IAEA-TECDOC-1173

Review of data and methods recommended in the international code of practice for dosimetry IAEA Technical Reports Series No. 381, The Use of Plane Parallel Ionization Chambers in High Energy Electron and Photon Beams

Final report of the Co-ordinated Research Project on Dose Determination with Plane Parallel Ionization Chambers in Therapeutic Electron and Photon Beams

INTERNATIONAL ATOMIC ENERGY AGENCY IAEA

October 2000

The originating Section of this publication in the IAEA was:

Dosimetry and Medical Radiation Physics Section
International Atomic Energy Agency
Wagramer Strasse 5
P.O. Box 100
A-1400 Vienna, Austria

REVIEW OF DATA AND METHODS RECOMMENDED IN THE INTERNATIONAL CODE OF PRACTICE FOR DOSIMETRY IAEA TECHNICAL REPORTS SERIES No. 381, THE USE OF PLANE PARALLEL IONIZATION CHAMBERS IN HIGH ENERGY ELECTRON AND PHOTON BEAMS

IAEA, VIENNA, 2000
IAEA-TECDOC-1173
ISSN 1011–4289

Printed by the IAEA in Austria
October 2000

FOREWORD

In 1987 the IAEA published a Code of Practice entitled "Absorbed Dose Determination in Photon and Electron Beams: An International Code of Practice" (IAEA Technical Reports Series No. 277), to advise users on how to obtain the absorbed dose in water from measurements made with an ionization chamber, calibrated in terms of air kerma. The Code of Practice described procedures and provided data for the use of ionization chambers to obtain the absorbed dose in high energy photon and electron beams. It was so designed that a variety of cylindrical chambers could be used, which represented the existing conditions worldwide. However, most national and international dosimetry protocols recognized the advantages of plane parallel ionization chambers, explicitly for electron beams and especially for low energy electron beams (below 10 MeV). Although this was acknowledged in TRS-277, recommended procedures for the calibration and use of these chambers were not fully developed.

Another Code of Practice entitled "The Use of Plane Parallel Ionization Chambers in High Energy Electron and Photon Beams: An International Code of Practice for Dosimetry" (IAEA Technical Reports Series No. 381) was published in 1997 to update TRS-277 and complement it with respect to the area of parallel plate ionization chambers. TRS-381 describes options on how to calibrate plane parallel chambers, against air kerma or absorbed dose to water standards at ^{60}Co gamma ray energies, in order to determine the absorbed dose to water in reference conditions. The use of these chambers to calibrate therapy electron beams, as well as to perform relative dose measurements for photon and electron beams, is included in the Code of Practice which also updates some of the data and concepts in TRS-277. It is considered that the Code of Practice TRS-381 fills the gaps that existed in TRS-277 with respect to plane parallel chambers and will result in improved accuracy in radiotherapy dosimetry when these chambers are used. In order to minimize searching and interpolation errors, the calculational procedures of the Code of Practice have been implemented in a computerized worksheet (Excel), which has been made available to users in Member States.

Dosimetry recommendations in the form of Codes of Practice or protocols include "state of the art" data in a given field at the time of their development. Subsequent scientific developments usually confirm or improve some of these data, or even reveal deficiencies in some of the data recommended. Codes of Practice also include new recommended procedures for performing measurements that have to be carefully verified and compared with existing recommendations in all possible situations found in clinical practice with therapeutic electron and photon beams.

In order to investigate the accuracy of the data and procedures included in TRS-381, a Co-ordinated Research Project was formed, its scientific scope including also the task of analysing and quantifying possible differences with other dosimetry recommendations. The main goal of the project was to ascertain that TRS-381 satisfies the highest scientific standards and yields the most accurate results available today with plane parallel ionization chambers. The Code of Practice replaces also various aspects of the recommendations in TRS-277, which most Member States use today, and evidence of improvement in practical dosimetry is necessary to advocate its implementation.

The Co-ordinated Research Project was conducted for three years and the present publication is a compilation of the results and findings by groups of investigators from different countries. An appendix has been included listing scientific publications by the participants in relation with this project.

The IAEA staff member responsible for this publication was P. Andreo of the Division of Human Health.

EDITORIAL NOTE

This publication has been prepared from the original material as submitted by the authors. The views expressed do not necessarily reflect those of the IAEA, the governments of the nominating Member States or the nominating organizations.

The use of particular designations of countries or territories does not imply any judgement by the publisher, the IAEA, as to the legal status of such countries or territories, of their authorities and institutions or of the delimitation of their boundaries.

The mention of names of specific companies or products (whether or not indicated as registered) does not imply any intention to infringe proprietary rights, nor should it be construed as an endorsement or recommendation on the part of the IAEA.

The authors are responsible for having obtained the necessary permission for the IAEA to reproduce, translate or use material from sources already protected by copyrights.

CONTENTS

Review of data and methods recommended in the international code of practice for dosimetry IAEA Technical Reports Series No. 381, The Use of Plane Parallel Ionization Chambers in High Energy Electron and Photon Beams 1
A. Dusautoy, M. Roos, H. Svensson, P. Andreo

Determination of the $N_{D,air}$ factor of plane parallel chambers and h_m values 11
M. Brunetto, G. Vélez, A. Germanier, S. Bustos

Verification of the absorbed dose values determined with plane parallel ionization chambers in therapeutic electron beams using ferrous sulfate dosimetry 21
A. Van der Plaetsen, H. Thierens, H. Palmans

Procedures for the selection of stopping power ratios for electron beams: Comparison of IAEA TRS procedures and of DIN procedures with Monte Carlo results 35
M. Roos, G. Christ

Deviation of the effective point of measurement of the Markus chamber from the front surface of its air cavity in electron beams 45
M. Roos, K. Derikum, A. Krauss

The recombination correction and the dependence of the response of plane parallel chambers on the polarizing voltage in pulsed electron and photon beams 53
M. Roos, K. Derikum

Electron beam dosimetry. Calibration and use of plane parallel chambers following IAEA TRS 381 recommendations 65
M.C. Lizuain, D. Linero, C. Picón, O. Saldaña

Experimental determination of p_{cav} factors for cylindrical ionisation chambers in electron beams 81
Å. Palm, O. Mattsson

Calibration of plane parallel chambers and determination of p_{wall} for the NACP and Roos chambers for ^{60}Co γ-ray beams 91
Å. Palm, O. Mattsson, P. Andreo

Testing of the code of practice at different electron energies and phantom materials 97
A. Björeland, H. Svensson

APPENDIX: PUBLICATIONS ISSUED WITHIN THE FRAMEWORK OF THIS PROJECT 105

PARTICIPANTS IN THE CO-ORDINATED RESEARCH PROJECT 107

RECENT IAEA PUBLICATIONS ON DOSIMETRY AND MEDICAL PHYSICS 109

REVIEW OF DATA AND METHODS RECOMMENDED IN THE INTERNATIONAL CODE OF PRACTICE FOR DOSIMETRY IAEA TECHNICAL REPORTS SERIES No. 381, THE USE OF PLANE PARALLEL IONIZATION CHAMBERS IN HIGH ENERGY ELECTRON AND PHOTON BEAMS

Results of the co-ordinated research project

A. DUSAUTOY
National Physical Laboratory (NPL),
Centre for Ionising Radiation Metrology,
Teddington, Middlesex, United Kingdom

M. ROOS
Physikalisch-Technische Bundesanstalt (PTB),
Gruppe für Photonen- und Elektronendosimetrie,
Braunschweig, Germany

H. SVENSSON
Radiation Physics Department,
Norlands Universitetssjukhus (NUS),
University of Umeå,
Umeå, Sweden

P. ANDREO
Dosimetry and Medical Radiation Physics Section,
Division of Human Health,
International Atomic Energy Agency,
Vienna

Abstract

An IAEA Co-ordinated Research Project was designed to validate the data and procedures included in the International Code of Practice Technical Reports Series (TRS) No. 381, "The Use of Plane Parallel Ionization Chambers in High Energy Electron and Photon Beams". This work reviews and analyses the procedures used and the data obtained by the participants of the project. The analysis shows that applying TRS-381 generally produces reliable results. The determination of absorbed dose to water using the electron method in reference conditions is within the stated uncertainties (2.9%). Comparisons have shown TRS-381 is consistent with the AAPM TG-39 protocol within 1% for measurements made in water. Based on the analysis, recommendations are given with respect to: (i) the use of plane parallel ionization chambers of the Markus type, (ii) the values for the fluence correction factor for cylindrical chambers, (iii) the value of the wall correction factor for the Roos chamber in ^{60}Co beams, and (iv) the use of plastic phantoms and the values of the fluence correction factors.

1. Introduction

An International Code of Practice for Dosimetry entitled "The Use of Plane Parallel Ionization Chambers in High Energy Electron and Photon Beams" (Technical Reports Series No. 381) [1] was published by the IAEA in 1997 in order to complement and extend the widely used Code of Practice Technical Reports Series No. 277 [2] for the determination of absorbed dose in radiotherapy photon and electron beams. The scope of TRS-381 was the calibration and use of plane parallel ionization chambers in electron beams, as well as relative dose measurements in photon and electron beams.

A Co-ordinated Research Project was designed to investigate the accuracy of the data and the procedures included in the Code of Practice TRS-381 [1]. The main objectives of the project were:

- to compare absorbed dose to water determinations under reference conditions with different detectors and methods that have shown high accuracy in other circumstances,
- to compare absorbed dose to water determinations under conditions that include the use of plane parallel ionization chambers in different plastic materials commonly used as dosimetry phantoms,
- to compare TRS-381 [1] with TRS-277 [2] and other dosimetry protocols recently issued by different national organizations (AAPM TG-39 [3]) using different types of plane parallel ionization chambers and phantom materials included in the TRS-381 [1].

The Co-ordinated Research Project operated between 1996 and 1999, during which time two research co-ordination meetings took place (Vienna, 1996; Barcelona, 1998) where the project participants presented their results and discussed their findings. As a result of a fruitful scientific interaction, agreements were reached with regard to the adoption of common set-ups and conditions for measurements made by the participants. These agreements minimized the likelihood of systematic errors and enabled more accurate comparisons.

By September 1999 participants submitted to the IAEA a final report on their activities carried out in relation to the project. These reports have been compiled in the present publication. A consultants meeting was convened in Vienna in November–December 1999 in order to analyse the contributions from a general perspective and to extract conclusions of interest for radiation dosimetry performed with plane parallel ionization chambers using TRS-381 [1]. The following analysis is the result of that meeting.

Results are grouped by topic and discussed from a global perspective. Contributions are referred to in the text by the code assigned in the third column of Table I, giving the list of participants. The topics included are:

(i) measurement of dose distributions in electron beams;
(ii) determination of the $N_{D,air}$ factor of plane parallel chambers;
(iii) selection of stopping power ratios;
(iv) absolute dose determination with Fricke dosimetry;
(v) use of plastic phantoms;
(vi) comparison with other dosimetry protocols; and
(vii) cavity perturbation correction factor, ρ_{cav}, for Farmer type ionization chambers.

2. Measurement of dose distributions in electron beams

Contributors: BEL, GER-2, SPA.

There are different detectors available for the measurement of dose distributions as a function of depth along the central axis. The detectors recommended in TRS-381 [1] for this purpose are plane parallel chambers. It is, however, convenient to use solid state detectors such as diodes and diamonds. Usually it is assumed that the reading of the diodes and diamonds is proportional to absorbed dose to water and the measured relative distributions are then taken directly as dose distributions without correction.

2.1. Use of different types of plane parallel chambers

Results using ionization chambers show that the range parameters agree when ion chambers that comply with the properties recommended in TRS-381, Table I, p. 15, are used (e.g. NACP, Roos). When a Markus type chamber is used in electron beams the effective point of measurement has been found to be shifted by about 0.5 mm from the front surface of the cavity towards its center. This may be essential for dose measurements in the vicinity of steep dose gradients.

TABLE I. PARTICIPANTS IN THE CO-ORDINATED RESEARCH PROJECT

Scientific investigators	Affiliation (of chief scientific investigator)	Contribution reference
BRUNETTO, M. VELEZ, G. GERMANIER, A.	Grupo de Espectroscopía Facultad de Matemática, Astro y Física Universidad Nacional de Córdoba Ciudad Universitaria 5000 Córdoba, ARGENTINA	ARG
VAN DER PLAETSEN, A.	Radiotherapie-Oncologie A.Z. St. Lucas Groene Briel 1 B-9000 Ghent, BELGIUM	BEL
ROOS, M.	Laboratorium 6.43 Physikalisch-Technische Bundesanstalt Bundesallee 100 D-38023 Braunschweig, GERMANY	GER-1 GER-2 GER-3
LIZUAIN, M.C. LINERO, D. PICON, C.	Institut Català d'Oncologia Av. Gran Vía s/n, km 2,7 E-08907 L'Hospitalet, Barcelona, SPAIN	SPA
MATTSSON, O. PALM, Å.	Department of Radiation Physics Sahlgren University Hospital S-413 45 Göteborg, SWEDEN	SWE G-1 SWE G-2
SVENSSON, H. BJÖRELAND, A.	Department of Radiation Physics University Hospital S-901 85 Umeå, SWEDEN	SWE U

2.2. Use of diode and diamond detectors

For the type of diode and diamond detectors used in the present investigations, the range parameters R_{100}, R_{50} and R_p agree with those from measurements using NACP and Roos chambers within the estimated experimental uncertainties.

A small uncertainty in the range, e.g. of the order of 0.5 mm, affects the determination of the mean beam energy at the phantom surface by the order of 0.1 MeV approximately. This has a small effect on the resulting stopping power ratio (and therefore in dose determination) except at the lowest energies.

3. The $N_{D,air}$ chamber factor of plane parallel chambers

In this section ratios of the $N_{D,air}$ factors, ρ_{wall} values for the Roos chamber and recombination correction factors are discussed.

3.1. Comparison of $N_{D,air}$ factors derived in cobalt-60 and electron beams

Contributors: ARG, BEL, SPA, SWE G-2.

The preferred method for the determination of the $N_{D,air}$ chamber factor is the electron beam method described in Section 9.1.1 of TRS-381 [1], where a plane parallel chamber is cross calibrated in a high-energy electron beam against a cylindrical reference chamber. The determinations of $N_{D,air}$ in a cobalt-60 beam by the in-air or in-phantom methods are therefore compared with this method in Table II. All participants used the NE2571 as the reference chamber. In one case a Capintec chamber was also used; unfortunately, these measurements could not be taken into account due to technical problems.

TABLE II. RATIOS OF $N_{D,air}$ VALUES DETERMINED IN COBALT-60 (IN-PHANTOM AND IN-AIR) WITH THOSE DETERMINED IN A HIGH ENERGY ELECTRON BEAM

$N_{D,air}$ values: cobalt-60 in water method/electron beam method		
Markus: 1.004	NACP: 0.995	Roos:1.012
std dev 0.003	2 chambers from 2 centres	std dev 0.02
4 chambers from 4 centres		12 chambers from 4 centres

$N_{D,air}$ values: cobalt-60 in air method/electron beam method
Markus: 1.008
1 chamber from 1 centre

It is unclear whether all the measurements reported take into account the water equivalent thickness of the front wall of the chambers. In high-energy electron beams the influence of this omission is negligible due to the small dose variation with depth around R_{100}. It is more important, however, for the cobalt-60 in-phantom measurements where a steep dose gradient exists.

$N_{D,air}$ values derived using the cobalt-60 in-phantom method are compared first in Table II with those derived using the electron beam method. The two methods agreed, within 0.5% approximately, for measurements made with the Markus and NACP chambers. However the methods did not agree for measurements made with the Roos chamber (the average ratio was 1.012). These results are discussed under Section 3.2 on ρ_{wall} (see also Section 8 on ρ_{cav}).

Next in Table II, $N_{D,air}$ values derived using the cobalt-60 in-air method are compared with those derived using the electron beam method. Measurements were only made with a Markus chamber at one Centre, giving an average ratio of 1.008.

$N_{D,air}$ values derived using the cobalt-60 in-air method have been compared with those derived using the cobalt-60 in-phantom method. Measurements were made with two Markus chambers at each of two Centres obtaining an average ratio of 1.003.

3.2. Value of the ρ_{wall} factor for the Roos chamber in cobalt-60

Contributors: ARG, BEL, SPA, SWE G-2.

Two different methods can be mentioned for the determination of ρ_{wall}.

1. The value of ρ_{wall} given in TRS-381 [1] is based on a comparison of dose determinations based on primary standards of air kerma and absorbed dose to water for cobalt-60. Therefore, in addition to the uncertainties introduced by the assumptions and data involved in using TRS-381 [1] (e.g. the omission of wall effects of all chambers in electron beams, ρ_{cav} and ρ_{cel} of the reference chamber in the electron beam and k_{att}, k_m and k_{cel} of the reference chamber in the cobalt-60 beam) the uncertainty of the air kerma calibration of the reference chamber and the uncertainty of the absorbed dose to water calibration of the plane parallel chamber, including the uncertainties of the respective primary standards also enter into this determination.

2. The second determination of ρ_{wall} uses a cross calibration between cylindrical and plane parallel chambers in a phantom, in a cobalt-60 beam and in a high-energy electron beam. Since $N_{D,air}$ is assumed to be independent of beam quality in TRS-381 [1], the results can be used to determine ρ_{wall} of the plane parallel chamber. The assumptions, and the data, are similar to those of method 1 (instead of the factors k_{att}, k_m and k_{cel} of the reference chamber, the factors ρ_{wall} and ρ_{cel} of this chamber in the cobalt-60 beam enter into the respective expression). However, only the quotient of the corrected readings of both chambers in the electron beam and in the cobalt-60 beam enter into this determination of ρ_{wall}. No reference is required to the primary standards.

The value recommended in TRS-381 [1] for the Roos chamber (p_{wall} = 1.003) has been used in the determination of the $N_{D,air}$ ratios included in Table II. Applying the second method, the results of Table II indicate that the value for ρ_{wall} is underestimated by 1.2% (i.e. ρ_{wall} should be 1.015). This is discussed further in Section 8.

3.3. Recombination correction

Contributor: GER-3.

The determination of the recombination correction may be facilitated by the application of analytical relations. Based on an experimental investigation a relation was deduced including the initial recombination and the proper contribution of the free electron in plane parallel chambers. It has been shown that the use of the Boag formula (as recommended in TRS-381 [1]) usually leads to uncertainties of the order of only 0.1% for conventional beams. However, it has been shown that these simple relations are not applicable in all cases.

Additionally, experimental results of the voltage dependence of the response for various chambers demonstrate again the importance of applying the two voltage method twice (e.g. in the cobalt-60 beam and the electron beam) as recommended in TRS-381 [1].

4. Stopping power ratios

Contributor: GER-1.

The selection of stopping power ratios according to DIN 6800-2 [4] may produce a slight improvement compared to TRS-381 [1] for typical clinical beams with a broad energy distribution when compared with the Monte Carlo results of Ding et al. [5]. However, in order to draw definite conclusions, experimental results (obtained using, for example, Fricke dosimeters) from different clinical accelerators are necessary.

A comparison between the water/air stopping powers given in TRS-381 [1] and those recommended in the forthcoming International Code of Practice based on standards of absorbed dose to water [6] has been carried out by the reviewers. The latter set of data originate from calculations by Ding et al. [5] using Monte Carlo simulations which included details of the accelerator heads of clinical accelerators for a variety of accelerator types (see Appendix B in the new Code of Practice [6]). To enable the comparison, the values in TRS-381 [1] have been recasted to the conditions used in the new Code of Practice [6], namely, electron beam quality specified in terms of R_{50} and depths scaled according to R_{50}. The two sets of data are shown in Fig. 1, where very good agreement can be observed except at large depths; this is expected, according to the discussion on beam contamination included in Appendix B of TRS-381 [1].

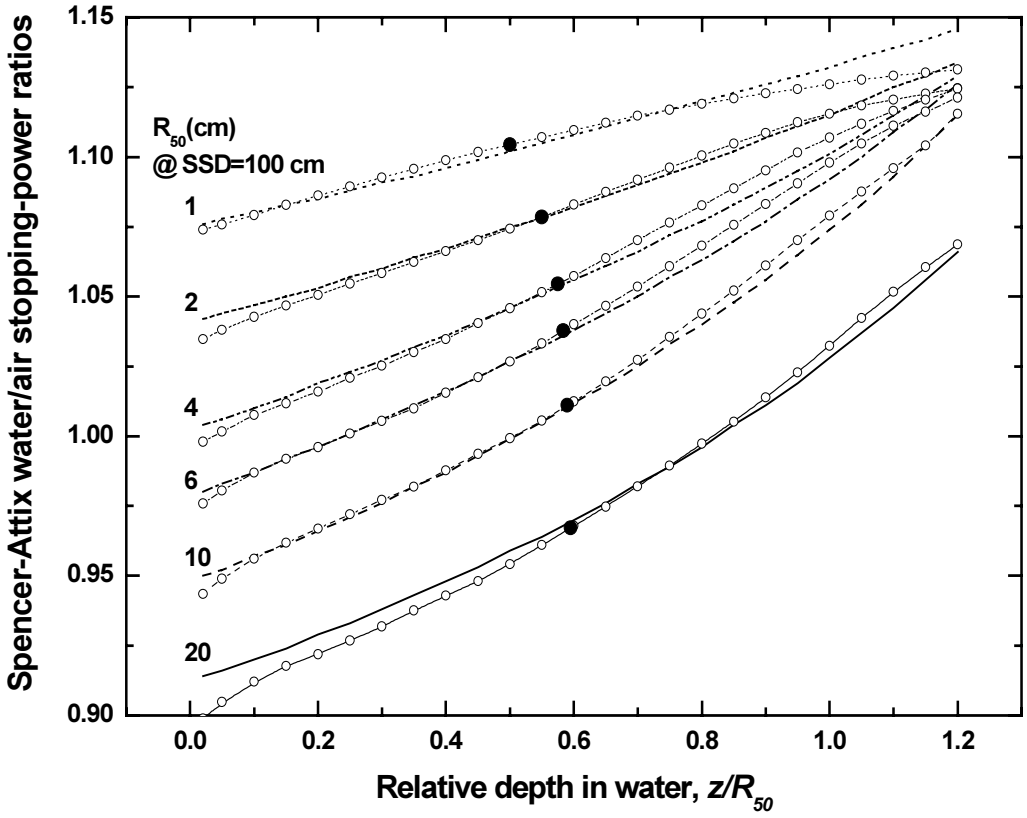

Figure 1. Stopping power-ratios for electron beams in TRS-381 [1] (circles) and in the forthcoming International Code of Practice based on standards of absorbed dose to water [6] (lines without symbols). The filled circles correspond to $s_{w,air}$ values at the reference depths in each case.

It is interesting to emphasize, however, that the largest difference occurs for beams with an energy close to 50 MeV (R_{50} = 20 cm approximately); this is striking, as the values in TRS-381 are for monoenergetic electrons whereas the new values at this energy correspond to a *racetrack* microtron, whose beams are almost monoenergetic. The reasons for the discrepancy are not well understood but are believed to be related to the different Monte Carlo calculations, even if in the two cases they were made with the same code (EGS4).

5. Absolute dose determination with Fricke dosimetry

Contributors: BEL, SWE-U.

One group (BEL) reported measurements made in PMMA, but they were difficult to interpret with regard to the quantity determined. Therefore they have been omitted from this discussion.

The ratio of D_w using the electron beam method to that found by using the Fricke method was determined at two laboratories. The Fricke results have been normalized at cobalt-60. The results from the Belgian laboratory were difficult to interpret. As the results for the Markus chamber do not appear to be consistent with the others, they have been omitted from the following analysis.

There is no energy dependence in absorbed dose to water determinations for beams with energies E_0 in a range from 5.7 to 45 MeV. The mean ratio of the electron beam method divided by the Fricke method was found to be 0.998 with a standard deviation of 0.003 and a standard deviation of the mean of 0.0008.

6. Use of plastic phantoms

Although water is recommended as the phantom material, measurements are also possible in plastics. If plastic phantoms are used, the required quantity is still absorbed dose to water in a water phantom.

Three steps are required to use plastic phantoms:

1. Determine the range parameters in water from those measured in plastic by range scaling.
2. Convert the depth of interest in water to an equivalent depth in plastic by depth scaling.
3. Apply the fluence correction h_m to the reading obtained in plastic to determine absorbed dose in water using the stopping power ratios water to air for the water phantom.

6.1. Scaling of depths and ranges

Contributors: BEL, SPA, SWE-U.

It has been demonstrated that the density of plastic must be measured and taken into account in order to get accurate range scaling. Density figures provided by the manufacturer may not be accurate.

Good agreement was found between the $R_{50,w}$ /$R_{50,PMMA}$ measured and that given in the TRS-381 [1].

No significant differences were found between the R_{100} measured in PMMA and its scaled depth measured in water for the energy range 4–20 MeV (from BEL & SWE-U) taking the width of the dose maximum into account.

6.2. Fluence correction factor, h_m

Contributors: ARG, BEL, SPA, SWE-U.

The correction factor h_m is determined as the quotient of the reading at depth in water and the reading at the scaled depth in plastic.

Measurements of h_m by the participants presented at the meeting in Barcelona (ARG, BEL, SPA) showed a large spread. This was attributed to the large dose variation with depth when the depth is not near R_{100} (particularly at low energies), so these data have not been not taken into account in the discussion.

The correction factor h_m was re-evaluated (by ARG, SPA, SWE-U) using depths in water and plastic at R_{100}, where the dose variation with depth is small. It was shown that R_{100} in water coincides approximately with the scaled R_{100} in plastic. The results are plotted in Figure 2.

The measured values of h_m for PMMA are about 0.4% low compared with the values given in TRS-381 [1] at all energies. The results for three types of plane parallel chamber, from three centres agree within about ±0.2%. The measurements of h_m with Farmer chambers appears to be approximately 0.6% lower than those recommended in TRS-381. However, the data are almost entirely from one laboratory.

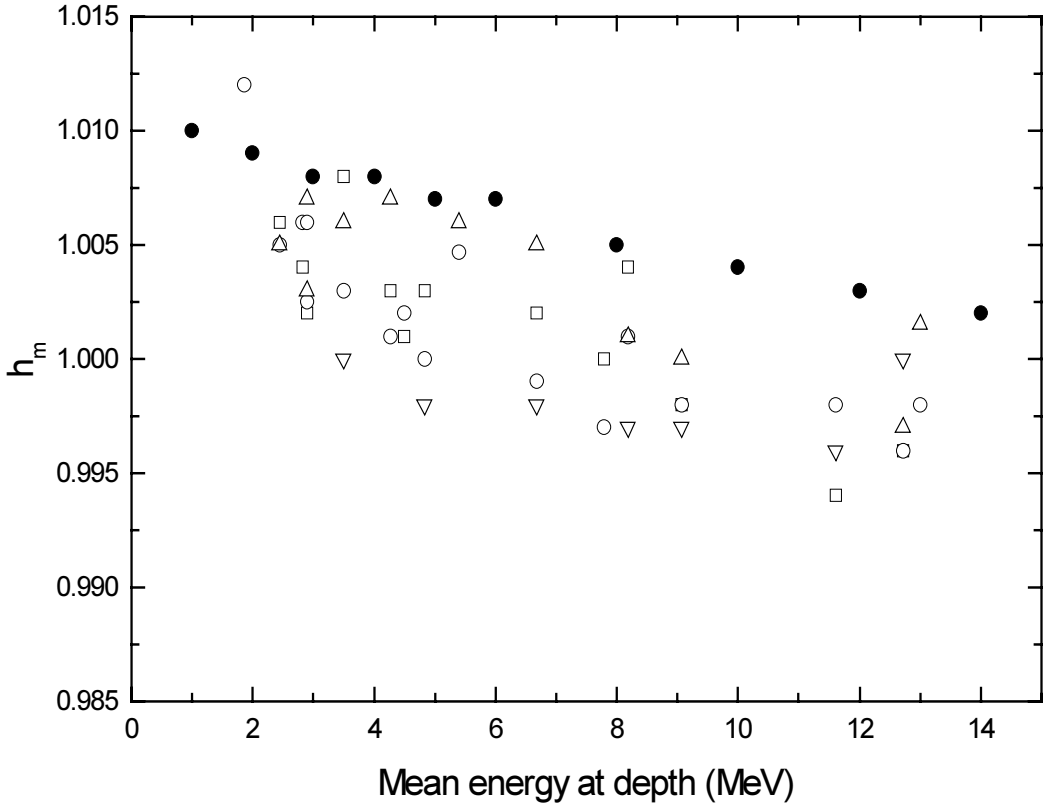

Figure 2. Factor h_m to correct for the difference in the electron fluence in a PMMA phantom compared to that in water at equivalent depths. Data shown correspond to TRS-381 [1], filled circles; NACP plane parallel chamber, triangles; Roos plane parallel chamber, circles; Markus plane parallel chamber, squares; Farmer NE 2571 cylindrical chamber, inverted triangles.

7. Comparison with other protocols

Contributors: GER-1, SPA, SWE-U.

For a Philips SL75/20 linear accelerator, in the reference conditions, the change in stopping power ratios between DIN 6800-2 [4] and TRS-381 [1] caused by the different selection procedures, amount to 0.8% at most. The difference is however decreased by 0.2% due to the polynomials used to determine the mean energies. Therefore the resulting stopping power ratios in these two protocols differ by less than 0.6%.

TRS-381 and IPEMB96 essentially use the same data and methods, so there is very little difference between the results obtained with these two Codes of Practice.

The differences in $N_{D,w}$ determined according to the protocols TG-39 [3], TRS-277 [2] and TRS-381 [1] for the Roos and NACP chambers (when the Farmer chamber was used as the reference chamber) were less than 1%, when measurements were made in water phantoms, (except for the lowest energies). However, up to 2% difference was found for measurements made in PMMA phantoms.

D_w determined from TG-39 [3] using a NACP chamber is between 0.5% and 0.7% lower than that found by following TRS-381 [1]. There appears to be a small trend with energy: The ratio D_w found from TG-39 [3] divided by D_w found from TRS-381 [1] is lower at high energies (e.g. above 10 MeV).

8. Cavity perturbation correction factor, $\rho_{cav,}$ for Farmer type chambers

Contributors: SWE G-1.

The ρ_{cav} values used in all current dosimetry protocols are based on the values determined by the SWE-G1 group in 1978, and these are also used in TRS-381 [1]. The original values were measured in a PMMA phantom using cylindrical ionization chambers with different radius and walls made of a mixture of graphite and epoxy resin. These results have been confirmed using the same set of ionization chambers but different electron beams. Additional measurements have been made using an improved experimental set up, where graphite ionization chambers of different radii have been used in water and in graphite phantoms. The measurements in water with graphite chambers were made in order to determine perturbation correction factors for Farmer type chambers in situations encountered in hospitals. The measurements in graphite were made in order to avoid mixing cavity and wall effects; in these cases, which correspond to using wall-less chambers, the linear relation between ρ_{cav} and the chamber radius measured in 1978 was also verified.

The new ρ_{cav} values are closer to 1 than the previous values. For energies relevant to the calibration of plane parallel ionization chambers in high-energy electron beams the change is up to about 1%, decreasing with energy.

If the current ρ_{cav} values were replaced with the new values, the $N_{D,air}$ factor would be reduced by the same amount for all the chambers when the recommended electron beam method is used. If new ρ_{cav} values are adopted, all the determinations of the absorbed dose based in the electron beam method would change.

Some remarks on the above results can be elaborated, based on the results of the comparisons between the electron beam method and the cobalt-60 in-phantom method. Using the current ρ_{cav} values an inconsistency in the value for ρ_{wall} of the Roos chamber at cobalt-60 has been found; this can be resolved with the use of a different ρ_{wall} factor for the Roos chamber, which would need to be increased by about 1% compared with the recommended data, as already described. If, on the other hand, the latest ρ_{cav} values (reported by the SWE-G1 group) were used, then the inconsistency of the data for the Roos chamber would be removed, but then an inconsistency in the data for the NACP chamber would appear; this could be resolved using a different ρ_{wall} factor for the NACP chamber, which would need to be reduced by about 1% compared with the recommended data. Due to the large impact of a change in the values used for $\rho_{cav,}$ further investigations on this correction factor would be necessary before recommendations can be made on the use of the new values.

9. Conclusions

The present analysis shows that the results of applying the Code of Practice TRS-381 [1] generally produces reliable results. The determination of D_w using the electron method in reference conditions is well within the stated uncertainties (i.e. 2.9%); this has been demonstrated by comparison with results obtained with the Fricke method for measurements made in water (having an accuracy within 1% relative to cobalt-60).

Different comparisons have shown that TRS-381 [1] is consistent with the AAPM TG-39 protocol [3] within 1% for measurements made in water. However it has been demonstrated that if measurements are performed in plastic phantoms the differences increase considerably. Therefore, the use of plastics is not recommended.

Based on the present analysis, the following specific recommendations can be given to the users of TRS-381 [1]:

- If a Markus type chamber (which does not comply with the desirable chamber properties recommended by TRS-381) is used for the dosimetry of electron beams, a shifted effective point of measurement must be used; this is situated 0.5 mm from the surface of the cavity towards its centre.
- The values of the fluence correction factor ρ_{cav} for cylindrical chambers, used as reference for the calibration of plane parallel chambers, given in TRS-381 appear to be low according to the latest investigations. Considering the large impact of a change in $\rho_{cav,}$ it is recommended that the values for ρ_{cav} given in TRS-381 continue being used until further results are available.
- To resolve the discrepancy found for the ρ_{wall} correction factor at cobalt-60 of the Roos chamber (which may be related to the current values of $\rho_{cav,}$ for the cylindrical reference chamber) it is recommended to increase the perturbation correction factor ρ_{wall} for the Roos chamber by 1.2% at cobalt-60, resulting in a ρ_{wall} value equal to 1.015.
- There are considerable technical problems with measurements made in plastic phantoms. For this reason it is recommended not to use plastic phantoms if at all possible. If the use of plastics is unavoidable, then the value of the factor h_m for plane parallel chambers in PMMA phantoms (Table XVIII, in TRS-381) should be reduced by 0.4%. The density of the plastics should always be determined.

There is a typographical error in Table IX of TRS-381, where the central electrode material of the chamber NE 0.6 cm^3 Robust Farmer has been erroneously written (twice) as “aluminium”; it should read A-150.

REFERENCES

[1] INTERNATIONAL ATOMIC ENERGY AGENCY, The Use of Plane Parallel Ionization Chambers in High Energy Electron and Photon Beams — An International Code of Practice for Dosimetry, Technical Reports Series No 381, IAEA, Vienna (1997).

[2] INTERNATIONAL ATOMIC ENERGY AGENCY, Absorbed Dose Determination in Photon and Electron Beams — An International Code of Practice, Technical Reports Series No 277, IAEA, Vienna (1987).

[3] P.R. ALMOND, F.H. ATTIX, S. GOETSCH, L.J. HUMPHRIES, H. KUBO, R. NATH, D.W.O. ROGERS, The calibration and Use of Plane Parallel Ionization Chambers for Dosimetry of Electron Beams: An Extension of the 1983 AAPM Protocol, Report of AAPM Radiation Therapy Committee Task Group 39, Med. Phys. **21** (1994) 1251–1260.

[4] DEUTSCHES INSTITUT FÜR NORMUNG, Dosismeßverfahren nach der Sondenmethode für Photonen- und Elektronenstrahlung: Ionisationsdosimetrie, Deutsche Norm DIN 6800-2, Berlin (1996).

[5] G.X. DING, D.W.O. ROGERS, T.R. MACKIE, Calculation of Stopping-Power Ratios Using Realistic Clinical Electron Beams. Med. Phys. **22** (1995) 489–501.

[6] INTERNATIONAL ATOMIC ENERGY AGENCY, Absorbed Dose Determination in External Beam Radiotherapy — An International Code of Practice for Dosimetry Based on Standards of Absorbed Dose to Water, Technical Reports Series No. 398, IAEA, Vienna (2000).

DETERMINATION OF THE $N_{D,air}$ FACTOR OF PLANE PARALLEL CHAMBERS AND h_m VALUES

M. BRUNETTO
FaMAF (UNC) – Centro Médico Dean Funes

G. VÉLEZ
FaMAF (UNC) – Hospital San Roque

A. GERMANIER
CEPROCOR

S. BUSTOS
CEPROCOR – CONICOR

Córdoba, Argentina

Abstract

The use of plane parallel ionization chambers for the dosimetry of electron beams has been recommended by most national and international dosimetry protocols. The International Code of Practice TRS-381 provides recommendations for the calibration and use in reference conditions of plane parallel chambers in radiotherapy electron beams, as well as for relative dose measurements in electron and photon beams. The present investigations focus mainly on two topics: (i) determinations of the $N_{D,air}$ factor for the plane parallel chambers PTW-23343 Markus and PTW-34001 Roos, using different methods proposed in TRS-381; and (ii) experimental determinations of the fluence correction factor h_m in PMMA. For the Markus chamber the results show no difference between the $N_{D,air}$ obtained with ^{60}Co in water and the electron beam method. The discrepancies found for the Roos chamber lead us to question the value of ρ_{wall} for ^{60}Co recommended in TRS-381. The h_m values obtained are lower than those in TRS-381 for all the energies measured, and show no difference for the different chambers used.

1. Calibration of plane parallel ionization chambers against cylindrical chambers

During the duration of this research project, the different methods for the calibration of plane parallel ionization chambers described in TRS-381 [1] were investigated in detail.

Our study has been focused on two plane parallel chambers commonly used in radiotherapy dosimetry, PTW 23343 Markus and PTW 34001 Roos. As reference cylindrical chambers this investigation has used the chambers NE 2571 and Capintec PR06-G, whose main characteristics are listed in Table I.

TABLE I. CHARACTERISTICS OF THE CYLINDRICAL CHAMBERS USED AS REFERENCE

	NE 2571	Capintec PR06-G
cavity radius	3.15 mm	3.20 mm
central electrode material	Aluminium	C-552
wall material	Graphite	C-552
wall thickness, t_{wall}	0.065 g/cm^2	0.050 g/cm^2
build-up cap material	Delrin	Polystyrene
build-up cap thickness, t_{cap}	0.551 g/cm^2	0.530 g/cm^2

1.1. Determination of $N_{D,air}$ for the PTW Markus plane parallel chamber

The study of the PTW Markus chamber is the former part of our work. Measurements were made at the Hospital San Roque in a Teradi 800 ^{60}Co unit, and at the Centro Médico Dean Funes in a Varian Clinac 18 linear accelerator and an AECL Theratron-80 ^{60}Co unit.

Twelve independent determinations of $N_{D,air}$ were made for the Markus chamber: four were cross-calibrations against an NE 2571 chamber and eight were against a Capintec PR06-G chamber.

1.1.1. Measurements in a ^{60}Co gamma-ray beam

The main recommendation in TRS-381 is to perform the determination of $N_{D,air}$ using the electron beam method. However, if it is not possible to follow that procedure two alternative methods are given based on measurements in a ^{60}Co gamma-ray beam: (i) ^{60}Co in-phantom method (usually performed in the user's beam at the hospital); and (ii) ^{60}Co in-air method (usually performed at the Standards Laboratory).

(i) ^{60}Co in-water method

The reference conditions used were based on a 10 × 10 cm^2 field size at the phantom surface and an SSD of 80 cm. Both chambers, the plane parallel and the reference cylindrical chamber, were situated at the reference depth of 5 cm (their effective point of measurement placed at this depth). The results of these measurements are given in Table II, where the mean value and its standard deviation have been included.

TABLE II. VALUES OF $N_{D,air}$ FOR A PTW MARKUS PLANE PARALLEL CHAMBER USING THE ^{60}Co IN-WATER METHOD

Radiation Treatment Unit	$N_{D,air}$ vs NE 2571 (× 10^{-2} Gy/div)	$N_{D,air}$ vs Capintec PR06-G (× 10^{-2} Gy/div)
Theratron-80	–	9.38
Theratron-80	–	9.48
Teradi-800	9.52	9.46
Mean value	9.46 ± 0.03	

(ii) ^{60}Co in-air method

The experimental procedure yields N^{pp}_K from the measurement of air-kerma, obtained using a reference cylindrical chamber with known N^{ref}_K. For the plane parallel chamber, the $N_{D,air}$ factor is derived according to

$$N_{D,air} = N_K\,(1-g)\,k_m k_{att} \qquad (1)$$

Four independent determinations of $N_{D,air}$ for the Markus plane parallel chamber were made, out of which three were against a Capintec PR06-G chamber and one against an NE2571 chamber. The reference conditions were 10 × 10 cm^2 field size at the depth of measurement and SCD = 90 cm. Each ionization chamber was provided with its corresponding build-up cap. As the Markus plane parallel chamber does not have an appropriate build-up cap provided by the manufacturer, a special build-up cap of PMMA was

manufactured in order to perform these measurements in air. It had the same diameter as the waterproof sleeve and was 3.6 mm thick (equivalent to 4 mm of water); thus, the total build-up was 5 mm water equivalent. A value of 0.985 for the product $k_m k_{att}$ (Table XV in TRS-381) was used to determine the $N_{D,air}$ factor from the measured N_K. The results of these measurements are given in Table III.

TABLE III. VALUES OF $N_{D,air}$ FOR A PTW MARKUS PLANE PARALLEL CHAMBER USING THE ^{60}Co IN-AIR METHOD

Radiation Treatment Unit	$N_{D,air}$ vs NE 2571 ($\times 10^{-2}$ Gy/div)	$N_{D,air}$ vs Capintec PR06-G ($\times 10^{-2}$ Gy/div)
Theratron-80	–	9.59
Theratron-80	–	9.59
Teradi-800	9.54	9.56
Mean value	9.57 ± 0.01	

1.1.2. Measurements in a high-energy electron beam

Four independent determinations of $N_{D,air}$ were made using the electron beam method using the Capintec PR06-G as a reference chamber. An external monitor was placed in water. The reference conditions used were:

Radiation treatment unit	Varian Clinac 18
Phantom material	water
E_o	17.54 MeV
depth	R_{100} (2.45 cm)
E_z	11.55 MeV
SSD	100 cm
Field size (cone delimited)	15 cm × 15 cm
Nominal dose rate	300 MU/min

The four values of $N_{D,air}$ ($\times 10^{-2}$ Gy/div) were: 9.44, 9.41, 9.48 and 9.46. Their mean value was 9.45 ± 0.01.

1.1.3. Comments on the results of $N_{D,air}$ for the PTW Markus chamber

The number of determinations of $N_{D,air}$ with the ^{60}Co in-air method was not enough statistically; however, the spread of the $N_{D,air}$ values obtained by using the Capintec PR06-G as the reference chamber was less than 0.2%. The difference between the $N_{D,air}$ values obtained using Capintec and NE2571 cylindrical chambers as reference is less than 0.4%. In this method, it is difficult to reproduce the exact position of the chambers for conditions other than at a Standards Laboratory; for example, hospitals have no proper devices to perform these measurements as accurately as they should be done.

No differences were found between the values of $N_{D,air}$ obtained with the ^{60}Co in-water and electron beam method. However, there is a discrepancy of about 1.3% between the value obtained with the ^{60}Co in-air method and with the electron beam method. This leads us to believe that the value 0.985 used for $k_m k_{att}$ for the build-up manufactured by us may not be correct.

Comparing the value of $N_{D,air}$ obtained with what can be considered our best estimate, e.g. the electron beam method, with that for the ^{60}Co in-air method (Eq. 1), we can experimentally determine the value of $k_m k_{att}$ for our build-up cap. In that case we obtain $k_m k_{att} = 0.978$.

1.2. Determination of $N_{D,air}$ for the PTW Roos plane parallel chamber

The reference conditions for the Roos chamber were the same as those used for the Markus chamber. We did not test the ^{60}Co in-air method for this chamber because of the drawbacks cited above.

1.2.1. Measurements in a ^{60}Co gamma-ray beam

Eight independent determinations of $N_{D,air}$ were performed against an NE2571 chamber and ten against a Capintec PR06-G chamber. The reference conditions were a 10 × 10 cm^2 field size and SSD of 80 cm; both chambers were situated at the reference depth of 5 cm. The results of this set of measurements are given in Table IV.

TABLE IV. VALUES OF $N_{D,air}$ FOR A PTW ROOS PLANE PARALLEL CHAMBER USING THE ^{60}Co IN-WATER METHOD

$N_{D,air}$ vs NE 2571 ($\times 10^{-2}$ Gy/div)	$N_{D,air}$ vs Capintec PR06-G ($\times 10^{-2}$ Gy/div)
1.405	1.398
–	1.378
–	1.381
–	1.389
1.394	–
1.400	1.393
1.396	1.390
1.393	1.385
1.386	1.379
1.403	1.388
1.399	1.390
mean: 1.397±0.002	mean: 1.387±0.002

1.2.2. Measurements in a high-energy electron beam

The reference conditions used were:

Radiation treatment unit	Varian Clinac 18
Phantom material	water
E_o	17.54 MeV
Depth	2 cm
E_z	12.84 MeV
SSD	100 cm
Field size (no cone)	20 cm × 20 cm
Nominal dose rate	300 MU/min

The results are given in Table V.

TABLE V. VALUES OF $N_{D,air}$ FOR A PTW ROOS PLANE PARALLEL CHAMBER USING THE ELECTRON BEAM METHOD

$N_{D,air}$ vs NE2571 ($\times 10^{-2}$ Gy/div)	$N_{D,air}$ vs Capintec PR06-G ($\times 10^{-2}$ Gy/div)
1.371	1.355
1.380	1.356
1.380	1.361
1.385	–
1.380	–
mean: 1.379±0.002	mean: 1.357±0.002

1.2.3. Comments on the results of $N_{D,air}$ for the PTW Roos chamber

We can observe that for the Roos chamber using the ^{60}Co in-phantom method the $N_{D,air}$ results for the two reference chambers agree within 0.7%. However, the values with the two chambers differ by about 1.6% when the electron beam method is used. This lead us to investigate if there was a problem with the Capintec chamber, mainly because it had originally agreed well with the NE 2571 chamber for an absorbed dose determination in ^{60}Co. A new comparison between the two chambers in ^{60}Co was made, and these measurements confirmed our suspicion, as we found a difference of about 1% between the two absorbed dose values. Due to this discrepancy, in what follows only the NE2571 results will be used; no attempt is made to re-analyse the results for the Markus chamber (see 1.1.3).

During the second Research Co-ordination Meeting (1998), several participants presented significant discrepancies between the values of $N_{D,air}$ for the PTW Roos plane parallel chamber when measurements were made in a ^{60}Co beam and in an electron beam. These discrepancies prompted the need for a re-evaluation of ρ_{wall} (^{60}Co) of the Roos chamber.

Comparing the $N_{D,air}$ obtained using the electron beam method with that derived from ^{60}Co in-water using NE2571 as a reference chamber, the ratio is 1.013. This may question the ρ_{wall} value of 1.003 recommended in Table XIII of TRS-381.

As a general comment about the calibration of the plane parallel chambers in the user beam, we want to emphasize the importance of using an external monitor chamber placed in water near the plane parallel and reference chambers for the electron beam method, as recommended in TRS-381. It is necessary to perform several independent determinations to achieve a reliable mean value. Further, the study of the polarity and recombination correction factors for the chambers involved must be taken into account. Finally, the cylindrical chamber used as reference chamber should preferably be a "tertiary standard".

2. Experimental determination of h_m in PMMA

The factor h_m corrects for the differences in the electron fluence in a plastic phantom compared to that in water at an equivalent depth. According to TRS-381, it can be calculated as the ratio of ionization chambers readings in the two media:

$$M_{Q,w}(z_{ref,w}) = M_{Q,plastic}(z_{ref,plastic})\, h_m \quad (2)$$

and the equivalent depth can be obtained by using the relationship:

$$z_{ref,w} \approx z_{ref,plastic} \frac{\rho_{user}}{\rho_{table}} C_{pl} \tag{3}$$

2.1. First set of determinations (1998)

The values of h_m were measured in a PMMA phantom, using two plane parallel chambers, under the following experimental conditions:

Reference chambers	PTW Markus, PTW Roos, NE2571
Monitor chamber	NE 2571
Radiation treatment unit	Varian Clinac 18
Nominal dose rate	300 MU/min
Nominal energy and depths in water [mm]	6 MeV (12.2, 13.4); 12 MeV (24.5, 28.1); 15 MeV (24.5, 28.1); 18 MeV (24.5)
SSD	100 cm
Cone	15 cm × 15 cm
MU/reading	200 MU
Plastic material	PMMA (PTW)

The density of the PMMA used was measured giving ρ_{user} = 1.18 gcm^{-3}. The Markus chamber was placed in PMMA without a waterproof sleeve. An external monitor detector (em) was positioned in air to normalize the readings for both, water and PMMA. It was placed in the electron cone because it is necessary to interchange the water and the PMMA phantoms, without disturbing it. Thus, the position of the external monitor was very close to the x-rays jaws, and it is possible that in that place there were fluctuations in the temperature that could not be registered. The h_m value was calculated for all the chambers using the following expression:

$$h_m = \frac{M_{Q,w}(z_{ref,w}) \Big/ M_{em,air}}{M_{Q,PMMA}(z_{ref,PMMA}) \Big/ M_{em.air}} \tag{4}$$

No correction for temperature was made here. Results are presented in Table VI and they are also shown in Fig. 1. No other influence quantities were corrected for.

These values were presented during the Second Research Co-ordination Meeting (1998). All the values obtained by the participants were compared and there was a very large scatter between the various determinations.

TABLE VI. FIRST RESULTS FOR THE FACTOR h_m, TO CONVERT ELECTRON FLUENCE FROM PMMA TO WATER, FOR DIFFERENT MEAN ELECTRON ENERGIES AT DEPTH, USING TWO PLANE PARALLEL CHAMBERS, COMPARED WITH THE DATA IN TABLE XVIII (TRS-381)

E_z[MeV]	TRS-381	PTW Markus	% difference	PTW Roos	% difference
2.81	1.008	1.010	0.2	1.014	0.6
3.09	1.008	1.009	0.6	1.011	0.4
4.60	1.008	1.020	1.2	1.014	0.6
5.39	1.007	1.009	0.2	1.011	0.4
7.00	1.006	1.012	0.4	1.010	0.4
7.79	1.005	1.006	0.1	1.008	0.3
11.62	1.003	0.998	–0.5	1.004	0.1

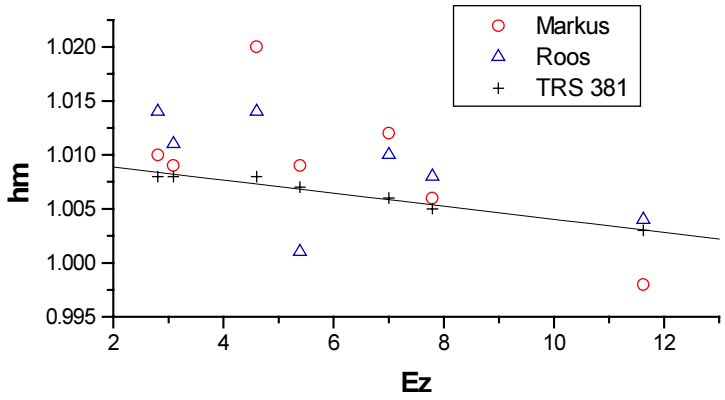

FIG. 1. A comparison of h_m, as a function of the mean electron energy at depth, using different ionization chambers (PTW Roos, PTW Markus and NE2571) with the values in TRS-381.

2.2. New set of measurements of h_m (1999)

In order to clarify the discrepancies mentioned above, it was agreed to use common measurement conditions to obtain new values of h_m: use constant SCD if possible, 15 × 15 cm^2 field size, no electron cones, external monitor to be placed in the lowest position in the treatment head, avoid use of scaling rules, do measurements at z_{max} in each medium, perform water/PMMA/water or PMMA/water/PMMA triple measurements at each energy during the same session, use $f_{P,T}$ for water and plastic, and perform a minimum of three independent measurements for each data point.

We performed new determinations of h_m in PMMA for the two PTW plane parallel chambers, Markus and Roos, as well as for the cylindrical chamber NE 2571. Special fixation accessories were designed and manufactured in order to have good reproducibility in mounting the ionization chambers in water phantom. The reference conditions were:

Radiation treatment unit	Varian Clinac 18
Mode	electrons
Nominal energy	6, 9, 15 and 18 MeV
SSD	100 cm
Field size	15 cm × 15 cm (no electron cones)
MU/reading	200 MU
Nominal dose rate	300 MU/min
Reference chambers	PTW Markus, PTW Roos, NE2571
Monitor chamber	NE2571
Phantom materials	PMMA, water

Four different mean electron energies at depth were selected with the purpose of determining h_m as a function of E_z for each chamber. These are listed in Table VI.

TABLE VI. ENERGIES AND DEPTHS USED TO PERFORM MEASUREMENTS OF h_m

E_{nom} [MeV]	E_o [MeV]	E_z [MeV]	$R_{100,,w}$ [mm]	$R_{100,,w\ PMMA}$ [mm]
6	5.8	2.83	13.4	12
9	8.5	4.49	17.8	16
15	13.5	7.79	24.5	22
18	17.4	11.62	24.5	22

The results are given in Tables VII–IX for the Markus chamber, for the Roos chamber and for the NE 2571 chamber. All the values of h_m vs E_z are given along with its average and standard deviation of the mean value. A compilation of the results is given in Fig. 2.

In general, our first set of results were higher than the new values. This may be because some of the new conditions were different; the set-up was easier because we could work without the electron cone, the positioning of the chambers in water was better, and the Markus chamber was placed with the waterproof sleeve in both phantoms (water and PMMA). Also, we did more measurements for the second run.

TABLE VII. DETERMINATIONS OF THE FACTOR h_m, FOR DIFFERENT MEAN ELECTRON ENERGIES AT DEPTH, USING A PTW MARKUS CHAMBER

E_z [MeV]	h_m (Markus)					Mean.
2.83	1.005	1.007	0.999	1.008	1.002	1.004±0.002
4.49	0.999	0.996	0.998	1.010	1.003	1.001±0.002
7.79	1.003	0.997	0.994	1.007	0.999	1.000±0.002
11.62	1.000	0.997	0.990	0.986	0.999	0.994±0.002

TABLE VIII. DETERMINATIONS OF THE FACTOR h_m, FOR DIFFERENT MEAN ELECTRON ENERGIES AT DEPTH, USING A PTW ROOS CHAMBER

E_Z [MeV]	h_m (Roos)						Mean.
2.83	1.001	0.995	1.006	1.008	1.010	1.005	1.004±0.002
4.49	1.006	0.990	1.002	1.000	1.004	1.003	1.001±0.002
7.79	0.997	0.990	0.995	1.006	–	1.000	0.998±0.003
11.62	0.998	0.991	0.992	1.005	–	0.998	0.997±0.003

TABLE IX. DETERMINATIONS OF THE FACTOR h_m, FOR DIFFERENT MEAN ELECTRON ENERGIES AT DEPTH, USING A CHAMBER NE2571

E_z [MeV]	h_m (NE2571)					Mean.
11.62	0.996	0.999	0.992	0.995	0.998	0.996±0.001

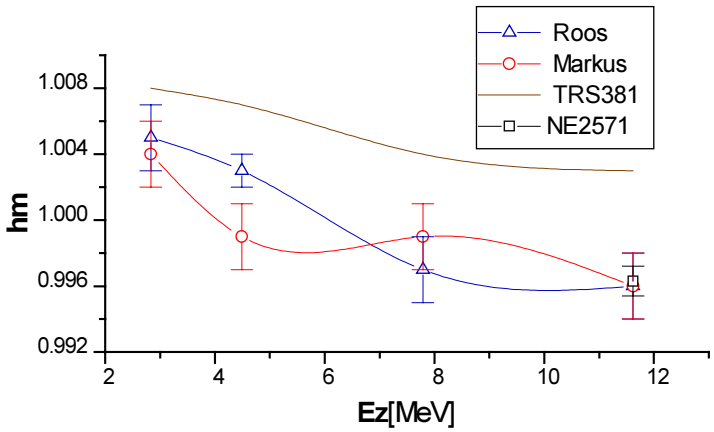

FIG. 2. Comparison of h_m, as a function of the mean electron energy at depth, using different ionization chambers (PTW Roos, PTW Markus and NE2571) with the values in TRS-381.

However, we consider that the main difference was that for the first set of determinations we did not correct for the possible difference in the temperature of water and PMMA. In the new set of measurements, we applied the temperature corrections to the h_m values. It is difficult to determine the temperature of PMMA. In general, the temperature of PMMA was always higher than the temperature of water by about 2°C; thus the h_m values with this correction become lower. On the other hand, we cannot be sure that the external monitor was at the same temperature while we did the measurements in water and in PMMA. In order to take into account this effect in an approximate manner, we compared the h_m values obtained directly with Eq. (4), with those resulting from the same expression multiplied by the corresponding mean value of the external monitor. That is:

$$h_m = \frac{\left\langle M_{Q,w}(z_{ref,w}) \Big/ M_{em,air}^{(1)} \right\rangle \left\langle M_{em,air}^{(1)} \right\rangle}{\left\langle M_{Q,PMMA}(z_{ref,PMMA}) \Big/ M_{em,air}^{(2)} \right\rangle \left\langle M_{em,air}^{(2)} \right\rangle} \quad (5)$$

where (1) refers to the measurements in water, and (2) refers to the measurements in PMMA. We found that the differences with this correction did not differ from the values obtained without correction.

A comparison with the values included in TRS-381 indicates that our values are generally lower than those in TRS-381 by about 0.7%.

With regard to the variation of the h_m values for the different chambers, our results show no appreciable difference between them, and their ratios are very close to unity.

REFERENCE

[1] INTERNATIONAL ATOMIC ENERGY AGENCY, The Use of Plane Parallel Ionization Chambers in High Energy Electron and Photon Beams — An International Code of Practice for Dosimetry, Technical Reports Series No. 381, IAEA, Vienna (1997).

VERIFICATION OF THE ABSORBED DOSE VALUES DETERMINED WITH PLANE PARALLEL IONIZATION CHAMBERS IN THERAPEUTIC ELECTRON BEAMS USING FERROUS SULFATE DOSIMETRY

A. VAN DER PLAETSEN
Department of Radiotherapy,
A.Z. Sint Lucas

H. THIERENS, H. PALMANS
Standard Dosimetry Laboratory,
University of Ghent

Ghent, Belgium

Abstract

Absolute and relative dosimetry measurements in clinical electron beams using different detectors were performed at a Philips SL18 accelerator. For absolute dosimetry, ionization chamber measurements with the PTW Markus and PTW Roos plane parallel chambers were performed in water following the recommendations of the TRS-381 Code of Practice, using different options for chamber calibration. The dose results obtained with these ionization chambers using the electron beam calibration method were compared with the dose response of the ferrous sulphate (Fricke) chemical dosimeter. The influence of the choice of detector type on the determination of physical quantities necessary for absolute dose determination was investigated and discussed. Results for d_{max}, R_{50} and R_p were in agreement within statistical uncertainties when using a diode, diamond or plane parallel chamber. The effective point of measurement for the Markus chamber is found to be shifted 0.5 mm from the front surface of the cavity. Fluence correction factors, h_m, for dose determination in electron beams using a PMMA phantom were determined experimentally for both plane parallel chamber types.

1. Introduction

The IAEA Code of Practice TRS-381 [1] describes the use of plane parallel ionization chambers in high-energy electron beams and gives options to calibrate this type of chambers. The different calibration methods were applied to PTW Markus and PTW Roos chambers. Fricke measurements [2] in water in a high-energy electron beam confirmed the value of the $N_{D,air}$ factors of the Markus and the Roos chambers determined in a high-energy electron beam. The $N_{D,air}$ factor of the PTW/Roos chamber determined in water in a ^{60}Co beam was 1.7% higher than that determined in a high-energy electron beam.

Relative dosimetry measurements in clinical electron beams are performed with different detectors. The measured values of the different parameters were compared and the influence of the use of different detectors for determination of physical quantities on the absolute dose values is discussed. Measurements confirmed that the effective point of measurement of the PTW/Markus chamber is not in the front of the air cavity but approximately 0.5 mm towards the centre of the air volume.

Most protocols include the use of plastic phantoms for the dose determination to water in electron beams, especially for low energy beams. Correction factors for dose determination in electron beams in a PMMA phantom h_m were experimentally determined with both plane parallel chamber types. These values deviate from those specified by the TRS-381 protocol. The largest deviations were observed for the Markus chamber. Experiments also showed that these correction factors are dependent on the type of the chamber. The results confirm the recommendation in the protocol to determine the absorbed dose in a water phantom to avoid the plastic-dependent correction factors.

To investigate the accuracy of the new data and the procedures included in the TRS-381 Code of Practice, the calculated absorbed dose values determined with a PTW/Markus and a PTW/Roos plane parallel chamber types and using the $N_{D,air}$ factors determined in a high-energy electron beam, were compared with those obtained with an independent dosimeter, the Fricke dosimeter, in a PMMA phantom.

2. Electron beam characteristics: relative dosimetry

To determine the absolute dose in an electron beam, the electron beam parameters related to the physical quantities such as mean electron energy at depth and at the surface of the phantom have to be determined [1, 3].

We have experimentally determined the depth of dose maximum R_{100}, the half value depth R_{50} and the practical range R_p using different detectors: the PTW/Markus (type PTW 23343) and PTW/Roos (type PTW 34001) plane parallel ionization chambers, a diode (Scanditronix p-Si) and a diamond detector (PTW ITP Dubna). Measurements were performed in an automatic water phantom (PTW MP3). Some measurements were repeated in a PMMA phantom. All depth values reported in the following tables are specified as depth (mm) in water.

2.1. Determination of the depth of dose maximum in an electron beam

To determine the value of the depth of dose maximum with a plane parallel ionization chamber, the measured ionization values were converted to dose values by multiplication with the stopping power ratios and with the appropriate correction factors (ρ_{cav}, ρ_{pol}, ρ_s). The effective point of measurement is located at the inner surface of the front window. The diode and diamond detector can be used directly without depth dependent corrections. The results are given in Table Ia. The uncertainties are given as one standard deviation of the measured values with the different detectors. The measurements were performed using an SSD of 100 cm and a 10 cm × 10 cm field.

TABLE Ia. DEPTH OF MAXIMUM DOSE DETERMINED WITH DIFFERENT DETECTORS IN A WATER PHANTOM FOR A 10 × 10 FIELD AND SSD = 100 cm

Energy (MeV)	(R_{100}) Roos (mm)	(R_{100}) diamond (mm)	(R_{100}) diode (mm)	(R_{100}) mean (mm)	σ (mm)
4	8.8	8.9	8.9	8.83	0.06
6	12.6	12.6	12.3	12.5	0.2
8	16.4	17.1	17.0	16.8	0.4
10	20.5	21.5	21.3	21.1	0.5
12	26.7	26.8	26.7	26.73	0.06
15	27.7	27.9	27.7	27.8	0.1
18	30.0	29.5	30.0	29.8	0.3

Results for the Markus chamber are given in Table Ib. These different from the values determined with the Roos chamber, the diode and the diamond detector: if one determines the std dev for all the other values, the results for the Markus chamber are outside 3*std dev. This is indicating a possible shift in the position of P_{eff} of the Markus chamber.

For some energies, especially the low energies, the measurements were repeated with the Markus plane parallel ionization chambers in a PMMA slab phantom. The results are given in Table II. These values are specified as depth in water. The scaling method proposed in the TRS-381 Code of Practice was used to calculate the corresponding depth in water.

TABLE Ib. DEPTH OF MAXIMUM DOSE DETERMINED WITH A PTW/MARKUS PLANE PARALLEL CHAMBER IN A WATER PHANTOM FOR A 10 × 10 FIELD AND SSD = 100 cm

Energy (MeV)	(R_{100}) Markus (mm)
4	8.4
6	12.2
8	16.0
10	19.8
12	26.0
15	27.3
18	29.4

TABLE II. DEPTH OF MAXIMUM DOSE DETERMINED WITH A PTW/MARKUS PLANE PARALLEL IONIZATION CHAMBER IN A PMMA SLAB PHANTOM

Energy (MeV)	R_{100} (mm water equiv)
4	9.0
6	12.6
8	17.0
18	30.0

Taking the spread of the results for the depth of dose maximum into account, it can be concluded that no significant difference was found between the values obtained with the ionization chambers in water and in PMMA. From these results it can be concluded that the proposed scaling procedure given in the TRS-381 protocol to convert the depth in a PMMA phantom to the depth in water is satisfactory. In low-energy electron beams where the dose maximum is only a few millimetres, measurements in water are difficult and the determination in a plastic phantom can be seen as a check of the water measurements. However, the plastic measurements are too laborious in clinical circumstances.

We conclude, under the assumption that the detector reading is proportional to absorbed dose to water, that in clinical practice the diode is the most practical detector. The diamond detector needs to be pre-irradiated to give accurate results. Ionization chamber measurements need multiple calculations (to include stopping power ratios and perturbation correction factors) to determine depth-dose values from measured ionization values.

2.2. Determination of the practical range R_p

The practical range is determined in a 14 cm × 14 cm field for an SSD of 100 cm. The results are shown in Table III.

TABLE III. PRACTICAL RANGE DETERMINED WITH DIFFERENT DETECTORS IN A WATER PHANTOM

Energy (MeV)	(R_p) Markus (mm)	(R_p) Roos (mm)	(R_p) diamond (mm)	(R_p) diode (mm)	(R_p) mean (mm)	σ (mm)
4	20.8	21.1	20.9	21.1	21.0	0.2
6	29.0	29.4	29.1	29.2	29.2	0.2
8	38.4	39.0	38.7	38.8	38.7	0.2
10	45.6	45.9	45.7	46.0	45.8	0.2
12	59.3	60.4	59.9	59.8	59.9	0.3
15	70.3	71.4	71.1	71.1	71.0	0.2
18	83.3	83.5	83.0	82.2	83.0	0.7

Similar conclusions can be drawn for these results as for the experimental determination of the depth of dose maximum.

2.3. Effective point of measurement of the PTW Markus ionization chamber

The effective point of measurement for a plane parallel ionization chamber is assumed to be situated in the center at the inner surface of the front window. TRS-381 has specified the properties for the recommended plane parallel ionization chambers. The chamber properties for the PTW/Markus chamber however deviate from these recommended values: the ratio of the diameter of the cavity to the height of the cavity is only 3 and the guard ring is too small.

We compared the values of maximum ionization at the depth and at half value depth, measured with both the PTW/Markus and the PTW/Roos plane parallel ionization chambers in a water phantom. The measured ionization values were corrected for polarity and recombination effects. Results are given in Tables IV and V.

Due to the cavity properties and the negligible guard ring which can introduce in-scattering via the side walls, an average shift of 0.5 mm (σ = 0.2 mm) of the effective point of measurement of the Markus ionization chamber from its front surface of the air volume towards the center of the air volume is measured by comparison with the PTW/Roos chamber.

2.4. Determination of R_{50}

For dosimetry purposes it is customary to specify the beam quality of an electron beam by the mean energy at the phantom surface. This parameter is required for the selection of different physical quantities and parameters used to calculate the absorbed dose, and is determined from empirical relationships between the mean energy and the parameter R_{50}.

We compared the values for R_{50}^J derived from an ionization curve measured with a plane parallel ionization chamber and given in Table V, and R_{50}^D the half value depth determined with a diode or a diamond detector. The measurements were performed using an SSD of 100 cm and a 14 × 14 field. The results are given in Table VI.

TABLE IV. SHIFT OF THE EFFECTIVE POINT OF MEASUREMENT OF THE PTW/MARKUS CHAMBER IN COMPARISON WITH THE PTW/ROOS CHAMBER BASED ON MEASUREMENTS AT THE DEPTH OF MAXIMUM IONIZATION

Energy (MeV)	R_{100}^{J} (Markus) (mm water)	R_{100}^{J} (Roos) (mm water)	shift = $z_{Markus} - z_{Roos}$
4	8.3	8.6	–0.3
6	11.5	12.1	–0.5
8	15.1	15.4	–0.3
10	18.2	19.0	–0.8
12	24.7	25.5	–0.8
15	26.5	26.9	–0.4
18	29.2	29.6	–0.4

TABLE V. MEASURED SHIFT OF THE EFFECTIVE POINT OF MEASUREMENT OF THE PTW/MARKUS CHAMBER IN COMPARISON WITH THE PTW/ROOS CHAMBER BASED ON HALF VALUE DEPTH

Energy (MeV)	R_{50}^{J} (Markus) (mm water)	R_{50}^{J} (Roos) (mm water)	Shift Markus – Roos
4	16.0	16.7	–0.7
6	22.5	23.1	–0.6
8	30.2	30.6	–0.4
10	36.4	36.9	–0.3
12	47.6	48.4	–0.8
15	56.9	57.2	–0.3
18	66.9	67.2	–0.4

TABLE VI. R_{50}^{J}, DERIVED FROM AN IONIZATION CURVE MEASURED WITH A PLANE PARALLEL IONIZATION CHAMBER AND R_{50}^{D}, THE HALF VALUE DEPTH DETERMINED WITH A DIODE OR A DIAMOND DETECTOR

Energy (MeV)	(R_{50}^{D}) diode (mm water)	(R_{50}^{D}) diamond (mm water)
4	16.5	16.7
6	23.2	23.3
8	31.0	31.1
10	37.2	37.5
12	49.1	49.3
15	58.2	58.5
18	69.2	68.9

The mean energy at phantom surface was calculated using the 2 polynomial expressions (10.3a) and (10.3 b) in TRS-381 depending on the use of R_{50} from ionization measurements or from a depth dose distribution. We obtained a difference up to 4% between the two calculated values of the mean energy at phantom surface. However, the maximum difference found in the s-ratios determined from these two values of the eman energy was only 0.4%, see Table VII. In conclusion, the difference in the absorbed dose using s-ratios based on Eo(J) and Eo(D) values is maximum 0.4%.

TABLE VII. INFLUENCE OF THE USE OF R_{50}^{J} AND R_{50}^{D} ON THE STOPPING POWER RATIOS AT THE DOSE MAXIMUM

Energy (MeV)	$\overline{E_0^J}$ (MeV)	$s_{w,air}$	$\overline{E_0^D}$ (MeV)	$s_{w,air}$	% difference
4	4.02	1.0917	4.11	1.0899	0.2
6	5.37	1.0837	5.55	1.0790	0.4
8	7.05	1.0714	7.25	1.0684	0.3
10	8.41	1.0677	8.62	1.0644	0.3
12	10.93	1.0503	11.30	1.0476	0.3
15	13.12	1.0291	13.62	1.0247	0.4
18	15.55	1.0144	15.84	1.0132	0.1

3. Determination of the h_{m} factor for PMMA (1998)

Water is the preferred medium to determine the absorbed dose. However, for low energy beams due to position uncertainties, some protocols often suggest the use of plastic phantoms. Ideally, a plastic phantom should be water-equivalent i.e. should have the same linear collision stopping power and linear scattering power as water. If the phantom is not water-equivalent the ranges and depths must be scaled to the water equivalent depths. Besides, a fluence correction factor converts the ionization measured in the plastic to the ionization in water. This fluence correction factor is experimentally determined as the ratio of the measured ionization in the water phantom to that in the plastic phantom at the corresponding reference depth.

We have determined this factor for PMMA with the PTW/Markus and the PTW/Roos plane parallel ionization chambers. Measurements were performed in a 14 cm × 14 cm field at the depth of maximum dose in water and in PMMA using a fixed SSD The Markus chamber is fitted with a 1 mm thick PMMA cap during the measurements in water. Temperature and pressure were monitored throughout the measurements and the readings were converted to a common temperature for both phantoms. The equivalent water depth in PMMA is calculated with the scaling procedure of TRS-381. The reproducibility of the measurement conditions is very important but is difficult for the lowest energies.

The results are presented in Fig. 1. The indicated uncertainty is equal to one standard deviation on several measurements. Values of h_{m} for the Markus chamber were obtained with three different chambers, showing no significant chamber-to-chamber differences.

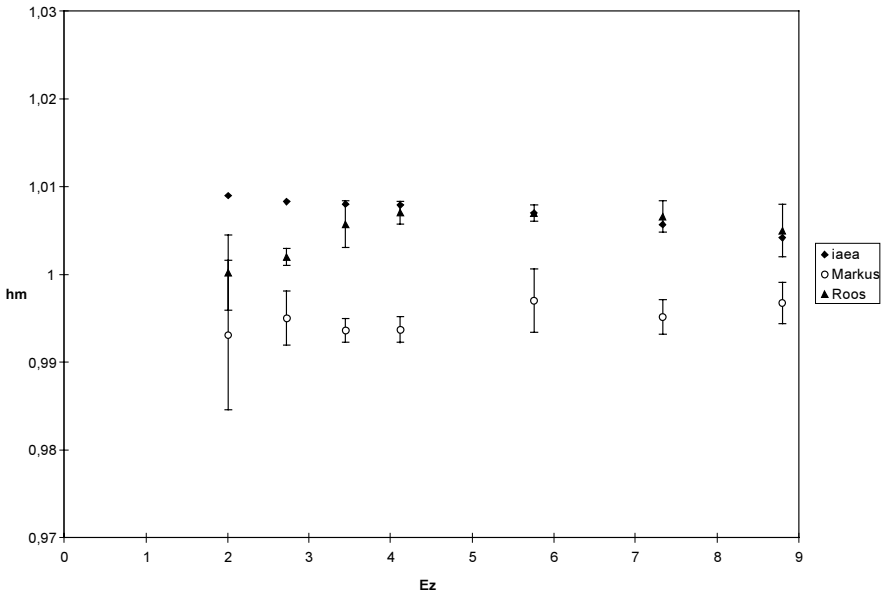

FIG. 1. Experimental h_m factors compared to the values from the TRS-381 protocol.

It can be concluded that the values measured with the PTW/Roos ionization chamber are in agreement with the protocol, except for the lower energies.

The values resulting from the measurements with the PTW/Markus chamber are up to 1.7% lower than the values of the protocol. These results show that we have to consider perturbation effects in different phantom materials, and that these differences are dependent on the type of the chamber. Measurements with three different Markus chambers revealed no chamber to chamber variations.

4. Calibration of plane parallel ionization chambers

Since previous protocols for electron dosimetry did not include enough details for the calibration procedures of plane parallel chambers, the TRS-381 Code of Practice was published in 1997 as a complement and extension of TRS-277. It describes how to calibrate therapeutic electron beams specifically with plane parallel chambers. Different options for calibrating plane parallel chambers are also given.

4.1. Calibration against a cylindrical chamber in a high-energy electron beam

The TRS-381 Code of Practice is strongly recommending the calibration of a plane parallel chamber in a high-energy electron beam against a reference ionization chamber with known calibration factor. With this method, both chambers are alternatively positioned at the reference depth in a phantom. The calibration factor for the plane parallel chamber is obtained from equating the absorbed doses obtained with the two chambers.

The energy of the electron beam should be as high as possible to minimize the cavity perturbation effect of the reference cylindrical chamber – ρ_{cav} should be within 2% of unity. For a Farmer type chamber with an internal radius of approximately 3 mm the mean energy at the phantom surface should be higher than 15 MeV. In electron beams, the effective point of measurement for a cylindrical chamber is taken at 0.55r (r = internal radius) from the center towards the source.

We have determined the $N_{D,air}$ calibration factor of the PTW/Markus and the PTW/Roos plane parallel ionization chambers in the electron beam with a nominal energy of 18 MeV. The calibrations were performed with an NE2571 and a PTW-30001 cylindrical chamber in a water phantom. The N_K calibration factors for these cylindrical chambers were determined at the Standard Dosimetry Laboratory of the University of Ghent. The effective point of measurement for the chambers was placed at the depth of maximum dose. The field size was 14 cm × 14 cm and SSD was 100 cm. The mean energy at the phantom surface was 15.8 MeV. This results in a ρ_{cav} for the cylindrical chamber of 0.977 [6].

For the Markus chamber a calibration factor $N_{D,air}$ = 0.476 ± 0.003 cGy/reading was obtained. The uncertainty is the standard deviation on different measurements. The calibration factor determined in the electron beam of the Roos chamber was 0.0707 ± 0.0003cGy/reading.

4.2. Calibration in a ^{60}Co beam free in air

4.2.1. The N_K calibration factor

The air kerma calibrations were again performed in ^{60}Co at the Standard Dosimetry Laboratory of the University of Ghent. The calibration in-air method in a ^{60}Co beam gives the N_K calibration factor. The plane parallel chamber with appropriate build-up material is placed free in air in a ^{60}Co beam with its center positioned where K_{air} is known. The calculation of $N_{D,air}$ from N_K requires the correction factors $k_{att}\,k_m$, since $N_{D,air}$ is derived from the N_K calibration factor using the relation $N_D = N_K\ (1\text{-}g)\ k_{att}\,k_m$. Since the calibrations were performed with the same set-up as for the N_K determination of the NE 2571 chamber in the previous method, any differences in $N_{D,air}$ values for the plane parallel chambers are due to inconsistent values of $k_{att}\,k_m$ and ρ_Q for the plane parallel and cylindrical ion chambers.

For the Markus chamber, $k_{att}\,k_m$ = 0.985 when calibrated with 4.2 mm PMMA as build-up (TRS-381). We obtained $N_{D,air}$ = 0.480 ± 0.002 cGy/reading. Using $k_{att}\,k_m$ = 0.993 for the calibration with 0.54 g cm^{-2} graphite build-up as proposed in the protocol for electron dosimetry published by the Netherlands Commission on Radiation Dosimetry, the $N_{D,air}$ factor has the same value; this shows consistency in the $k_{att}\,k_m$ values for this type of chamber.

4.2.2. Experimental determination of $k_{att}\,k_m$ for the PTW/Roos chamber

Knowing $N_{D,air}$ for a certain chamber from the calibration in a high-energy electron beam and knowing its in-air calibration factor $N_{K,}$ the value of $k_{att}\,k_m$ for this chamber could be derived.

For the PTW/Roos chamber, this results in $k_{att}\,k_m$ = 0.974 when the chamber is calibrated in the ^{60}Co beam with an additional build-up of 4.2 mm PMMA and using a PMMA insert piece in the back of the chamber. This value is in close agreement with the value found by Nilsson and Johansson [5] ($k_{att}\,k_m$ = 0.978), who also used the PMMA insert (Nilsson, personal communication). Their $k_{att}\,k_m$ value was experimentally determined with a large plane parallel chamber simulating the walls of the Roos chamber.

4.3. Calibration in a ^{60}Co beam in phantom

This calibration was performed in the Standard Dosimetry Laboratory of the University of Ghent. When the plane parallel chamber is calibrated in a phantom in a ^{60}Co beam, the chamber is compared with an air-calibrated reference chamber with known $N_{D,air}^{ref}$. The main

uncertainty when using this method is the wall perturbation factor p_{wall}^{pp}. The absorbed dose to water is determined with a cylindrical chamber NE 2571 with its center at 5 cm depth. The data for the cylindrical chamber in the ^{60}Co beam were calculated according to, or taken from, TRS-381, including the effect of a 0.5 mm thick waterproofing sleeve. This results in a total conversion factor $C_{w,Q} = 1.088$ in the overall expression for the absorbed dose determination $D_w = M N_K C_{w,Q}$.

The center of the front surface of the plane parallel chamber cavity is positioned at 5 cm depth in the water phantom, taking into account the water equivalent thickness of the front window. The field size at the measuring point was 12 cm × 12 cm. The $N_{D,air}$ calibration factors of the PTW/Markus and the PTW/Roos plane parallel ionization chambers are obtained by equating the absorbed doses for the two chambers. The correction factor p_{wall}^{pp} for the plane parallel chambers must be known. Because this factor is introducing the major source of uncertainty in this procedure, the electron beam method is recommended for the calibration of plane parallel chambers. Following this procedure, an $N_{D,air}$ calibration factor of 0.478 ± 0.003 cGy/reading is obtained for the Markus chamber which is in agreement with the value determined in the electron beam. However, the $N_{D,air}$ calibration factor obtained for the Roos chamber equals 0.0719 ± 0.0002 cGy/reading and differs by 1.7% from the factor obtained with the electron beam method. This indicates that the value of $p_{wall}^{pp} = 1.003$, assumed in TRS-381 for the Roos chamber, is too low.

4.4. The $N_{D,w}$ calibration factor of plane parallel chambers

The $N_{D,w,Co}$ calibration factor for the plane parallel chambers was determined in a ^{60}Co beam against the absorbed dose to water standard of the Standard Dosimetry Laboratory of the University of Ghent. The plane parallel chambers were calibrated against the average dose response of three NE 2571 transfer chambers that were calibrated directly against the water calorimeter. The design and performance of this water calorimeter have been described by Seuntjens and Palmans [7].

For the Markus chamber, $N_{D,w,Co}$ was 0.5443 Gy/nC and for the Roos chamber $N_{D,w,Co}$ was 0.08139 Gy/nC. The response of the water calorimeter in the ^{60}Co beam was 0.4% lower than the dose to water measured with the NE 2571 ion chamber based on an air kerma calibration factor and applying TRS-381, as described in the previous section. It should be noticed that the Belgian absorbed dose to water standard is 0.55% lower than BIPM whereas the air kerma standard is higher than BIPM by the same amount; these differences should be takedsdn into account to interprete the difference between the two methods, based on $N_{D,w}$ and N_K calibration factors.

This calibration method provides an in-water calibration factor $N_{D,w}^{pp}$ from which the in-air calibration factor could be derived through the relation $N_{D,w}^{pp} = N_{D,air}^{pp} (s_{w,air})_Q \rho_Q$, with Q being the user's beam quality. However, the $N_{D,w}$ calibration factor is intended to be used with an $N_{D,w}$ based dosimetry formalism only, as described in Section 6 of TRS-381.

4.5. Calibration based on the Fricke dosimeter

If the absorbed dose to water can be determined in an electron beam with the Fricke dosimeter, another method to calibrate an ionization chamber is introduced. It is possible to derive the $N_{D,w,E}$ factor for a chamber by equating the dose to water determined with the Fricke dosimeter and with the plane parallel chamber using TRS-381.

We determined the dose with the Fricke dosimeter in an 18 MeV electron beam. Specifications of the cells and the Fricke dosimeter system are described later on. An εG value of 351.5×10^{-6} m^2 kg^{-1} Gy^{-1} has been used, which is the value recommended by Svensson and Brahme [8]. The value of εG that results from calibration against the water calorimeter of the Standard Dosimetry Laboratory of Ghent is 350.3×10^{-6} m^2 kg^{-1} Gy^{-1}, which is 0.34% lower. Ionometric and Fricke measurements were performed in water. The $N_{D,air}$ factors of the PTW/Markus and the PTW/Roos plane parallel chambers calculated using the relationship $D_{Fricke} = N_{D,w,E} \times M^{pp}$ are in agreement with those obtained in a high-energy electron beam comparing against a reference ionization chamber with a known calibration factor.

Table VIII summarizes the results for the $N_{D,air}$ factors of the PTW/Markus and the PTW/Roos plane parallel chambers.

Agreement within 0.5% was obtained between the $N_{D,air}$ factors of the Markus chamber.

Fricke measurements in the 18 MeV beam confirm the results for the calibration factors of both plane parallel chambers, the Markus and the Roos, based on the comparison with a Farmer chamber in an electron beam.

For the Roos chamber, the $N_{D,air}$ cannot be derived from N_K because of lack of the $k_{att}k_m$ value in the TRS-381 protocol. A discrepancy of 1.7% is found between the $N_{D,air}$ factor of the PTW/Roos chamber when calibrated in water in a ^{60}Co beam and the $N_{D,air}$ determined in an electron beam. This difference is focusing on the uncertainty in the wall perturbation factor ρ_{wall} for this type of chamber in a ^{60}Co beam.

TABLE VIII. $N_{D,air}$ VALUES FOR THE PTW/MARKUS AND THE PTW/ROOS IONIZATION CHAMBERS DETERMINED FOLLOWING DIFFERENT METHODS SPECIFIED IN THE TRS-381 PROTOCOL

	PTW/Markus	PTW/Roos
$N_{D,air}$ derived from N_K	0.480 (0.002)	–
$N_{D,air}$ determined in an electron beam against a cylindrical chamber	0.476 (0.003)	0.0707 (0.003)
$N_{D,air}$ determined in a water phantom in ^{60}Co	0.478 (0.003)	0.0719 (0.0002)
$N_{D,air}$ derived from Fricke measurements in water in the 18 MeV electron beam	0.471 (0.003)	0.0705 (0.0003)

5. Absolute dosimetry in PMMA with plane parallel chambers compared with Fricke dosimetry

We have determined the absorbed dose to water from measurements in a PMMA phantom with the Markus and the Roos chamber in the electron beams of a Philips SL18 accelerator. Ionometry was performed following the specifications of the TRS-381 Code of Practice and compared with the dose values obtained with an independent dosimetry system, the Fricke dosimeter.

The measurements were performed in a PMMA slab phantom at the reference depth, which was for these beams the depth of maximum dose. The field size was 10 cm × 10 cm. The recombination correction factor for the Markus chamber was less than 0.5%. The polarity correction factor was less than 1%. The Roos chamber showed a negligible polarity effect (<0.2%) and the recombination correction was less than 0.5%.

The ferrous sulphate cells, made of PMMA, were cylindrical in shape with outer diameter 40 mm, inner diameter 35 mm and total thickness 4 mm. The irradiation was carried out with the cell axis parallel to the beam axis. The mean absorbed dose to the dosimeter solution is deducted from a spectrophotometric measurement of the difference in absorbance between the irradiated and the unirradiated solution. The technique is described in the ICRU Report No. 35 [3]. For all electron beams, an εG value of 351.5×10^{-6} m^2 kg^{-1} Gy^{-1} was used. The dose to the ferrous sulfate solution was converted to the dose to water using a constant mass stopping power ratio $s_{w,Fricke} = 1.004$ (ICRU 35).

The ionometric dose values are calculated following the procedures and correction factors of the TRS-381 Code of Practice. The $N_{D,air}$ calibration factor was based on the calibration of the chamber in the high-energy electron beam. Similar experiments were performed with the PTW/Roos chamber.

Figures 2 and 3 give the ratio of the dose to water determined with the plane parallel ionization chambers to the dose determined with the Fricke dosimeter. The indicated uncertainties for the Fricke measurements, and they correspond to one standard deviation, obtained between repeated readings of the absorbance of the irradiated solution.

The results reveal good agreement, within the experimental uncertainty, between the dose values obtained ionometrically using the TRS-381 Code of Practice, and the Fricke values.

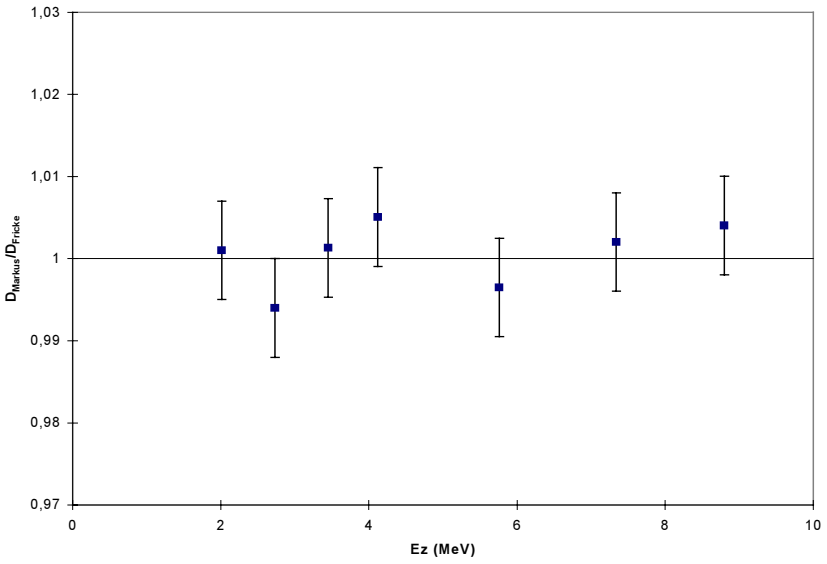

FIG 2. Ratios of the absorbed dose to water in electron beams, determined in a PMMA phantom, obtained with a PTW/Markus chamber (based on TRS-381 [1]) and with Fricke dosimetry.

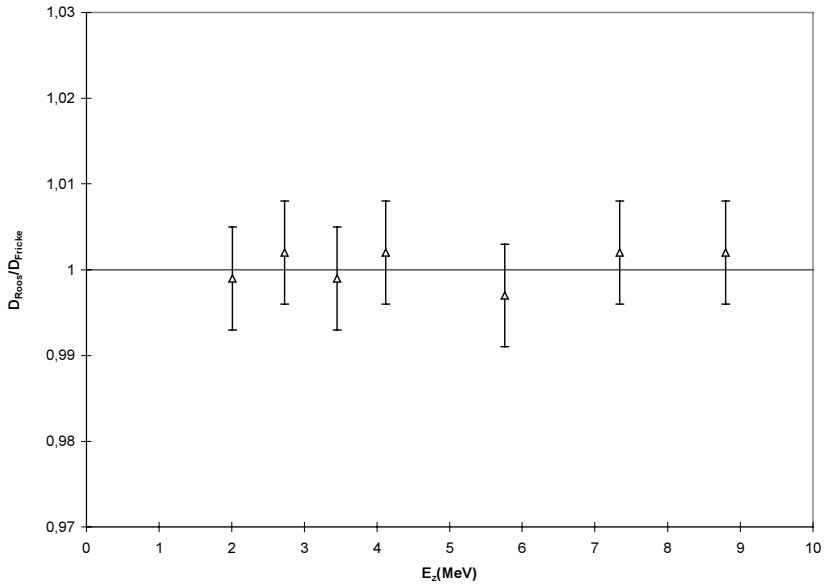

FIG 3. Ratios of the absorbed dose do water in electron beams, determined in a PMMA phantom, obtained with a PTW/Roos chamber (based on TRS-381 [1]) and with Fricke dosimetry.

6. Conclusions

For relative dosimetry, agreement within the statistical uncertainty was obtained in the present work between the values for R_{100}, R_{50} and R_p using a diode, a diamond and plane parallel chambers. [1]

Due to cavity properties and the small guard ring, the effective point of measurement of the Markus chamber is shifted towards the center of the air volume. This shift of 0.5 mm was determined by comparison of the depth-ionization distributions measured with the Markus and the Roos chambers.

It is recommended to use a water phantom to determine the absorbed dose in an electron beam to minimize uncertainties, which are present when using a plastic phantom. These uncertainties arise from depth scaling, charge storage problems and the fluence ratios which are expressed through the h_m factors. These factors were determined for PMMA with the Roos and the Markus chamber, and the values obtained with the Roos chamber are in agreement with the protocol, except at the lower energies ($\overline{E_z}$ <3 MeV). Regarding the results of the Markus chamber, h_m is 1–1.5% lower than the recommended values. These results show the dependence of the fluence correction factor on the type of chamber which is used for its determination. [2]

For the calibration of a plane parallel chamber and the determination of $N_{D,air}$, TRS-381 strongly recommends the use of the method that is based on a comparison with a cylindrical chamber in a high-energy electron beam performed in a water phantom.

[1] Note added by reviewers. The results may, however, depend on the type of diode, as differences in ranges of up to 1 mm have been reported in the literature.

[2] Note added by reviewers. It should be noticed that the experimental conditions to determine h_m in this work are different from the settings adapted after a meeting in 1998, which have been used in all the other contributions of this report.

The agreement between the $N_{D,air}$ factors determined with different methods was within 0.5% for the Markus chamber. On the other hand, a discrepancy of 1.7% was found between the $N_{D,air}$ factor of the Roos chamber when calibrated in water in a ^{60}Co beam and that determined in an electron beam. Fricke measurements in water confirm the electron method for calibration of both chambers.

Dose values determined in PMMA with Fricke and with plane parallel chambers following the procedures and recommendations of the TRS-381 protocol agree within 1%.

REFERENCES

[1] INTERNATIONAL ATOMIC ENERGY AGENCY, The Use of Plane Parallel Ionization Chambers in High Energy Electron and Photon Beams — An International Code of Practice for Dosimetry, Technical Reports Series No 381, IAEA, Vienna (1997).

[2] VAN DER PLAETSEN, A., SEUNTJENS, J., THIERENS, H., VYNCKIER, S., Verification of absorbed dose determined with thimble and parallel-plate ionization chambers in clinical electron beams using ferrous sulfate dosimetry, Med. Phys. **21** (1994) 37.

[3] INTERNATIONAL COMMISSION ON RADIATION UNITS AND MEASUREMENTS, Radiation Dosimetry: Electron Beams with Energies Between 1 and 50 MeV, ICRU Report 35, ICRU, Bethesda, MD (1984).

[4] NCS, Code of Practice for the dosimetry of high-energy electron beams, Nederlandse Commissie voor Stralingsdosimetrie, NCS Report No. 5, Bilthoven, Netherlands (1989).

[5] NILSSON, JOHANSSON, Comparison of three methods to calibrate plane parallel ionization chambers according to the IAEA TRS-381 Protocol, Abstract World Congress on Medical Physics and Biomedical Engineering, Nice (1997).

[6] JOHANSSON, K.A., MATTSSON, L.O., LINDBORG, L., SVENSSON, H., "Absorbed-dose determination with ionization chambers in electron and photon beams having energies between 1 and 50 MeV", National and International Standardisation of Radiation Dosimetry (Proc. Symp. Atlanta, 1977), Vol. 2, IAEA, Vienna (1978) 243.

[7] SEUNTJENS, J.P., PALMANS, H., The University of Ghent sealed water calorimeter: construction, correction factors and performance at ^{60}Co gamma rays, Phys. Med. Biol. **44** (1999) 627–646.

[8] SVENSSON, H., BRAHME, A., Ferrous sulfate dosimetry for electrons. A re-evaluation, Acta Radiol. Oncol. **18** (1979) 326–336.

PROCEDURES FOR THE SELECTION OF STOPPING POWER RATIOS FOR ELECTRON BEAMS: COMPARISON OF IAEA TRS PROCEDURES AND OF DIN PROCEDURES WITH MONTE CARLO RESULTS

M. ROOS
Physikalisch-Technische Bundesanstalt,
Braunschweig, Germany

G. CHRIST
Radiologische Universitätsklinik, Abt. Med. Physik,
Universität Tübingen,
Tübingen, Germany

Abstract

In the International Code of Practice IAEA TRS-381 the stopping power ratios water/air are selected according to the half-value depth and the depth of measurement. In the German Standard DIN 6800-2 a different procedure is recommended, which, in addition, takes the practical electron range into account; the stopping power data for monoenergetic beams from IAEA TRS-381 are used. Both procedures are compared with recent Monte Carlo calculations carried out for various beams of clinical accelerators. It is found that the DIN procedure shows a slightly better agreement. In addition, the stopping power ratios in IAEA TRS-381 are compared with those in DIN 6800-2 for the reference conditions of the beams from the PTB linac; the maximum deviation is not larger than 0.6%.

1. Introduction

Stopping power ratios water/air for clinical electron beams (for instance in the IAEA International Code of Practice TRS-381 [1]) are usually selected according to the parameters of half-value depth and depth of measurement, from ratios which have been calculated for monoenergetic beams.

An experimental investigation by Johansson and Svensson [2] of the energy dependence of response of plane parallel chambers at different types of accelerators shows that the stopping power ratios may vary by a few percent, depending on the accelerator type and the beam-defining system, if only the two parameters mentioned are used. The investigations show, however, that this selection may be improved if the practical range is taken into account in addition.

In IAEA TRS-277 [3] this has been accomplished by scaling the depth with the measured practical range and the calculated range for monoenergetic electrons. Since the results are not convincing, this procedure is no longer recommended in IAEA TRS-381 [1]. The German Standard DIN 6800-2 [4] recommends a different procedure, the “virtual initial energy method” [5]. It takes the energy and angular spread of the clinical electron beam into account in approximation by using a higher “virtual energy” of monoenergetic electrons which — after traversing an additional water layer — yield the same mean energy and the same practical range as measured for the actual beam at the phantom surface. This allows the stopping power ratios for monoenergetic electrons to be used (they are taken from IAEA TRS-381 [1]), which are calculated from the half-value depth, the practical range and the depth of measurement. It is obvious that this is a crude approximation, simulating the energy loss straggling, the generation of bremsstrahlung, etc. of a complex treatment-head by the respective degradation caused by a water layer. It allows, however, the incident beam to be characterized in addition by its practical range on the basis of a well-defined physical model, and it enables, nevertheless, to use the data for monoenergetic beams.

2. Results and discussion

2.1. Selection procedures

The accuracy of the selection procedures could best be checked if results from a variety of different accelerator types were available. Experimental data are, however, scarce. But recent work by Ding et al. [6] also allows the procedures to be checked. Ding et al. have numerically simulated clinical accelerators, including their beam defining systems, by means of the Monte Carlo Method. In addition, they have simulated the beam degradation within the water phantom and they have calculated the resulting depth dose distributions and the corresponding stopping power ratios water/air, with and without the influence of the electrons liberated by the contaminating photons from the treatment head.

Starting from the calculated depth dose distributions, the virtual initial energy method of DIN 6800-2 and the commonly used selection according to the half-value depth and the depth of measurement (as included in IAEA TRS-277 [3] and IAEA TRS-381 [1]) have been applied to all accelerators and beams investigated in [6]. The practical ranges and the half-value depths have been determined, and from the latter the mean energies at the phantom surface have been calculated. For the energy-range relationship the data of IAEA TRS-277 (Table IV) have been used, which form the basic of both, DIN 6800-2 and IAEA TRS-381. The values obtained serve as input parameters for the selection of stopping power ratios.

The accuracy of the selection does not essentially depend on the data set of stopping power ratios used, i.e., it does not matter whether the new set of IAEA TRS-381 is used or the set of IAEA TRS-277. Since the results given in the paper by Ding et al. [6] have been obtained using the same set of stopping power ratios as included in IAEA TRS-277, these data have also been chosen to check of the selection procedures in order to make a consistent comparison possible.

Figures 1–5 show the results for different beams of various accelerators.

The stopping power ratios calculated by Ding et al. [6] (“MC”), with the influence by contaminating photons (“electrons and photons”) and without this influence (“electrons only”), divided by the stopping power ratio according to the virtual initial energy method (“DIN”), have been plotted as a function of depth. The respective quotients for the stopping power ratios according to TRS-381 (“IAEA”) have also been included. It turns out that the virtual initial energy method usually makes a slight improvement in the selection of stopping power ratios in comparison with the method commonly used. This does not, however, hold for the narrow spectral distributions of the microtron beams, which are, however, not very common in clinical practice.

The virtual initial energy method takes contaminating photons from the treatment head into account only to a minor extent because, in the “additional water layer”, far less bremsstrahlung causing low energy electrons in the phantom, is produced than in a real treatment head. Correction for this influence should therefore in principal further improve the DIN results. Figures 1–5 show that this correction should amount to about 0.5% at most in the vicinity of the depth of maximum dose rate. The agreement between the DIN results and the Monte Carlo results is, however, not in all cases improved if this correction by a few tenths of a percent is applied to the DIN results. It must be borne in mind that, for instance, the uncertainties of the fit, included in the DIN Standard to facilitate the application of the virtual initial energy method, are in many cases comparable to the magnitude of the correction. In beams containing a large component of contaminating photons, however, the results may be essentially improved by the respective correction.

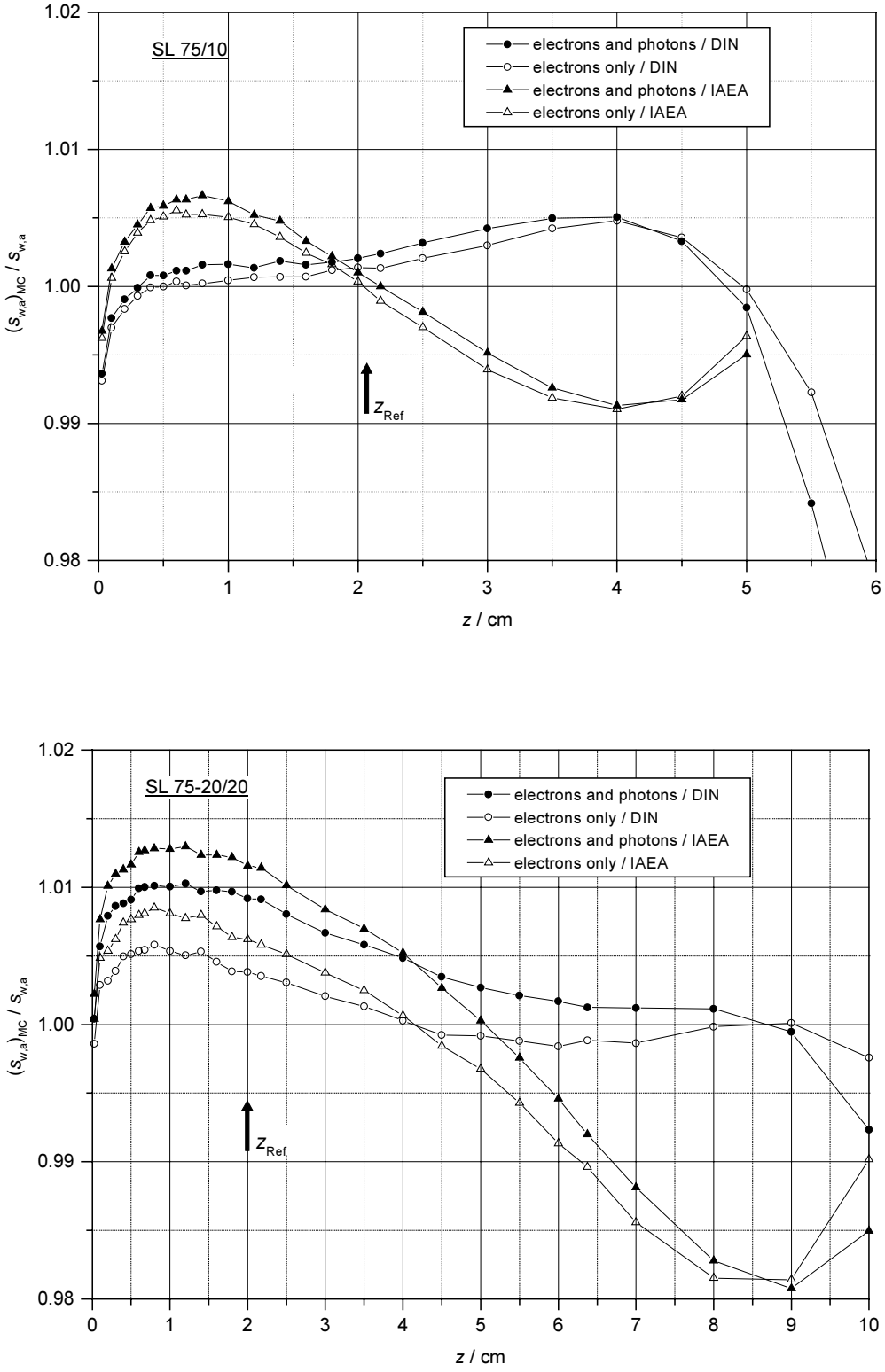

FIG. 1. Stopping power ratios water/air determined by Ding et al. [6] $(s_{w,a})_{MC}$*, with and without the influence of contaminating photons ("electrons and photons" and "electrons only" respectively), divided by the stopping power ratio* $s_{w,a}$ *according to IAEA TRS-381 and DIN recommendations as a function of depth z for different beams of a SL75 accelerator.*

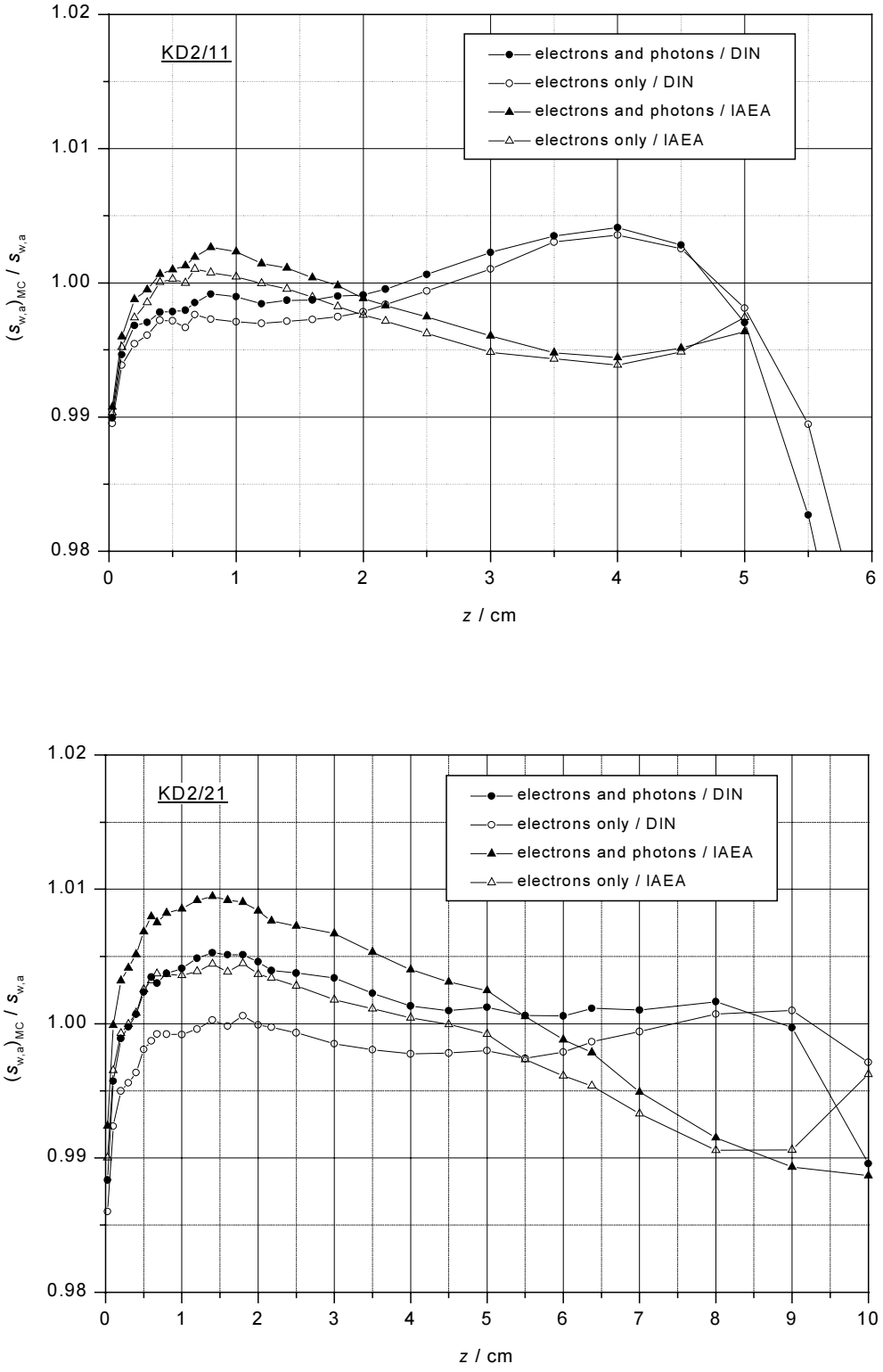

FIG.2. Stopping power ratios water/air determined by Ding et al. [6] $(s_{w,a})_{MC}$*, with and without the influence of contaminating photons ("electrons and photons" and "electrons only" respectively), divided by the stopping power ratio* $s_{w,a}$ *according to IAEA TRS-381 and DIN recommendations as a function of depth z for different beams of a KD2 accelerator.*

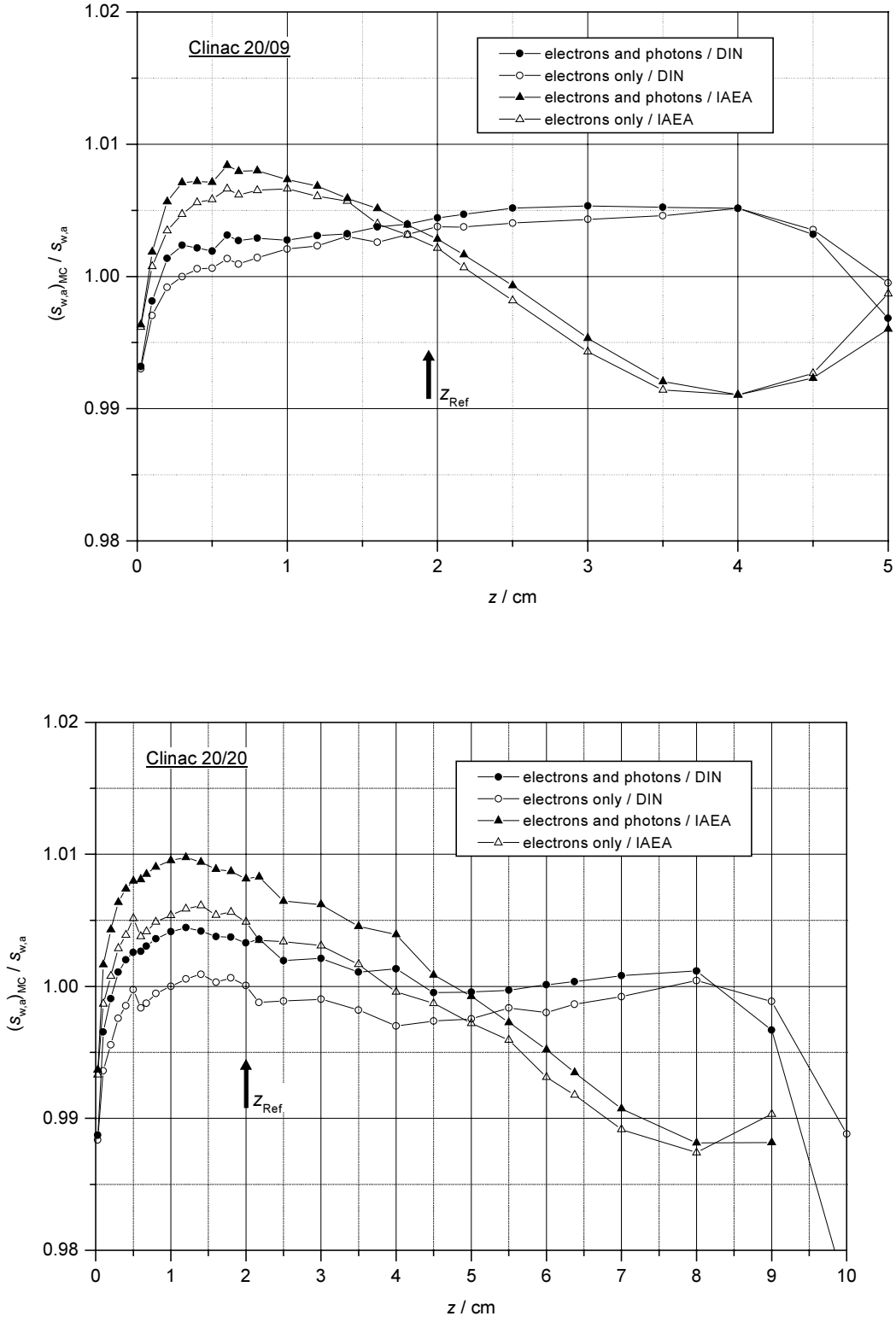

FIG.3. Stopping power ratios water/air determined by Ding et al. [6] $(s_{w,a})_{MC}$*, with and without the influence of contaminating photons ("electrons and photons" and "electrons only" respectively), divided by the stopping power ratio* $s_{w,a}$ *according to IAEA TRS-381 and DIN recommendations as a function of depth z for different beams of a Clinac 20 accelerator.*

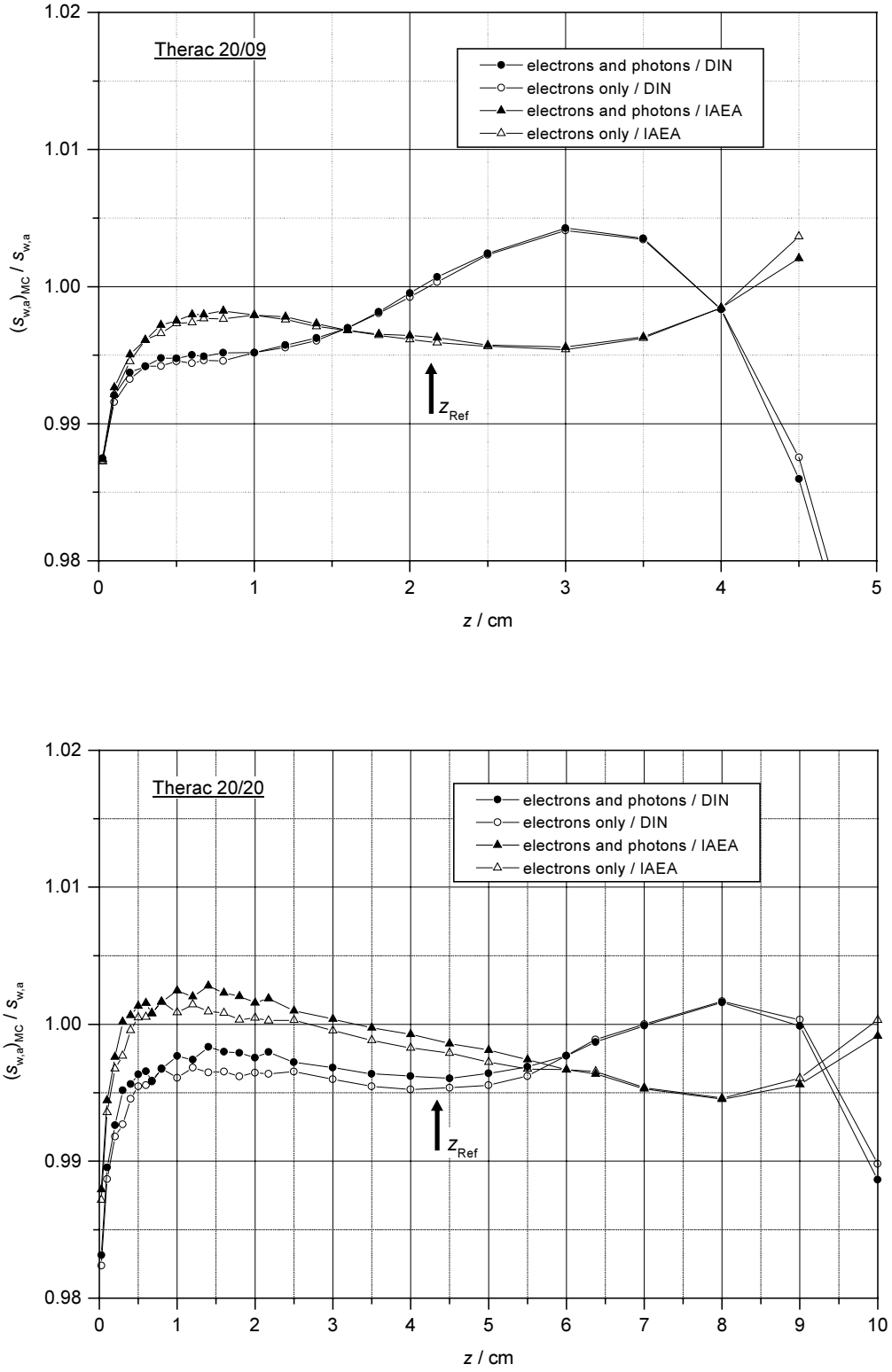

FIG.4. Stopping power ratios water/air determined by Ding et al. [6] $(s_{w,a})_{MC}$, with and without the influence of contaminating photons ("electrons and photons" and "electrons only" respectively), divided by the stopping power ratio $s_{w,a}$ according to IAEA TRS-381 and DIN recommendations as a function of depth z for different beams of a Therac 20 accelerator.

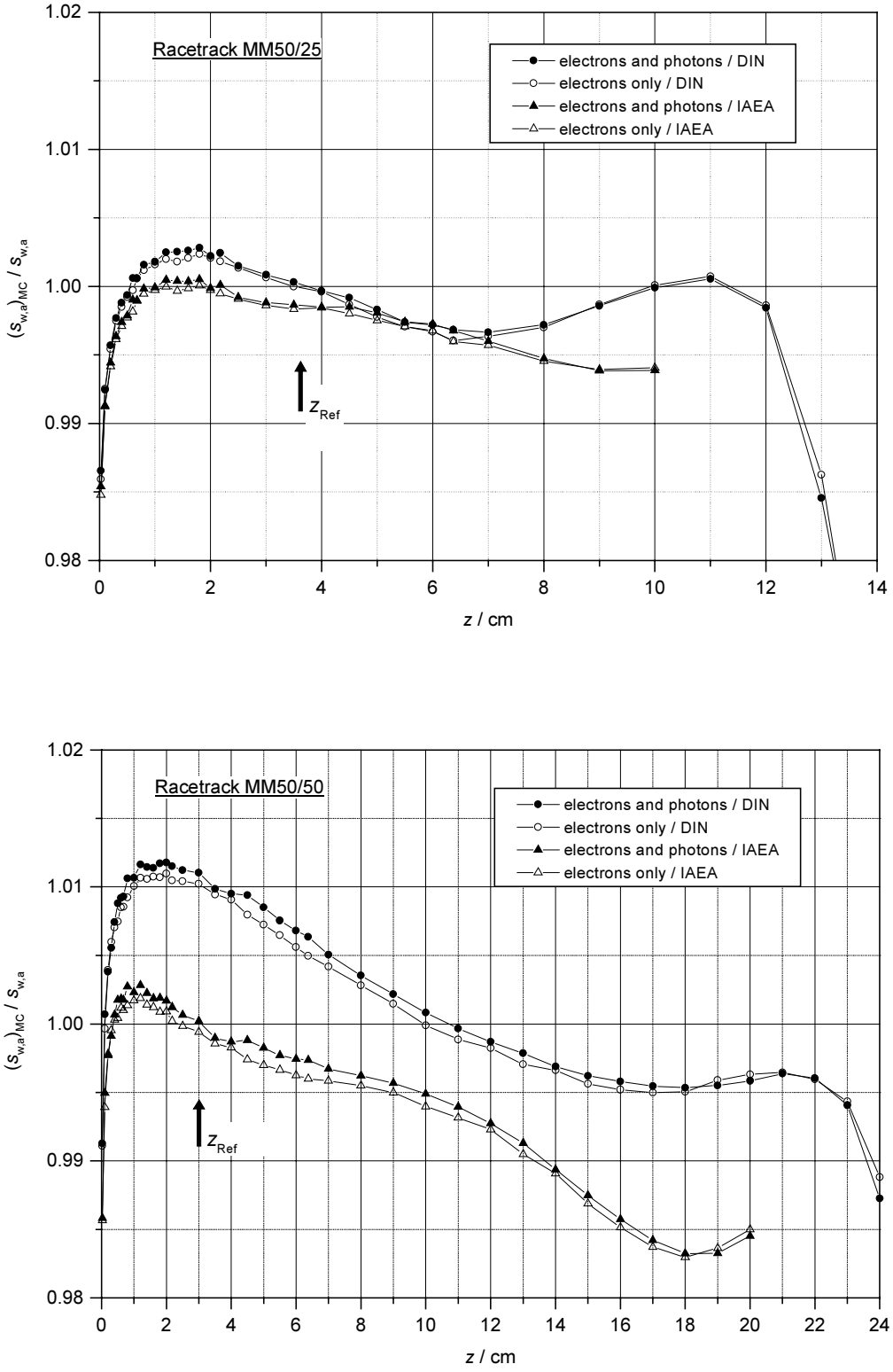

FIG.5. Stopping power ratios water/air determined by Ding et al. [6] $(s_{w,a})_{MC}$, with and without the influence of contaminating photons ("electrons and photons" and "electrons only" respectively), divided by the stopping power ratio $s_{w,a}$ according to IAEA TRS-381 and DIN recommendations as a function of depth z for different beams of a Racetrack MM50 accelerator.

2.2. Influence of the energy-range relationship

The IAEA Code of Practice TRS-381 and the Standard DIN 6800-2 recommend the use of the energy-range relationships to determine the mean energy at the phantom surface from half-value depths of absorbed dose and ionization distributions, which have already been included in NACP (1980) and in IAEA TRS-277 (Table IV).

In TRS-381, the table is replaced by formulae fitted to the data (second-order polynomials) for the whole range of energies from 1 MeV up to 50 MeV. In DIN 6800-2, the table is reproduced, and fitted formulae (second-order polynomials) for a restricted energy range from 3 MeV up to 35 MeV are recommended in addition.

Depth-ionization and absorbed dose distributions have been determined for the beams of the PTB SL 75-20 linac and the different formulae have been applied. Figure 6 (upper part) shows the deviation of the resulting energies from the "original results" according to IAEA TRS-277. The results based on the formulae of IAEA TRS-381 deviate by less than 3% and those based on the formulae of DIN 6800-2 deviate by not more than 1% from the original results.

Figure 6 (middle part) shows the resulting deviations of the stopping power ratios at the reference depths if the stopping power ratios are selected according to IAEA TRS-381 using these different energy values. The dose deviations caused by the deviations of the fitted formulae from the original data are within about 0.2% for the IAEA TRS-381 polynomials and within 0.1% for the DIN polynomials.

Figure 6 (lower part) shows that the resulting stopping power ratios according to DIN (virtual initial energy method, DIN polynomial) differ by less than 0.6% from the results according to IAEA TRS-381. The deviation caused by the different selection procedures amounts to 0.8% at most. It is, however, decreased by about 0.2% due to the deviating polynomials used to determine the mean energies.

3. Conclusions

The selection of stopping power ratios according to DIN 6800-2 [4], also taking account of the practical range, constitutes a slight improvement compared with the IAEA TRS-381 [1] procedure if the Monte Carlo results obtained by Ding et al. [6] are used as a reference.

In order to draw definite conclusions, experimental results (obtained using, for example, Fricke dosimeters) from different clinical accelerators would be extremely valuable. The most comprehensive set of data is still that obtained by Johansson and Svensson in investigations of the energy-dependence of the response of plane parallel chambers at different types of clinical accelerators [2]. Since that time, however, various new accelerator types have been put on the market.

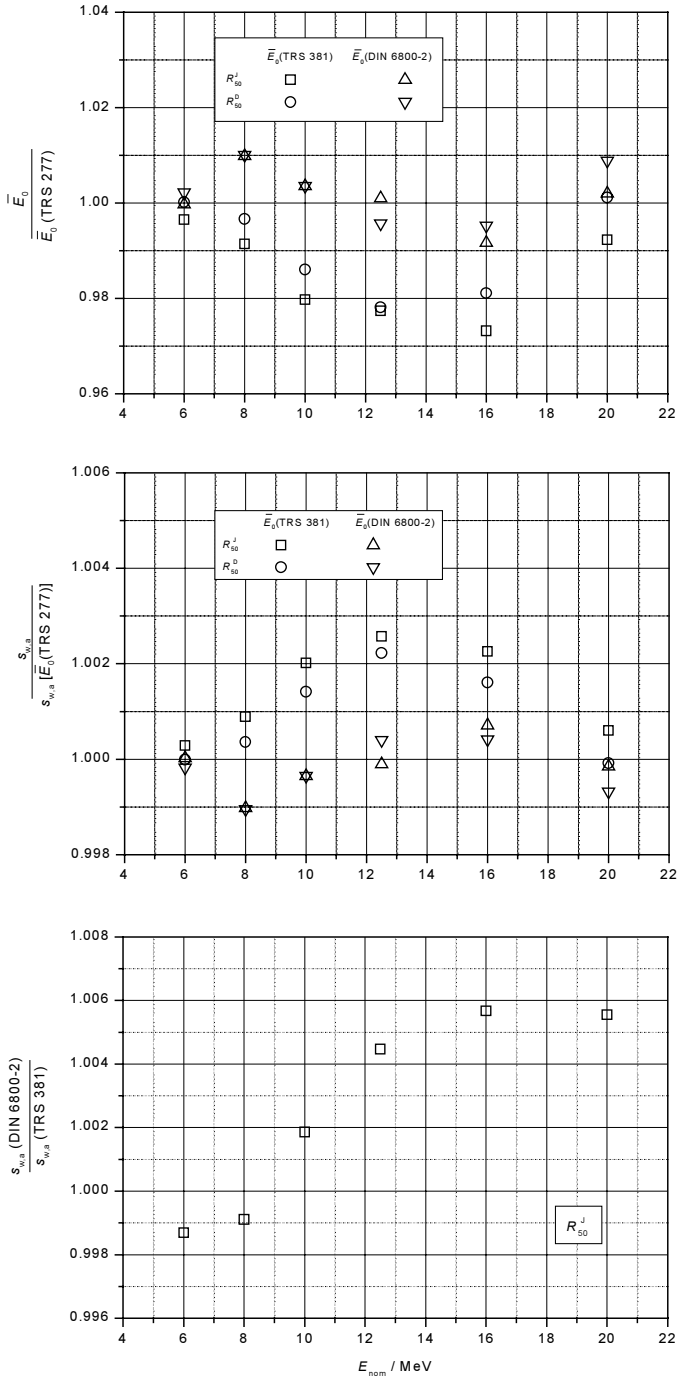

FIG. 6. UPPER PART: Mean energies $\overline{E}_0$ at the phantom surface using the fit formulae to the IAEA TRS-277 data for half-value depths from depth ionization R_{50}^J and depth absorbed dose R_{50}^D distributions as recommended in IAEA TRS-381 and in DIN 6800-2, divided by the energies according to the original data of TRS-277 for the beams of an SL 75-20 linac. MIDDLE PART: Resulting deviations of the stopping power ratios $s_{w,a}$ at the reference depths, if the stopping power ratios are selected from IAEA TRS-381 using the different energy values from Figure 2. The deviations are within about 0.2% for the IAEA TRS-381 polynomials and within 0.1% for the DIN polynomials LOWER PART: Stopping power ratios $s_{w,a}$ according to DIN 6800-2 (virtual initial energy method, DIN polynomial) divided by the corresponding ratios of IAEA TRS-381 at the reference depths for the beams of an SL 75-20 linac.

REFERENCES

[1] INTERNATIONAL ATOMIC ENERGY AGENCY, The Use of Plane Parallel Ionization Chambers in High Energy Electron and Photon Beams — An International Code of Practice for Dosimetry, Technical Reports Series No 381, IAEA, Vienna (1997).

[2] JOHANSSON, K.-A., SVENSSON, H., Dosimetric intercomparison at the Nordic Radiation Therapy Centres, Part II: Comparison between different detectors and methods, in JOHANSSON, K.-A., Thesis, Univ. of Gothenburg (1982).

[3] INTERNATIONAL ATOMIC ENERGY AGENCY, Absorbed Dose Determination in Photon and Electron Beams — An International Code of Practice, Technical Reports Series No 277, IAEA, Vienna (1987).

[4] DEUTSCHES INSTITUT FÜR NORMUNG, Dosismeßverfahren nach der Sondenmethode für Photonen- und Elektronenstrahlung: Ionisationsdosimetrie, Deutsche Norm DIN 6800-2, Berlin (1996).

[5] HARDER, D., GROSSWENDT, B., ROOS, M., CHRIST, G., BÖDI, R., Ermittlung des relativen Massenbremsvermögens für die Elektronenstrahlung klinischer Beschleuniger nach dem 'Ersatz-Anfangsenergieverfahren', in Nüsslin, Hrsg., Medizinische Physik 1988, Universität Tübingen (1988).

[6] DING, G.X., ROGERS, D.W.O., MACKIE, T.R., Calculation of stopping-power ratios using realistic clinical electron beams, Med. Phys. **22** (1995) 489.

DEVIATION OF THE EFFECTIVE POINT OF MEASUREMENT OF THE MARKUS CHAMBER FROM THE FRONT SURFACE OF ITS AIR CAVITY IN ELECTRON BEAMS

M. ROOS, K. DERIKUM, A. KRAUSS
Physikalisch-Technische Bundesanstalt,
Braunschweig, Germany

Abstract

The IAEA International Code of Practice TRS-381 recommends design requirements for plane parallel chambers, allowing to assume cavity perturbation effects to be negligible and the effective point of measurement to be situated on the front surface of the air volume. For the Markus chamber which does not meet these requirements it is shown that the effective point of measurement is shifted from the front surface by about 0.5 mm. Neglecting this effect may lead to dose errors of a few percent in the vicinity of the therapeutic range.

1. Introduction

In the International Code of Practice IAEA TRS-381 "The Use of Plane Parallel Ionization Chambers in High Energy Electron and Photon Beams: An International Code of Practice for Dosimetry" [1] as well as in other new dosimetry protocols, Spencer-Attix stopping power ratios water to air are used. According to the underlying formulation of the cavity theory, the walls of ionization chambers for measurements of water absorbed dose in a water phantom should be water equivalent and the air-filled cavity should not perturb the electron fluence above the cut-off energy Δ (for details, see for instance [2]).

These assumptions are not fulfilled by real ionization chambers. The necessary corrections are performed by selecting an effective point of measurement (P_{eff}) and applying an overall perturbation correction factor p_{Q}. The effective point of measurement is shifted from the centre of the cavity in order to correct for the displacement effect. The overall perturbation factor is the product of two factors p_{cav} and p_{wall}. The correction factor p_{cav} refers to the perturbation due to the air cavity (essentially caused by the in-scattering effect [2]) and the correction factor p_{wall} relates to effects which are due to the non-water equivalence of the wall and left over after the scaling of the front wall thickness (for details see [1, 3, 4]) the overall perturbation factor. Due to the lack of a sufficient database, the wall effects are not explicitly corrected in TRS-381 although it is recognized that the backscatter properties of a few chambers may considerably deviate from those of water.

For plane parallel chambers showing the desirable design properties of TRS-381, p_{cav} is assumed to be unity and P_{eff} to be at the centre of the front surface of the air volume. A very common chamber which is not in agreement with these requirements is the Markus chamber. TRS-381 gives experimental values for the resulting overall perturbation factor, which have, however, to be linked to P_{eff}. In the present paper the position of the P_{eff} of the Markus chamber is determined within the framework of TRS-381.

2. Design properties and methods of measurement

The properties the air-filled cavities of plane parallel electron chambers should have are [1]: the ratio of cavity diameter and cavity depth must be large (of the order of ten), the width of the guard electrode should not be smaller than 1.5 times the cavity height, and the cavity height should not exceed 2 mm.

Figure 1 (upper part) shows the corresponding proportions of the Roos chamber which are in agreement with these properties. For this design (as well as for the design of the NACP chamber) the overall perturbation factor p_{Q} is assumed to be unity [1, 3].

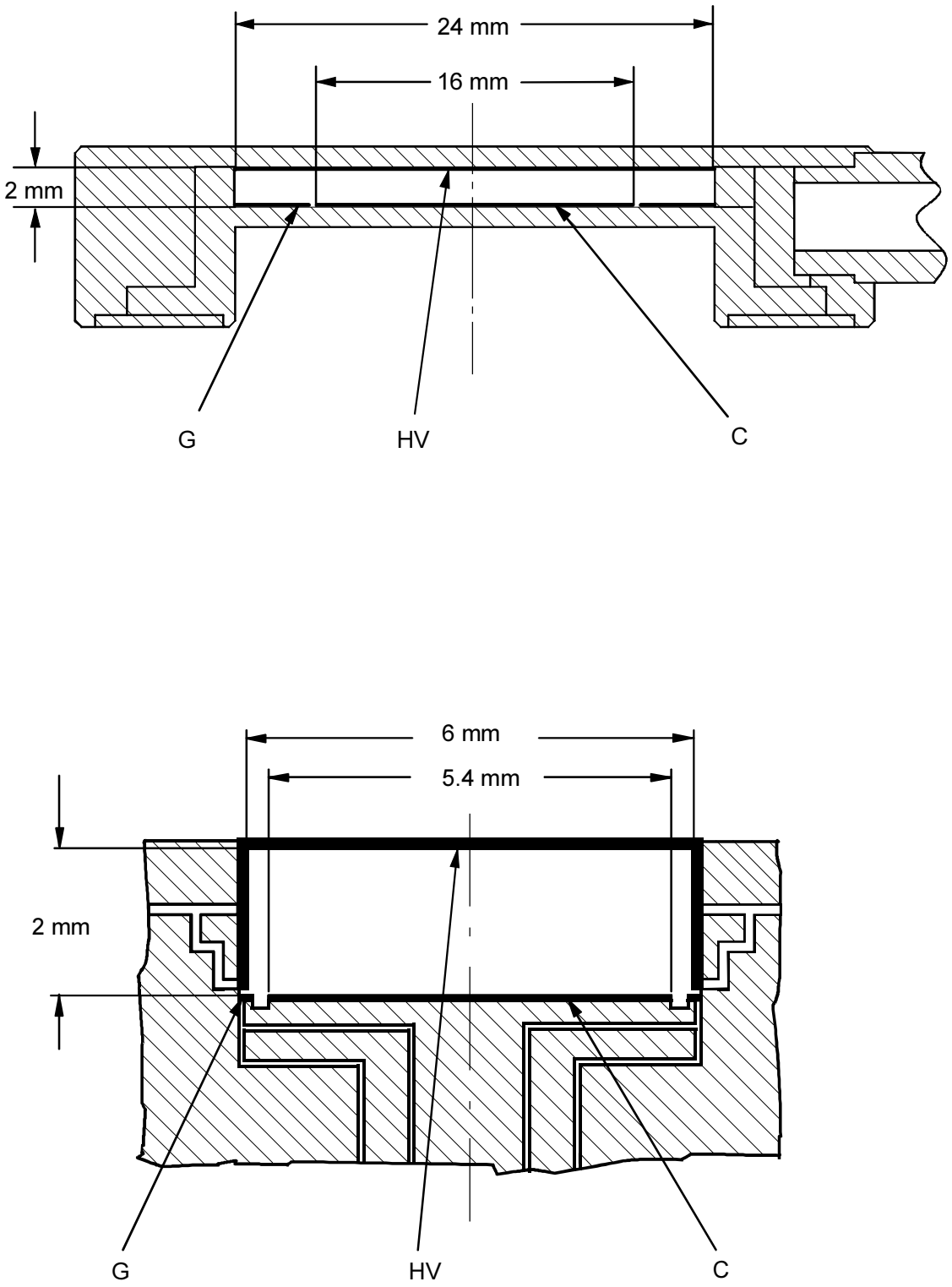

FIG. 1. Design features of the Roos chamber (upper part) and the Markus chamber (lower part) with high-voltage electrode (HV), collecting electrode (C) and guard ring (G).

For P_{eff}, the contribution to ionization in the collecting volume by the electrons entering through all parts of the surface has to be considered. The lower limit of the angular range of the electrons entering through the side walls from depths greater than that of the front surface is given by the ratio of the cavity depth to the width of the guard ring. Therefore, the broad guard ring substantially reduces the angular range and, in conjunction with the large diameter of the collecting volume, it reduces the contribution of electrons entering through the side walls to a negligible value.

The fluence of the backscattered electrons in the phantom is “measured” at the depth of the rear surface of the air volume. This means that the point of measurement of this component is displaced from the point of measurement of the component incident through the front surface by the depth of the air volume. For the irradiation conditions of practical interest, in a reasonable approximation (about 0.1 mm), the resulting P_{eff} of the chamber is still at the front surface of the air volume due to the small contribution of backscattered electrons.

Figure 1 (lower part) shows that the design requirements of TRS-381 are not fulfilled in the case of the Markus chamber. The diameter to height ratio is only 3 and the width of the guard ring is almost negligible. This leads to a pronounced in-scattering cavity effect. Furthermore, it is quite obvious that there is a wide angular range from which electrons may enter into the collecting volume through the side walls. These may substantially contribute to the signal, falsifying it or shifting P_{eff}.

Usually (for instance in the sense of [4]), for a gaseous detector, P_{eff} is defined as that point in the uniform water phantom at which the electron fluence is equal to the weighted mean fluence of the electrons at the surface of a volume, identical to the chamber volume, within the uniform phantom. The weighting of the fluence is performed according to the contribution to the detector signal, assuming that no scattering or attenuation occurs in the detector volume. This ensures that the influence of the in-scattering effect is excluded, avoiding a mix-up with p_{cav} . Also this definition refers to chambers having water equivalent walls to avoid mix-up with p_{wall}. Unfortunately, however, the experimental data currently available and recommended in TRS-381 do not allow straight separation of these corrections.

In order to get results consistent with TRS-381, the following procedure for the determination of the P_{eff} of the Markus chamber was followed. First, the overall perturbation factor p_Q of the Markus chamber was determined for the depths of maximum dose rate at the PTB linac by comparison with the Roos chamber. The procedure is described in [5] and the results are already included in TRS-381. Under these conditions, p_Q of the Roos chamber is assumed to be unity. The p_Q values of the Markus chamber were correlated with the mean electron energy at the measuring depth according to [1], and it was assumed that p_Q depends only on this energy. A generalization to depths deviating from those of the maximum dose rate is, for instance, very common in the case of cylindrical chambers [6]. It is, of course, only approximately correct since the in-scattering effect, included in this correction, additionally depends, for instance, on the depth due to the mean square angle of scattering [4]. The results of p_Q were used to correct depth ionization distributions measured by the Markus chamber. The resulting distributions were normalized to one at the depths of maximum dose rate and the position of the P_{eff} was obtained by comparison with the respective distribution measured by means of the Roos chamber.

3. Experimental methods and results

Depth ionization distributions in a water phantom were measured using a Markus chamber and a Roos chamber. The measurements were performed for SSD = 100 cm and FS = 15 cm × 15 cm at various electron energies. The thickness of the front walls was scaled according to the ratio of the electron densities of the respective wall materials and water. The reading of the Markus chamber as well as the reading of the Roos chamber were referred to the depth of the front surface of the air volume of the chambers as recommended in TRS-381.

The ionization chamber current was measured by a Keithley 616 electrometer. Its output voltage was converted to a frequency of pulses and the number of pulses was counted. The

reading was referred to the mean value of the reading of two monitor chambers placed to the right and to the left of the chamber under test, at a fixed depth in the phantom. In addition, a transmission chamber in front of the phantom was used for measurements at low electron energies. Before every series of measurements the electrometer including the voltage to frequency converter was calibrated so that it was traceable to the national standards at both polarities in order to avoid any influence from non-linearity and offset effects in the respective ranges of measurement.

For a given electron energy, first the measurements using the Roos chamber and a positive polarity of the polarizing voltage were performed. The zero depth was adjusted by a special device and then the depth dose distributions were measured in the forward and backward directions. This cycle, including zero adjustment, was repeated several times. Afterwards the same procedure was performed using the Markus chamber at both polarities, followed by the measurements using the Roos chamber at negative polarity. In order to estimate the uncertainties, above all the reproducibility of the depth position, the mean values of some range parameters and the corresponding standard deviation were calculated. The standard uncertainties of the range parameters in the descending part of the distributions are not higher than 0.03 mm.

In order to evaluate the resulting distributions, the mean values of all measurements at a given depth were calculated for all depths at both polarities. The resulting distributions were corrected for the polarity effect and for the recombination loss. In the case of the Markus chamber in addition the overall perturbation factor p_Q was applied. The resulting distributions were normalized to one at the depth of the maximum dose rate.

Figures 2 and 3 (upper part) show the results for the descending parts of the distributions for 6, 12.5 and 20 MeV electron beams. In addition, the results of the Markus chamber without application of the overall perturbation factor are included. The results show that the distributions measured using the Markus chamber are shifted towards lower depths by about $\delta = 0.5$ mm. This means that P_{eff} is shifted towards the center of the air volume by this distance. It may be seen that the resulting dose errors may amount to a few percent even in the vicinity of R_{85}.

The measurements were performed using the PTB version of the Roos chamber, denoted by FK6 [5]. A check showed that the distributions measured with the commercial Roos chamber PTW M34001 agree within 0.07 mm. Furthermore, the displacement of P_{eff} of the Markus chamber was determined by comparison with an NACP chamber in the 12.5 MeV beam. The results are shown in Figure 3 (lower part). The shift δ is similar as derived by comparison with the FK6 and PTW Roos chambers (Figure 2, lower part). Scaling of the front wall thickness according to the density of the material (instead of the electron densities) would change the shift δ obtained from the comparison with the Roos chamber by less than 0.01 mm. The shift δ from the comparison with the NACP chamber would be reduced by 0.06 mm.

The dependence of the shift on energy and depth is not very pronounced. Due to the mix-up of various properties, the interpretation of the results is complicated. Although the walls of the Roos chamber as well as those of the Markus chamber essentially consist of PMMA, the wall effects may differ. The thickness of the rear wall of the Roos chamber (1.3 mm) is only a fraction of the thickness necessary for backscatter saturation (about 4 mm [7]), and the backscatter deficiency relative to water is assumed to be small [1,4] since most of the backscattered electrons originate from water. In contrast to this, for the thick rear wall of the Markus chamber, the backscatter saturation values [7] should apply. Therefore the overall

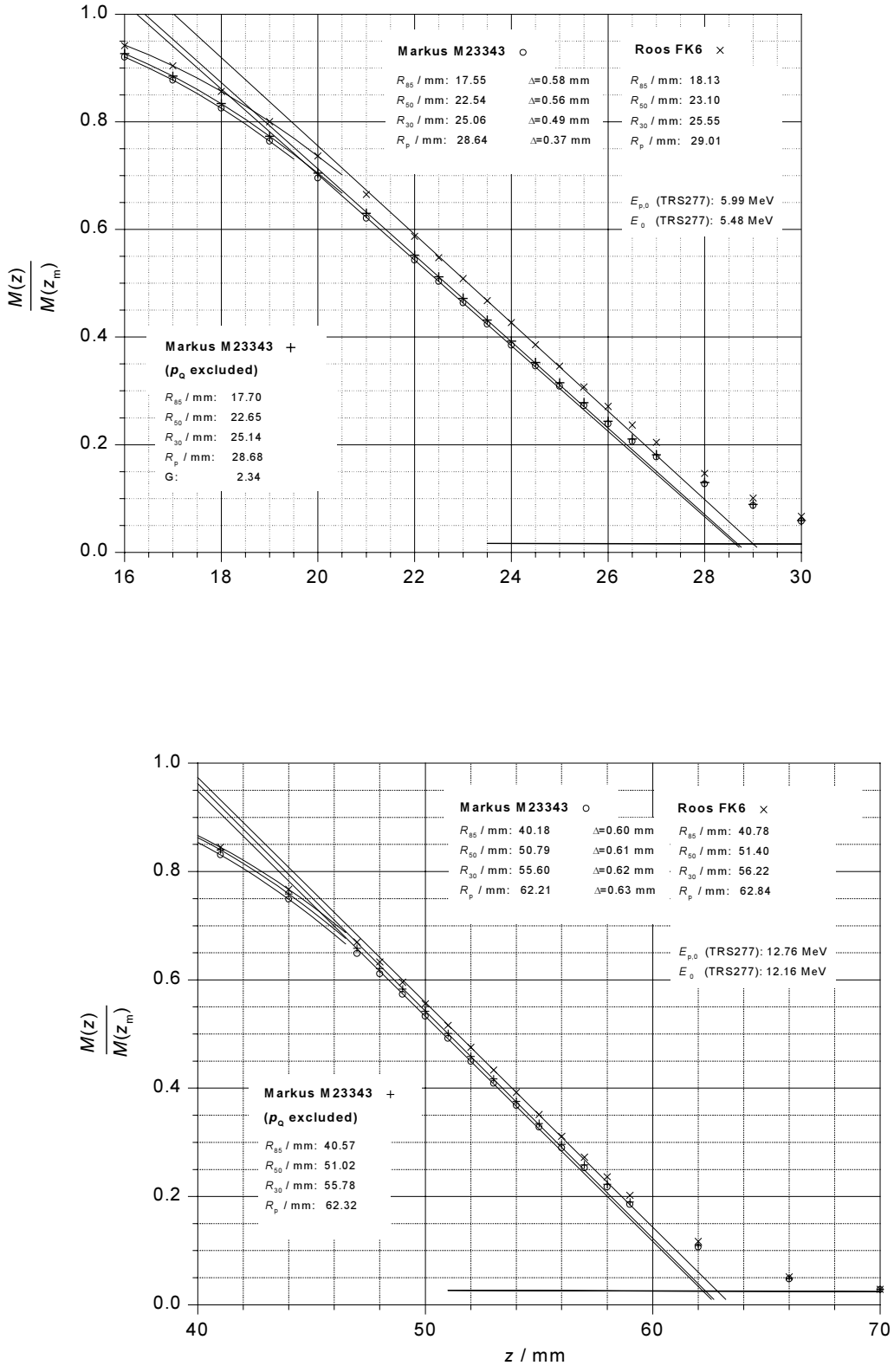

FIG. 2. Depth ionization distributions for 6 MeV and 12.5 MeV electrons measured with a Markus chamber and a Roos chamber. The readings are corrected for the polarity effect and for the recombination loss. In the case of the Markus chamber, the overall perturbation factor p_Q *was applied. In addition, the results obtained with the Markus chamber without this correction are included. The readings are normalized to one at the depth of maximum dose rate,* z_m.

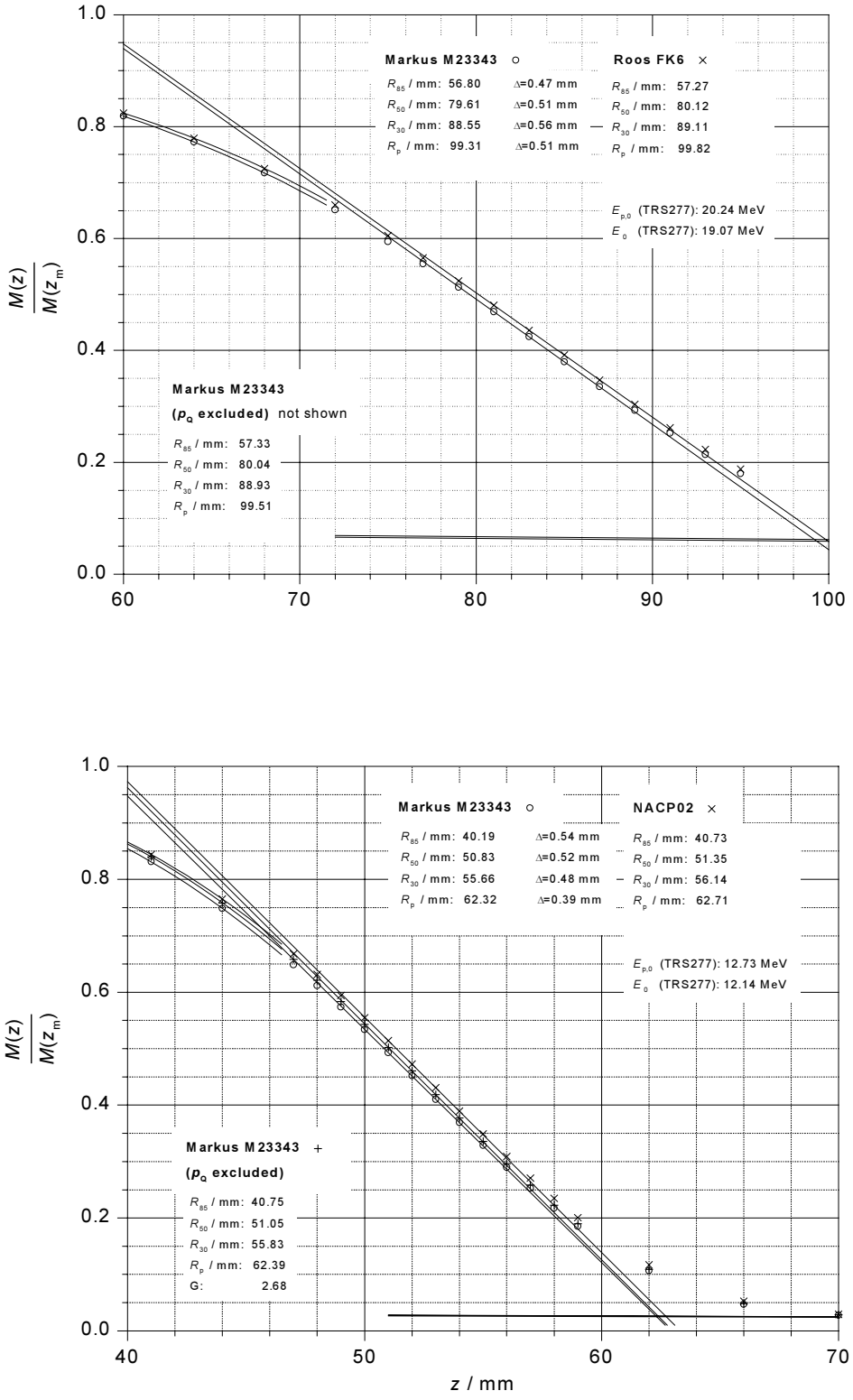

FIG. 3. Depth ionization distributions for 20 MeV electrons measured with a Markus chamber and a Roos chamber (upper part). Depth ionization distributions for 12.5 MeV electrons measured with a Markus chamber and an NACP chamber (lower part).The readings are corrected for the polarity effect and for the recombination loss. In the case of the Markus chamber, the overall perturbation factor p_Q *was applied. In addition, the results obtained with the Markus chamber without this correction are included. The readings are normalized to one at the depth of maximum dose rate,* z_m.

perturbation factor p_Q derived for the Markus chamber [5] corrects not only for the in-scattering effect but also for the differences in the backscatter deficiency.

The assumption that the product of the respective correction factor and the factor for the perturbation due to the air cavity depends only on the mean energy at depth is a rough approximation. The results for the apparent shift δ therefore cannot be consistently explained on the basis of the definition of the effective point of measurement (as cited above). It is a slightly deviating shift which appears within the framework of the TRS-381. It is the shift which has actually to be taken into account if the results of measurements obtained with the Markus chamber are compared with the results obtained with chambers meeting the design requirements.

4. Conclusions

The design requirements for plane parallel chambers recommended in IAEA TRS-381 constitute a compromise taking the requirements of practical dosimetry in clinical beams into account. The upper limit of the cavity depth of plane parallel chambers (2 mm), for instance, may be further reduced. This would allow to neglect the cavity perturbation effect and the shift of P_{eff} from the front surface of the air volume in even better approximation. It would, however, reduce the chamber response and it would impair the properties as regards the dependence of the response on the absolute value and on the polarity of the polarizing voltage, increasing the uncertainties of dose measurements.

In the present paper it is shown, on the other hand, that neglecting the design requirements of TRS-381 may substantially increase the uncertainties of dose measurements. In the case of the Markus chamber design, unsuitable cavity properties cause not only a pronounced cavity perturbation effect but also lead to a shift of the effective point of measurement. Neglecting this effect may result in dose errors of various percent at therapeutically important depths. This may be compensated by correction procedures only partly.

REFERENCES

[1] INTERNATIONAL ATOMIC ENERGY AGENCY, The Use of Plane Parallel Ionization Chambers in High Energy Electron and Photon Beams — An International Code of Practice for Dosimetry, Technical Reports Series No 381, IAEA, Vienna (1997).

[2] INTERNATIONAL COMMISSION ON RADIATION UNITS AND MEASUREMENTS, Radiation dosimetry: electron beams with energies between 1 and 50 MeV, ICRU Report 35, ICRU, Bethesda, MD (1984).

[3] NAHUM, A.E., Perturbation effects in dosimetry: Part I. Kilovoltage x-rays and electrons, Phys. Med. Biol. **41** (1996) 1531.

[4] SVENSSON, H., BRAHME, A., Recent Advances in Electron and Photon Dosimetry, Ch. 3, Radiation Dosimetry Physical and Biological Aspects, (ORTON, C.G., Ed.), Plenum Press, New York (1986).

[5] ROOS, M., The State of the Art in Plane-Parallel Chamber Hardware with Emphasis on the New 'Roos' and 'Attix' Chambers (Ref. [51] of IAEA TRS-381), Work commissioned by the IAEA plane-parallel working group (1993), in ROOS, M., DERIKUM, K., Plane-Parallel Chambers for Electron and Photon Dosimetry in Therapeutic Beams, PTB-Report DOS-33 (1999) to be published.

[6] INTERNATIONAL ATOMIC ENERGY AGENCY, Absorbed Dose Determination in Photon and Electron Beams: An International Code of Practice, Technical Reports Series No. 277, IAEA, Vienna (1987).
[7] HUNT, M.A., KUTCHER, G.J., BUFFA, A., Electron backscattering correction for parallel-plate chambers", Med. Phys. **15** (1988) 96–103.

THE RECOMBINATION CORRECTION AND THE DEPENDENCE OF THE RESPONSE OF PLANE PARALLEL CHAMBERS ON THE POLARIZING VOLTAGE IN PULSED ELECTRON AND PHOTON BEAMS

M. ROOS, K. DERIKUM
Physikalisch-Technische Bundesanstalt,
Braunschweig, Germany

Abstract

Based on an experimental investigation of the recombination effect in plane parallel chambers, a relation is deduced that allows the correction to be calculated from the electrode spacing and from the dose per pulse. It is shown that the uncertainties caused by the application of the Boag formula for volume recombination (recommended in the International Code of Practice TRS-381) amount to not more than about 0.1% for conventional beams. Calculated recombinations are compared with experimental results concerning the dependence of the response of various commercial plane parallel chambers on the polarizing voltage. Since it cannot be excluded that particular chambers collect a non-negligible amount of charge from regions outside the designated collecting volume or that the effective polarizing voltage is reduced by poor contacts, it seems advisable to experimentally check the chambers before use and before application of the analytical relations.

1. Introduction

The experimental determination of the recombination correction in pulsed beams is based on an extrapolation of the reciprocal of the reading $1/M$ as a function of the reciprocal of the polarizing voltage $1/U$ towards $1/U = 0$ in order to get the corrected value of 1/M [1, 2]. This implies, of course, that the voltage exclusively affects the degree of saturation. This assumption is, however, usually not fulfilled in the case of plane parallel chambers. Before the preparation of the International Code IAEA TRS-381 [3] it was shown [4] that most of the commercial plane parallel chambers show a pronounced curvature at the highest voltages, where theory essentially demands a straight line. This indicates that other effects may play an important role. As an example it was discussed that the dependence of the response of the Schulz chamber on the polarizing voltage is predominantly caused by the dependence of the collecting volume on this voltage. Any type of extrapolation therefore does not yield useful results as regards the degree of saturation in such cases.

Since the two-voltage method essentially consists in a linear extrapolation, it is strictly not applicable in such cases. It was therefore suggested to apply it twice, upon calibration (even if the recombination correction is in fact negligible as in the case of ^{60}Co-γ radiation) and in the users beam (using the same two voltages, of course). In this case the single corrections may be incorrect, but the quotient is approximately correct since the falsifying effects may, at least partly, cancel. This is obvious in the example of the voltage-dependent collecting volume.

It must, however, be borne in mind that, due to the long equilibration times of most of the chambers [5], the experimental determination of the correction (amounting to only a few tenths of a percent in most cases) seems to be unnecessarily laborious. In fact, depending on the equilibration time of the chambers and on the inherent drifts of the accelerator/ monitor/ dosimeter system, the uncertainty of the correction may be comparable to its magnitude. It was, therefore, suggested using the analytical formula by Boag, included in TRS-381 [3], for volume recombination [1] in such cases.

The present paper investigates the recombination in plane parallel chambers exposed to conventional pulsed beams and evaluates the uncertainties introduced by the application of the

Boag formula. In addition, the dependence of the response of commercial plane parallel chambers on the polarizing voltage is studied and compared with the respective saturation properties.

2. Results and discussion

2.1. Evaluation of the uncertainties introduced by the application of the Boag formula to volume recombination

The recombination in chambers with plane parallel orientation of the electrodes is well understood [1]. The restrictions as regards the applicability of the two-voltage method are not caused by a lack of theoretical knowledge but by peculiarities of chamber designs and of individual chambers. In fact, well designed and carefully constructed chambers show usually a more or less wide range of polarizing voltages where the dependence of response on the voltage is in accordance with the theoretically expected saturation behaviour. This allows a physically well-reasoned extrapolation of the reciprocal of the reading $1/M$ as a function of the reciprocal of the polarizing voltage $1/U$ towards $1/U = 0$.

The main mechanisms of ion loss are volume recombination, initial recombination and diffusion loss. Near saturation, the respective collection efficiencies may be calculated from the

initial recombination [6]: $$\mathrm{f_i} = 1 - e_i \cdot d / U \tag{1a}$$

diffusion loss [7]: $$\mathrm{f_d} = 1 - 2 \cdot k \cdot T / (U \cdot e) \tag{1b}$$

volume recombination [8]: $$\mathrm{f_v} = 1 - \frac{1}{2} \mu \cdot q \cdot d^2 / U \tag{1c}$$

The resulting collection efficiency f is the product of three factors:

$$\mathrm{f} = \mathrm{f_i} \cdot \mathrm{f_d} \cdot \mathrm{f_v} \tag{1}$$

The corresponding recombination correction factor $k_S = \mathrm{f}^{-1}$ is, therefore, a linear function of the reciprocal of the polarizing voltage U:

$$k_s = 1 + \mathrm{a} / U \tag{2}$$

with $$\mathrm{a} = e_i \cdot d + 2 \cdot k \cdot T / \mathrm{e} + \frac{1}{2} \mu \cdot q \cdot d^2$$

e	1.6022×10^{-19} C	electron charge
k	1.3807×10^{-23} J/K	Boltzmann constant
T	air temperature	
U	polarizing voltage	
d	electrode spacing	
q	initial charge density per pulse	
$\mathrm{e_i}$	constant with the dimension of a field strength	
μ	constant involving the recombination coefficient and the ionic mobilities [1]	

A plot of the reciprocal of the reading as a function of the reciprocal of the polarizing voltage should therefore result in a linear relation if the dependence of the response on the polarizing voltage is exclusively given by the recombination effects discussed. In the case of plane parallel chambers with small electrode separation, the free electron component has to be taken into account in addition [1]. It causes, in a first approximation, only a decrease of the slope of the $1/M$ vs. $1/U$ plot. Various models are available for the description of the influence of the free electron component [9]. Depending on the model used, the free electrons may cause a slight deviation from linearity in the direction of higher efficiency at the highest voltages (out-of-voltage range of the measurements). The maximum deviation caused by this curvature in comparison with a linear relation towards $1/U = 0$ is, however, in practice well below 0.1% in the range of the pulse charge densities of interest. If the free electron fraction is assumed to be proportional to the polarizing voltage (which is compatible with the data available [9]), or if it is independent of it, the linear extrapolation of the observed plot to 1/U = 0 furnishes the charge corresponding to complete saturation.

In order to determine the recombination correction experimentally, a plane parallel chamber of the type FK6 [4] with an electrode spacing of 2 mm (common with most of the commercial chambers used in electron dosimetry) was carefully checked in order to exclude effects such as gas multiplication, dependence of the collecting volume on the voltage and charge collection from regions outside the designated collecting volume. The charge (normalized to a monitor reading) was measured for various pulse charge densities around the range of interest, applying different polarizing voltages. The experimental features were described in [10].

Figure 1 shows the results for various pulse charge densities: the reciprocal of the reading normalized to 1 at 100 V has been plotted as a function of the reciprocal of the polarizing voltage. The polarity effect of this chamber is small and almost independent of the absolute value of the polarizing voltage. The dotted lines are linear fits to the data. The experimental data show the expected linear behaviour, and the corrected values were obtained by linear extrapolation towards $1/U = 0$.

Figure 2 shows the resulting charge deficit for a polarizing voltage of 100 V as a function of the pulse charge density (solid circles). In order to obtain a larger range of pulse charge densities, part of the measurements were performed in photon beams. The cross, obtained from measurements in an electron beam, demonstrates that the results hold for both high-energy photon and electron beams, as theoretically expected. A linear fit to the data yields

$$\mathrm{a} = 0.12\ \mathrm{V} + 0.51\ \frac{\mathrm{V}}{10^{-5}\,\mathrm{C/m^3}} \cdot q \qquad (3)$$

A comparison of Eq. (3) with Eq. (2) leads to

$$k_s = 1 + (e_i \cdot d + 2 \cdot k \cdot T / e + \frac{1}{2}\mu \cdot q \cdot d^2) / U$$

with $e_i = 35\ \frac{V}{m}$ and $\mu = 2.55 \cdot 10^{10}\,\mathrm{Vm/C}$

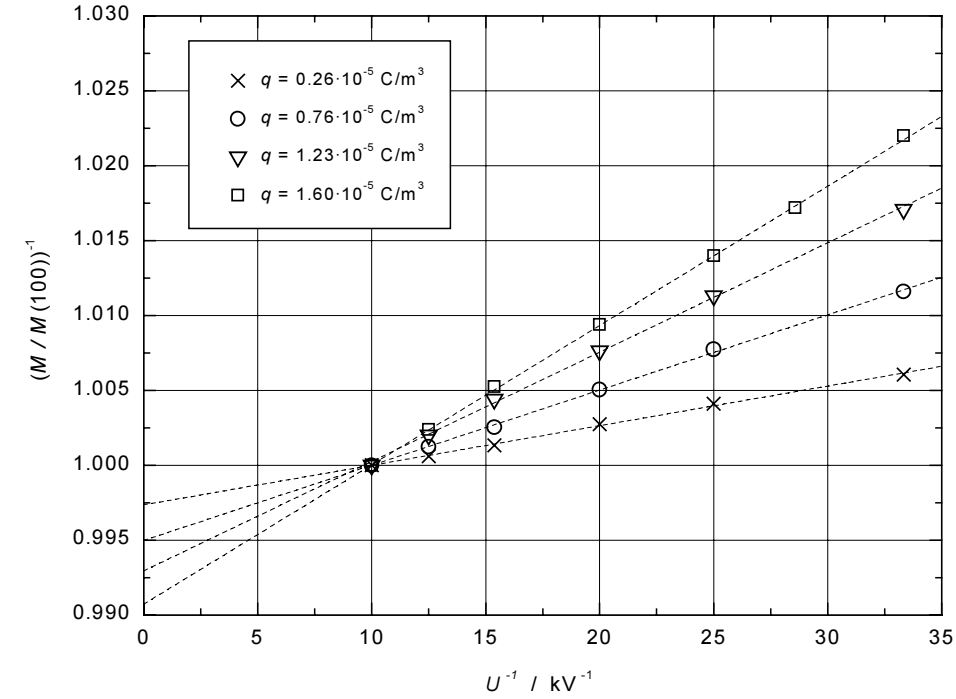

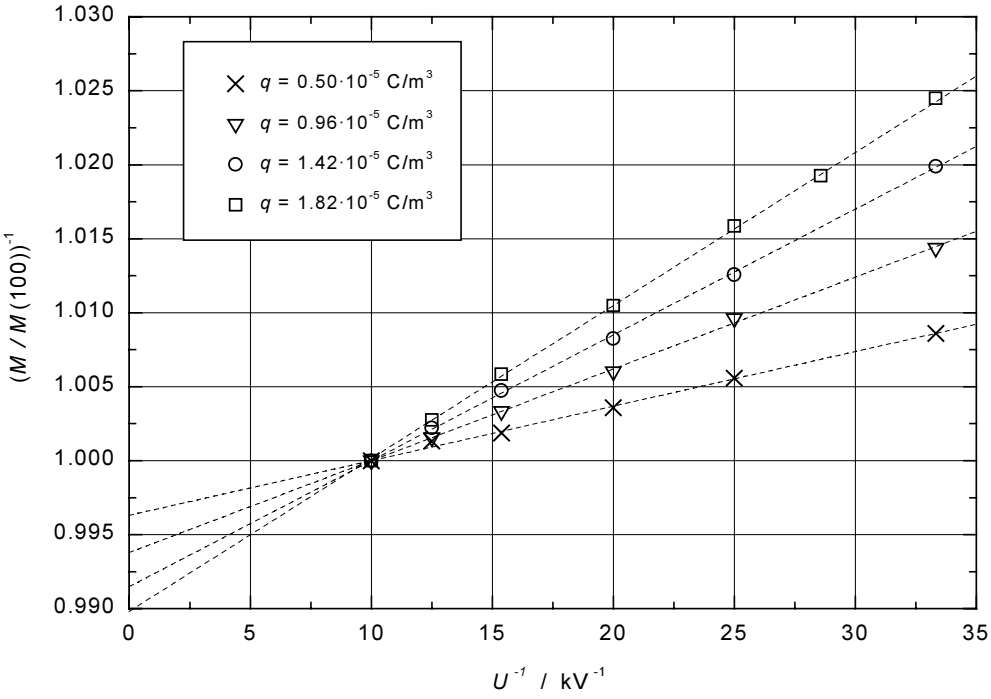

FIG. 1. Reciprocal of the reading M *of an FK6 chamber, normalized to 1 at 100 V, as a function of the reciprocal of the polarizing voltage* U *for various pulse charge densities* q*. The dotted lines are linear fits to the data (for discussion see text).*

This may be expressed as

$$k_s = 1 + (0.12 + 0.46 \cdot d^2 \cdot D_i) / U \qquad (4)$$

d = electrode spacing in mm

D_i = absorbed dose to air per pulse in mGy

U = polarizing voltage in volts

Equation (4) allows recombination correction factors to be calculated for well guarded plane parallel chambers with an electrode spacing d = 2 mm. It may, however, also be used for a spacing deviating by a few tenths of a millimetre from this value. It is sufficient to approximate the absorbed dose to air D_i per pulse by the absorbed dose to water per pulse.

The reason for the restriction of the electrode spacing is the dependence of the parameter μ [1] on the spacing. This parameter is implicitly contained in Eq. (4). It involves the ionic mobilities and the recombination coefficient and is defined [1] as a fitting parameter to the recombination models as used in the present work. It therefore allows in addition for the free electron component, space charge effects, etc. and, therefore, depends on the chamber type. For sufficiently guarded plane parallel chambers the μ value depends essentially on the electrode spacing because of the influence of the free electron component which depends on the spacing. The value μ = 2.55 10^{10} V m / C obtained from the above fit is considerably smaller than the value μ = 3.02 10^{10} V m / C included in the Boag formula [1]. It is valid for plane parallel chambers with an electrode spacing of about 2 mm, whereas the latter value is rather valid for different chamber types with a larger electrode spacing, resulting in a smaller free electron component (and sometimes in a considerably different space charge distribution).

The dotted line in Figure 2 represents Boag's relation for volume recombination only [1]. The deviation of this relation from the experimental results is essentially caused by the missing initial recombination and by the contribution of the free electron component, affecting the apparent value of parameter μ [1]. These deviations are, however, not larger than about 0.1% in the range investigated, and since the polarizing voltages of the different chamber types are usually considerably higher than 100 V, the deviations may be even smaller in practice. This can be inferred from the respective formulae (1c) and (4).

The results of investigations of the recombination correction made by Burns and McEwen [11] using NACP plane parallel chambers are in agreement with the present ones. McEwen, DuSautoy and Williams [12] also report recombination corrections for NACP chambers, which are in agreement with the results of [11] within about 0.1%. Nisbet and Thwaites [13] estimated ion recombination correction factors for NACP, Markus and Roos chambers using the two-voltage method. The authors claim accordance of their results with the Boag formula within about 0.2% for corrections which are not larger than about 1%. It has, however, to be borne in mind that the two-voltage method was not strictly applicable in most of the examples given there.

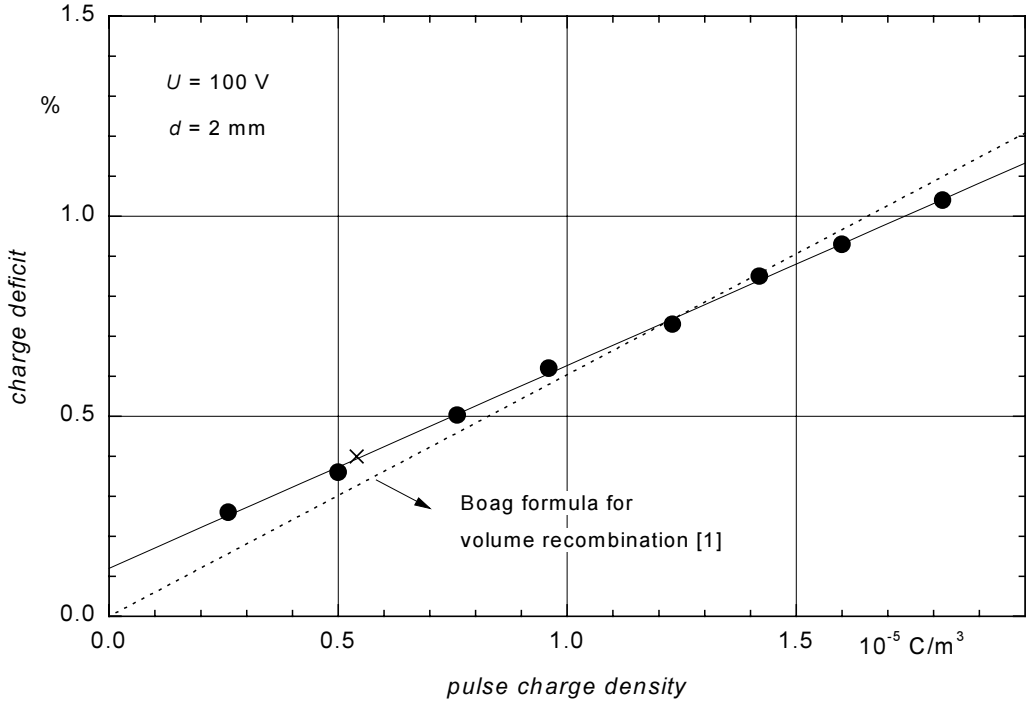

FIG. 2. Experimental results of the charge deficit as a function of the pulse charge density measured in photon beams (solid circles) and in an electron beam (cross) for an electrode spacing of 2 mm and a polarizing voltage of 100 V. The solid line is a linear fit to the data (expressed in Eq. (4) of the present work as a function of the absorbed dose to air per pulse D_i*). The dotted line is Boag's relation [1] for volume recombination.*

3. Investigation of the dependence of response on the polarity and the absolute value of the polarizing voltage

An investigation of the dependence of the response on the polarizing voltage of an ionization chamber requires that the "saturation curve" at both polarities be measured. The respective measurements were performed in the 12.5 MeV electron beam of an SL 75-20 linac using various commercial plane parallel chambers. The pulse repetition frequency was 300 Hz and the pulse length was not larger than 2 μs; the field size was 10 cm × 10 cm and the source-to-surface distance was 100 cm. The chambers were placed at the depth of maximum dose rate in a water phantom for the water-proved chambers and in a PMMA phantom for the others. The reading of the chambers was normalized to the mean value of the readings of two thimble chambers placed to the right and to the left of the chamber under test at the same depth in the phantom. Every day, the current measuring system was calibrated in a traceable route to the national primary standards over the whole measuring ranges at both polarities in order to eliminate the influence of non-linearity and of offset effects.

Since the equilibration times of various chamber types are rather long, each measurement at a given chamber voltage was followed by a measurement at a voltage of 100 V, in order to check the influence of drifts and to eliminate it.

Figures 3–5 show the results for various chambers at pulse doses D_i of about 0.17 mGy. The reciprocal of the reading $1/M$ (normalized to 1 at 100 V for both polarities) has been plotted as a function of the reciprocal of the voltage $1/U$ for both polarities. The arithmetic

means of the absolute values of both polarities have been connected by straight solid lines. All chambers, apart from the Roos chamber PTW34001, show an essential polarity dependence of the "saturation curves", or, vice versa, the polarity effect of these chambers depends on the absolute value of the polarizing voltage. It is particularly pronounced in the case of the NACP and RMI Attix chambers.

The dotted lines in Figures 3–5 represent the relation by Boag [1] and the relation of the present work, Eq. (4). Due to the normalization, the corrections to the reciprocal of the reading at 100 V may be taken directly from the intersections with the y-axis. This normalization to a relatively low voltage has been performed in order to make the effects clearly visible. To get the correction for a deviating voltage, a straight line must simply be drawn parallel to the dotted line of the relation of choice, through the respective data point. The correction is given by the difference of the reciprocal of the normalized reading at the voltage of choice and the intersection of this line with the y-axis.

Figure 4 shows the results for two Markus chambers, both manufactured by PTW. The only nominal difference is given by the plug: in the case of the chamber denoted W23343 (upper part of the figure), a different plug has been mounted, fitting the Wellhöfer electrometer system. In the case of this chamber, the slope of the curve is steeper than for the chamber denoted M23343 (lower part of the figure). This is accompanied by a more pronounced curvature at the highest voltages and a stronger dependence of the polarity effect on the polarizing voltage. A check showed that the different plugs are not responsible for the differing behaviour.

In the case of Markus chambers it must be taken into account that the electrodes are not essentially plane parallel, but most of the surface of the high voltage electrode is perpendicular to the collecting electrode. This can be seen in Figure 6. The high-voltage electrode (solid line) covers not only the entrance foil but in addition almost completely the side walls (reducing the polarity effect). The electrical field-strength is, therefore, essentially reduced over a large part of the collecting volume. Due to the saturation behaviour of the recombination the decrease of the collection efficiency within these regions may not be compensated by the increase within the regions of increased field strength close to the guard-ring. The relations for plane parallel chambers are, therefore, not strictly applicable in this case.

Figure 5 shows the results of the RMI Attix chamber. In addition to the results obtained according to the two formulae for the actual electrode spacing $d = 0.7$ mm [4] of this chamber, the results for the "nominal" spacing d = 1 mm, as stated by the manufacturer, have been included. It may be seen that, even for a polarizing voltage of 100 V, the respective deviations of the correction for 0.7 mm from those for 1 mm are far below 0.1%.

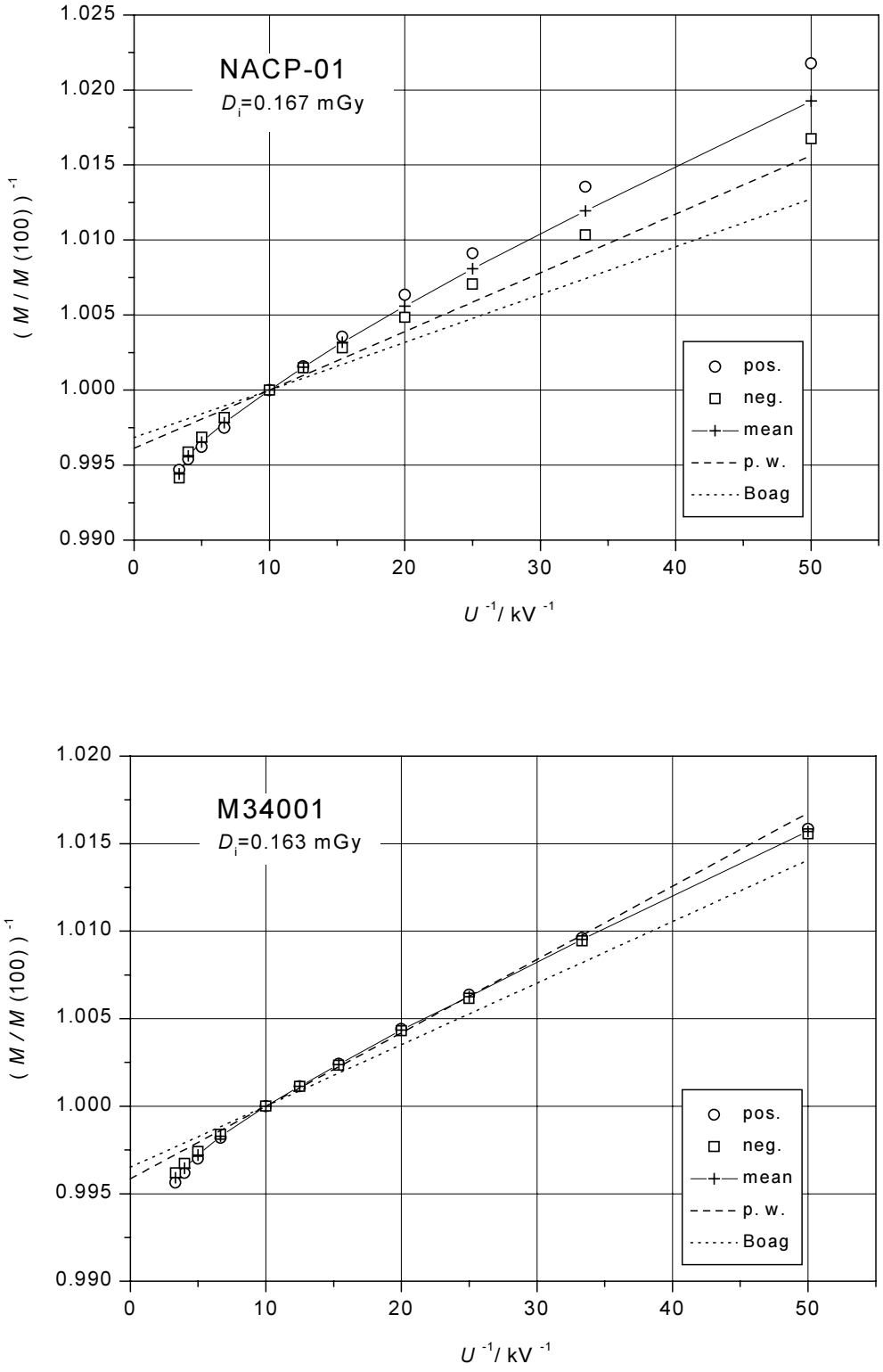

FIG. 3. Reciprocal of the reading M *(normalized to 1 at 100 V for both polarities) as a function of the reciprocal of the polarizing voltage* U *for both polarities of a chamber Scanditronix NACP-01 (upper part) amd PTW Roos M34001 (lower part) at pulse doses* D_i *of about 0.17 mGy. The means of the absolute values of both polarities have been connected by straight solid lines. The dotted lines are the results according to the Boag formula [1] and according to formula (4) of the present work, respectively.*

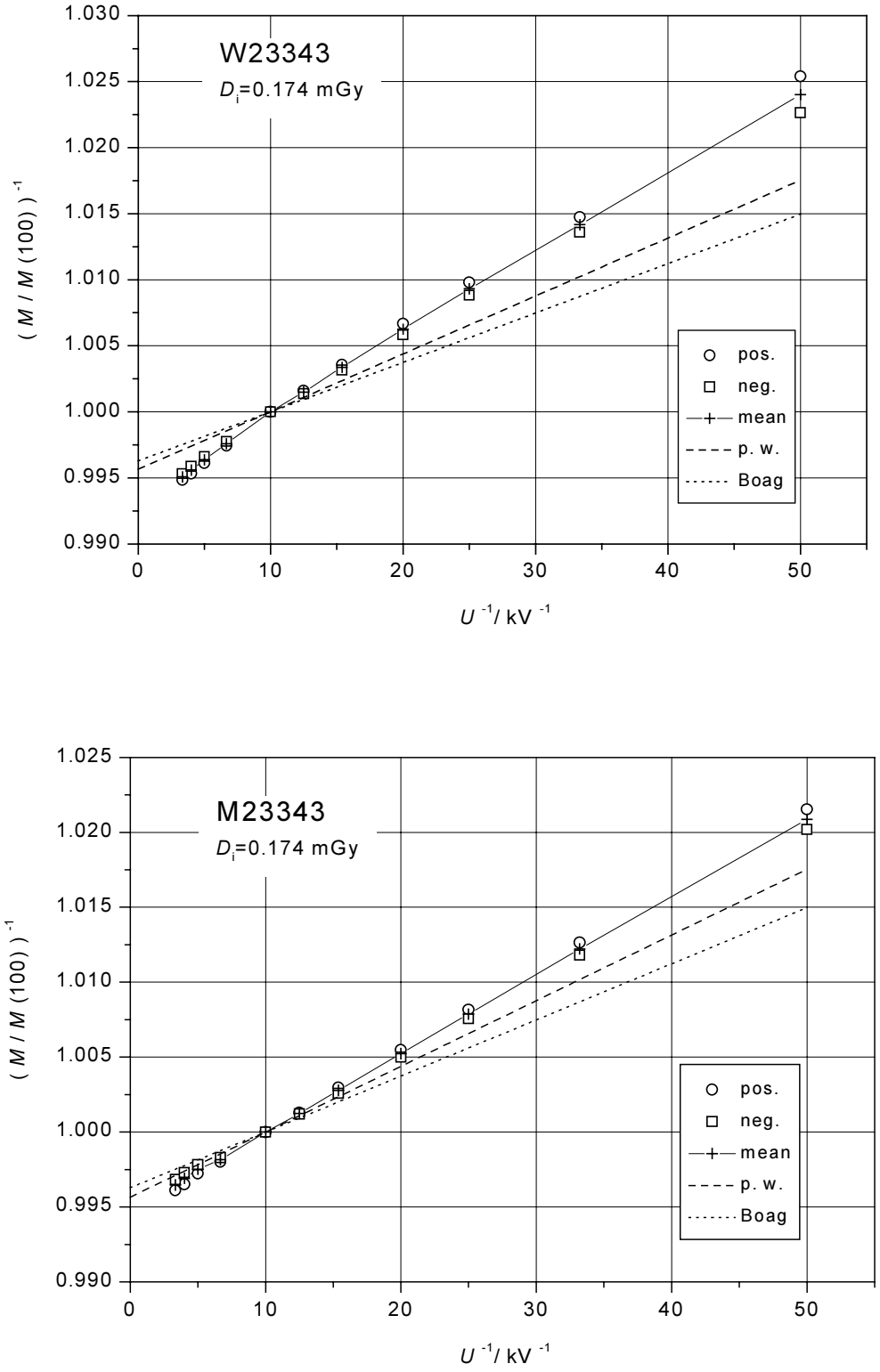

FIG.4. Reciprocal of the reading M *(normalized to 1 at 100 V for both polarities) as a function of the reciprocal of the polarizing voltage* U *for both polarities of a chamber PTW Markus W23343 (upper part) and M23343 (lower part), at pulse doses* D_i *of about 0.17 mGy. The means of the absolute values of both polarities have been connected by straight solid lines. The dotted lines are the results according to the Boag formula [1] and according to formula (4) of the present work, respectively..*

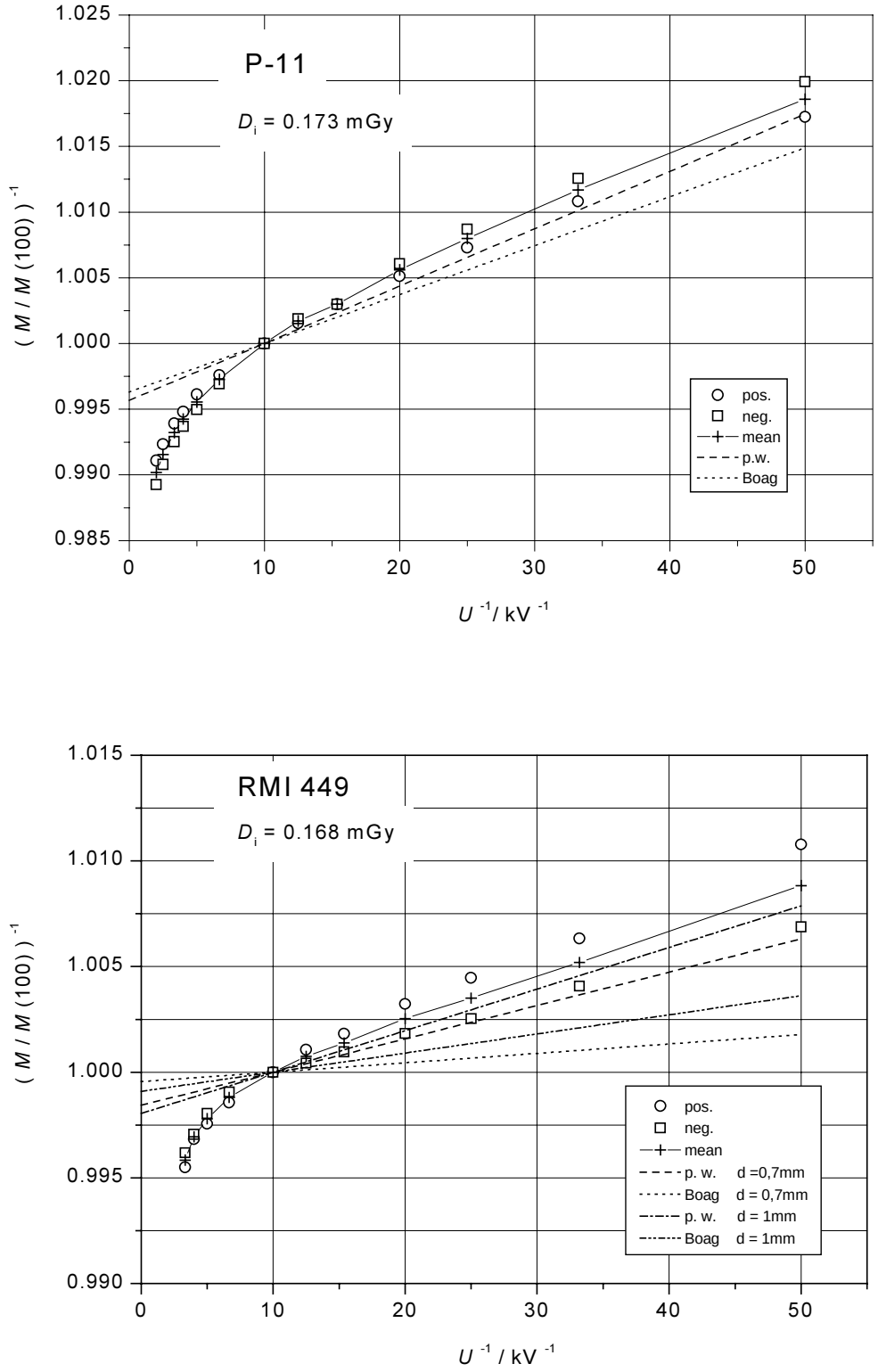

FIG. 5. Reciprocal of the reading M *(normalized to 1 at 100 V for both polarities) as a function of the reciprocal of the polarizing voltage* U *for both polarities of a chamber Exradin P-11 (upper part) and RMI Attix 449(lower part) at pulse doses* D_i *of about 0.17 mGy. The means of the absolute values of both polarities have been connected by straight solid lines. The dotted lines are the results according to the Boag formula [1] and according to formula (4) of the present work, respectively. The results for the nominal electrode spacing (1 mm) and for the actual spacing (0.7 mm) of the Attix chamber RMI 449 are included in the figure.*

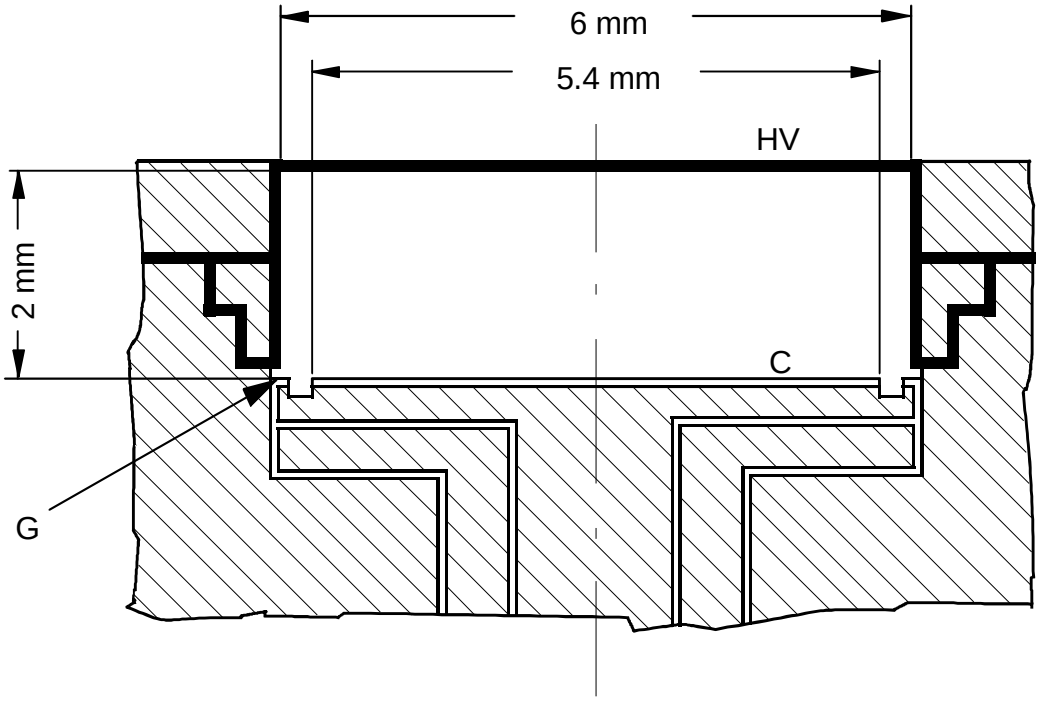

FIG. 6. Design features of the Markus chamber PTW 23343 with high-voltage electrode (HV), collecting electrode (C) and guard-ring (G). The high-voltage electrode (solid line) covers not only the entrance foil but in addition almost completely the side walls.

4. Conclusions

The determination of the recombination correction may be facilitated by the application of analytical relations allowing the correction factor to be calculated from the electrode spacing and from the pulse dose. Since the correction amounts to not more than about 1% for conventional beams, deviations of the electron spacing from the nominal value do not restrict applicability in practice.

The present investigations show, however, that particular chambers may collect a considerable amount of charge from regions outside the designated collecting volume, where the field strength may be far lower than in the designated volume. This is usually caused by an incomplete internal shielding of the chambers and shows a remarkable chamber-to-chamber dependence. This complicates the saturation behaviour, and the application of analytical relations for recombination tends to underestimate the recombination correction. In addition, in single cases poor contacts were observed which reduce the effective polarizing voltage in comparison with its nominal value. An experimental check of the chambers before use and before the application of analytical relations seems useful.

REFERENCES

[1] INTERNATIONAL COMMISSION ON RADIATION UNITS AND MEASUREMENTS, The Dosimetry of Pulsed Radiation, ICRU Report 34, ICRU, Bethesda, MD (1982).

[2] BOAG, J.W., Ionization chambers, Ch. 3, The Dosimetry of Ionizing Radiation, Vol. II, (KASE, K.R., BJARNGARD, B.E., ATTIX, F.H., Eds), Academic Press, London (1987).

[3] INTERNATIONAL ATOMIC ENERGY AGENCY, The Use of Plane Parallel Ionization Chambers in High Energy Electron and Photon Beams — An international Code of Practice for Dosimetry, Technical Reports Series No. 381, IAEA, Vienna (1997).
[4] ROOS, M., "The state of the art in plane parallel chamber hardware with emphasis on the new 'Roos' and 'Attix' chambers", (Ref. [51] of IAEA TRS-381) Work commissioned by the IAEA plane parallel working group (1993), in ROOS, M., DERIKUM, K., Plane parallel chambers for electron and photon dosimetry in therapeutic beams, PTB-Bericht DOS-33 (1999).
[5] ROOS, M., DERIKUM, K., Polarity effect and equilibration time of plane parallel ionization chambers in electron beams, PTB working notes.
[6] KARA-MICHAILOVA, E., LEA, D.E., The interpretation of ionization measurements in gases at high pressures, Proc. Camb. Phil. Soc. **36** (1940) 101.
[7] LANGEVIN, P., Mesure de la valence des ions dans les gaz, Le Radium **10** (1913) 113.
[8] BOAG, J.W., Ionization measurements at very high intensities, Br. J. Radiol. **23** (1950) 601.
[9] BOAG, J.W., HOCHHÄUSER, E., BALK, O.A., The effect of free electron collection on the recombination correction to ionization measurements of pulsed radiation, Phys. Med. Biol. **41** (1995) 885.
[10] DERIKUM, K., ROOS, M., Measurement of saturation correction factors of thimble-type ionization chambers in pulsed photon beams, Phys. Med. Biol. **38** (1993) 755.
[11] BURNS, D.T., MCEWEN, M.R., Ion recombination corrections for the NACP parallel-plate chamber in a pulsed electron beam, Phys. Med. Biol. **43** (1998) 2033.
[12] MCEWEN, M.R., DUSAUTOY, A.R., WILLIAMS, A.J., The calibration of therapy level electron beam ionization chambers in terms of absorbed dose to water, Phys. Med. Biol. **43** (1998) 2503.
[13] NISBET, A., THWAITES, D.I., Polarity and ion recombination correction factors for ionization chambers employed in electron beam dosimetry, Phys. Med. Biol. **43** (1998) 435.

ELECTRON BEAM DOSIMETRY. CALIBRATION AND USE OF PLANE PARALLEL CHAMBERS FOLLOWING IAEA TRS-381 RECOMMENDATIONS

M.C. LIZUAIN, D. LINERO, C. PICÓN
Servicio de Física y Protección Radiológica,
Institut Català d'Oncologia,
Barcelona, Spain

O. SALDAÑA
Instituto Oncológico Nacional,
Panamá, Panamá

Abstract

Using different plane parallel chamber types (NACP-02, PTW Roos and PTW Markus), and a cylindrical chamber NE-2571 as reference, the IAEA TRS-381 Code of Practice has been compared with the AAPM TG-39 dosimetry protocol for plane parallel chambers. $N_{D,air}^{pp}$ was determined following the *^{60}Co in-phantom method* and the *electron bean method* described in TRS-381, using water, PMMA and RMI-457 Solid Water phantoms. Differences were smaller than 0.5% between the two methods except for the PTW Roos chamber where the discrepancy was about 1.5%. The absorbed dose to water was determined according to the procedures and data of each protocol for electron beams between 4 and 18 MeV. Differences in absorbed dose were less than 1% when measurements were made in water, but a deviation of up to 2% was found between TRS-381 and TG-39 when PMMA phantoms were used. To validate the results obtained and to investigate differences between plastic and water phantoms in electron beam dosimetry, the scaling factor C_{pl} and *the fluence correction factor* h_m for PMMA and solid water RMI-457 were measured and compared to the data in TRS-381. Good agreement was found for C_{pl}, but only when the plastics density were taken into account. The experimental values of h_m have a large uncertainty but for PMMA a trend for h_m being lower than in TRS-381 has been obtained.

1. Introduction

Several Codes of Practice for the dosimetry of electron beams have been published in the last years. The data and methods recommended in these protocols are, in some cases, slightly different. These small differences can lead to different values of the determined absorbed dose in reference conditions, even when these conditions are the same or very similar.

The goals of this project were:

a) To evaluate the differences between IAEA TRS-381 [1], AAPM TG-39 [2], and IAEA TRS-277 [3] recommendations [1] for several types of ionization chambers, and to determine the absorbed dose to water under reference conditions in electron beams for several combinations of chambers and phantoms.

b) Following the recommendations of TRS-381 [1] for the PTW Roos plane parallel chambers, to study the polarity and recombination effects in various electron beams in the energy range from 6 to 20 MeV, and to determine the necessary correction factors.

c) To compare electron beam parameters measured with a PTW Roos chamber with those obtained with an NACP chamber.

d) To evaluate the absorbed dose to air chamber factor $N_{D,air}$ of PTW Roos, NACP and PTW Markus chambers in water and plastic phantoms for electron and ^{60}Co beams.

[1] The similarity between IAEA TRS 381 [1] and the IPEMB protocol [4] makes the results obtained with TRS 381 practically applicable to those that would be obtained with the IPEMB protocol.

e) To determine values of the fluence correction factor h_m for PMMA and Solid Water RMI-457 plastic materials and to compare them with those given in TRS-381 [1].

2. Materials and method

The measurements were carried out at three linear accelerators (Varian Medical Systems, models Clinac 2100 C and Clinac 18) and one ^{60}Co unit (Theratron 780 C).

The dose measuring systems are specified in Table I.

TABLE I. DESCRIPTION OF DOSE MEASURING SYSTEMS

Plane parallel ionization chambers

Chamber model	Window material	Window thickness	Electrode spacing	Collection electrode diameter	Guard ring width
NACP-02	Mylar foil and graphite	0.104 g/cm^2	2 mm	10 mm	3 mm
PTW-Markus	Graphite polyethylene foil	0.102 g/cm^2	2 mm	5.3 mm	0.2 mm
PTW-Roos	PMMA	0.118 g/cm^2	2 mm	16 mm	4 mm

Cylindrical ionization chambers

Chamber model	Air cavity volume	Wall material	Cavity inner radius	Central electrode
NE-2571	0.69 cm^3	Graphite 0.065 g/cm^2	3.5 mm	Aluminium 1 mm
Scanditronix RK83-05	0.12 cm^3	Graphite 0.07 g/cm^2	2 mm	Aluminium 1 mm

Plastic phantoms

Material	Slab thickness	Chamber cavity	Density	Scaling factor C_{pl}
PMMA	0.2, 0.5 and 1 cm	Cylindrical and	1.190	1.123
Solid water (RMI-457)	0.2, 0.3, 0.5, 1 and 2 cm	Plane parallel	1.062	0.967[a]

[a] Initially assumed to be identical to that given in TRS-381 for Solid Water (WT1) with $\rho = 1.020$. See Section 7 for experimental work on this topic.

Water phantoms

Automated radiation field analyser RFA 300 (Scanditronix)

Water phantom 30 × 30 × 30 cm^3 MED-TEC

The IAEA TRS-381 Code of Practice [1] has been followed for the determination of the absorbed dose to air chamber factors ($N_{D,air}$) and the absorbed dose to water in reference conditions. The methods and data recommended in the AAPM TG-39 [2] and IAEA TRS-277 [3] Codes of Practice for electron dosimetry were also used and the results compared to those obtained with TRS-381.

3. Determination of $N_{D,air}^{pp}$ for a plane parallel ionization chamber

$N_{D,air}^{pp}$ calibration factors have been determined for three types of plane parallel ionization chambers NACP, PTW Markus and PTW Roos. The determinations have been

made for electron beams in water, PMMA and RMI-457 phantoms, following *"the electron beam method"* recommended in TRS-381 [1]. Three linear accelerators were employed for these determinations, using the highest energy of each one. In addition, one set of determinations was made according to the "*^{60}Co in-phantom method*".

In all the cases, a cylindrical chamber NE-2571 was used as the reference chamber. The effective point of measurement of each chamber (plane parallel and cylindrical) was positioned in the "plateau" region of the depth-dose distribution of the electron beam. The readings of the two chambers (reference cylindrical and plane parallel) were corrected for the recombination, polarity (in the case of electron beams) and pressure and temperature effects in all the cases. For the *in-phantom* measurements in the ^{60}Co beam a reference depth of 5 cm was used.

When the measurements were carried out in the electron beams, an additional NE-2571 chamber was placed in the radiation field as an external monitor. It was placed close to the reference depth in the water phantom, and at the surface in the plastic phantoms. A summary of the measurement conditions is given in Table II.

TABLE II. MEASUREMENT CONDITIONS FOR DETERMINING $N_{D,air}^{pp}$ FACTORS

	Electron beams	^{60}Co beam
Energy $\overline{E}_0$ (MeV)	15.03, 17.11 and 19.28	–
SSD (cm)	100	100
Field size (cm × cm)	15 × 15	12 × 12
Reference depth	Depth of maximum absorbed dose, R_{100}, in water. Scaled depths in plastics	5 g cm^{-2}
Phantom material	Water, PMMA, SW RMI-457	Water, PMMA
Plane parallel chambers	NACP-02, Markus, Roos	NACP-02, Markus, Roos
Reference chamber	NE - 2571	NE - 2571
Monitor chamber	NE - 2571	No
$P_{P,T}$ correction	Yes	Yes
p_s, p_{pol} correction	Yes	No

Numerical values of $N_{D,air}^{pp}$ (expressed in mGy/nC) for the plane parallel chambers studied are given in Table III, where the uncertainties given correspond to the standard deviation of the mean value. The last column gives the ratio of the results obtained with the *^{60}Co in-phantom method* to those obtained with *electron beam method.* The perturbation factor p_{wall} used in the determination of $N_{D,air}^{pp}$ of the Roos chambers for the *^{60}Co in-phantom method* was 1.003 [1]. The differences for the NACP-02 and Markus chambers are of the same order as the standard deviation of the measurements. In the cases of the Roos chambers the discrepancy between the two methods is larger than 1%.

A set of determinations of the $N_{D,air}$ factor for the Roos chamber s/n 57 had been carried out in 1998 [5, 6], yielding a large discrepancy (up to 2.8%) between the two values determined using the electron method and the ^{60}Co method. The measurements in ^{60}Co had been made only in a PMMA phantom, and since no values are available for p_{wall} for the Roos chamber in PMMA, a value equal to one was assumed. This assumption most likely represented the largest contribution to the discrepancy found.

TABLE III. COMPARISON OF $N_{D,air}^{pp}$ FACTORS (mGy/nC) DETERMINED IN THIS WORK

Ionization chamber	Electron beam method [a]	In-phantom ^{60}Co method [b]	Ratio ^{60}Co/electron
NACP-02	151.7 ± 0.2	150.8 ± 0.1	0.994
PTW – Markus	483.4 ± 0.9	484.4 ± 1.3	1.002
PTW – Roos s/n 57	76.51 ± 0.06	77.54 ± 0.01	1.013
PTW – Roos s/n 253	71.98 ± 0.08	72.73 ± 0.11	1.010
PTW – Roos FK-06	69.72 ± 0.08	70.78 ± 0.09 [c]	1.015

[a] Average of values determined in water, PMMA and Solid Water.

[b] Average of values determined in water and PMMA, except (c).

[c] Average of values determined in water.

4. Electron beam quality specification with Roos and NACP chambers

The energy parameters that specify the quality of the electron beams have been determined from depth-ionization curves measured in a water phantom with Roos and NACP chambers for the conditions given in Table IV. The readings of the two ionization chambers have not been corrected for saturation and polarity effects. The thickness of the front wall of the chambers (in mm) has been taken into account, but these have not been converted into equivalent depths in water.

TABLE IV. REFERENCE CONDITIONS AND EXPERIMENTAL SET-UP FOR MEASURING DEPTH-DOSE CURVES IN ELECTRON BEAMS

Source Surface Distance (cm)	100
Field size (cm × cm)	25 × 25
Water phantom	Scanditronix RFA 300
Measurement chambers	Roos and NACP
Monitor chamber	Scanditronix RK 8305
Scan Step (mm)	0.5 and 1.0

$\overline{E}_0$ and $E_{p,0}$ have been calculated from the ranges R^{J}_{50} and R_{p} with the empirical relations recommended, respectively, in TRS-381 [1] and TRS-277 [3].

$$\overline{E}_0\ (MeV) = 0.818 + 1.935R_{50}^{J} + 0.040\left(R_{50}^{J}\right)^2 \quad (1)$$

$$E_{p,0}\ (MeV) = 0.22 + 1.98R_p + 0.0025R_p^2 \quad (2)$$

where, R_{50}^{J} and R_{p} are the average values obtained from ten depth-ionization curves. The standard deviation was less than 0.5 mm in all the cases. The difference between the average depth-ionization curves obtained with the two chambers varies between 0.4 and 1.1 mm, depending on the beam energy.

The measured depth-ionization curves have subsequently been converted into depth-dose curves and the parameters corresponding to these distributions re-evaluated. These are given in Table V.

TABLE V. ENERGY PARAMETERS OF ELECTRON BEAMS DETERMINED WITH NACP AND ROOS PLANE PARALLEL CHAMBERS

	R^{D}_{100} (mm)	R^{J}_{50} (mm)	R_p (mm)	$\overline{E}_0$ (MeV)	$E_{P,0}$ (MeV)
E_{nom} = 18 MeV					
Roos chamber	19.5 ± 6.0	71.3 ± 0.1	89.4 ± 0.0	16.7 ± 0.0	18.1 ± 0.0
NACP chamber	18.0 ± 6.0	71.0 ± 0.3	89.1 ± 0.1	16.6 ± 0.1	18.1 ± 0.0
Difference (%)	5.9 (1.1 mm)	0.5	0.4	0.5	0.5
E_{nom} = 15 MeV					
Roos chamber	19.0 ± 5.0	56.1 ± 0.1	70.3 ± 0.5	12.9 ± 0.0	14.3 ± 0.1
NACP chamber	20.0 ± 5.0	55.9 ± 0.2	70.1 ± 0.7	12.9 ± 0.1	14.2 ± 0.1
Difference (%)	3.6 (0.7 mm)	0.2	0.4	0.2	0.4
E_{nom} = 16 MeV					
Roos chamber	30.5 ± 4.2	64.8 ± 0.1	78.9 ± 0.1	15.0 ± 0.0	16.0 ±0.0
NACP chamber	30.5 ± 4.2	64.3 ± 0.2	78.6 ± 0.4	14.9 ± 0.1	15.9 ±0.1
Difference (%)	0.0	0.7	0.5	0.7	0.5
E_{nom} = 12 MeV					
Roos chamber	27.5 ± 2.5	49.0 ± 0.1	60.0 ± 0.2	11.3 ± 0.0	12.2 ± 0.0
NACP chamber	28.0 ± 2.5	48.7 ± 0.1	59.4 ± 0.1	11.2 ± 0.0	12.1 ± 0.0
Difference (%)	1.4 (0.4 mm)	0.7	1.1	0.7	1.1
E_{nom} = 9 MeV					
Roos chamber	20.4 ± 1.8	34.5 ± 0.1	42.4 ± 0.1	8.0 ± 0.0	8.6 ± 0.0
NACP chamber	20.5 ± 1.8	34.6 ± 0.1	42.4 ± 0.1	8.0 ± 0.0	8.7 ± 0.0
Difference (%)	0.5 (0.1 mm)	0.4	0.2	0.4	0.2
E_{nom} = 6 MeV					
Roos chamber	12.8 ± 1.4	22.9 ± 0.1	28.6 ± 0.0	5.5 ± 0.0	5.9 ± 0.0
NACP chamber	13.0 ± 1.3	23.0 ± 0.1	29.0 ± 0.1	5.5 ±0.0	6.0 ± 0.1
Difference (%)	0.8 (0.1 mm)	0.2	1.4	0.2	1.3
E_{nom} = 4 MeV					
Roos chamber	7.2 ± 1.0	13.2 ± 0.1	17.1 ± 0.6	3.4 ± 0.0	3.6 ± 0.1
NACP chamber	6.7 ± 1.0	13.3 ± 0.0	16.9 ± 0.1	3.5 ± 0.0	3.6 ± 0.0
Difference (%)	0.6 (0.4 mm)	0.4	1.2	0.3	1.1

The difference in the values of the energy parameters determined with the two chambers was of the same order as the standard deviation. Because of the small variations in the depth-dose curves, especially in the region close to the phantom surface, the depth of maximum dose (R^{D}_{100}) was calculated as the average value of the depth where the percentage dose was higher than 99.5%. The standard deviations of 5 or 6 mm correspond to high-energy electron beams having a wide "plateau" in the depth-dose distribution. Thus, the difference in the depth of maximum dose of 1.1 mm in the electron beam of 18 MeV is probably due to uncertainty in the chamber position. A comparison between the two sets of parameters shows that these are differences of about 0.5% in $\overline{E}_0$ and $R_{p;}$ these imply differences of less than 0.05% in $s_{w,air}$, and therefore in the absorbed dose determined for the reference conditions.

5. Determination of recombination and polarity correction factors for NE-2571, PTW Roos, NACP and PTW Markus ionization chambers

The determination of the recombination correction factor p_s for the chambers has been made using the *"two voltage"* method [7] and the polynomial fit included in TRS-277 [3]. The polarity factor p_{pol} has been determined as $\frac{|Q_+| + |Q_-|}{2|Q_-|}$.

Measurements have been performed in electron beams of mean energy $\overline{E}_0$ from 5.51 to 19.28 MeV (E_{nom} between 6 and 20 MeV) in water and Solid Water RMI-457 phantoms. In all cases, one external monitor chamber (NE-2571) was used, placed in the conditions described above.

The polarising voltages used were –300, +300 and –100 V for the cylindrical chambers and –100, +100 and –34 V for the plane parallel chambers. After changing the polarising voltage, enough time was allowed for reaching stable conditions, between 5 and 10 minutes.

The measurement conditions are given in Table VI.

TABLE VI. MEASUREMENT CONDITIONS FOR THE DETERMINATION OF RECOMBINATION AND POLARITY CORRECTION FACTORS

Mean energy at surface $\overline{E}_0$	5.51 – 19.28 MeV
Source to surface distance	100 cm
Field size	10 × 10 cm^2
Measurement depth	Depth of maximum of absorbed dose, R_{100}
Monitor chamber	NE 2571
Polarising voltage	± 300 V, ± 100 V and ± 34 V
Phantom	Water and solid water
Dose rate range	2.4 – 3 Gy/min

The numerical values obtained are given in Tables VII and VIII, together with the standard deviation of the mean values. The polarity correction is less than 0.1% for all chambers, but slightly higher for the PTW Markus chamber.

TABLE VII. POLARITY CORRECTION FACTOR

$\overline{E}_0\ (MeV)$	NE-2571	NACP	PTW-Markus	PTW-Roos
5.51	–	1.0000 ± 0.0005	0.9922 ± 0.0003	0.9996 ± 0.0001
8.16	–	1.0000 ± 0.0005	0.9940 ± 0.0005	1.0000 ± 0.0001
11.32	0.9987 ± 0.0002	1.0000 ± 0.0004	0.9959 ± 0.0005	1.0000 ± 0.0001
15.15	1.0000 ± 0.0003	1.0003 ± 0.0007	0.9953 ± 0.0004	1.0003 ± 0.0001
19.28	1.0005 ± 0.0001	1.0000 ± 0.0006	0.9981 ± 0.0005	1.0000 ± 0.0001

TABLE VIII. RECOMBINATION CORRECTION FACTOR

$\overline{E}_0\ (MeV)$	NE-2571	NACP	PTW-Markus	PTW-Roos
5.51	–	1.0112 ± 0.0008	1.0118 ± 0.0010	1.0094 ± 0.0002
8.16	–	1.0114 ± 0.0006	1.0134 ± 0.0006	1.0113 ± 0.0002
11.32	1.0109 ± 0.0003	1.0129 ± 0.0006	1.0140 ± 0.0023	1.0117 ± 0.0002
15.15	1.0113 ± 0.0005	1.0135 ± 0.0007	1.0147 ± 0.0025	1.0123 ± 0.0003
19.28	1.0005 ± 0.0003	1.0124 ± 0.0007	1.0156 ± 0.0008	1.0113 ± 0.0001

6. Determination of absorbed dose to water: comparison of different Codes of Practice

The absorbed dose to water in electron beams at different energies has been determined under reference conditions using several combinations of ionization chambers (cylindrical and plane parallel) and phantoms (water and PMMA). The determination has been made following the recommendations of TRS-381, TG-39 and TRS-277 Codes of Practice [1–3].

Measurements have been performed for a range of energies $\overline{E}_0$ between 3.3 and 17.1 MeV, at an SSD of 100 cm, with a field of 10 × 10 cm^2, in water and PMMA phantoms. The effective point of measurement of the chambers was placed at the reference depth in each phantom (scaled depths for plastics). Corrections for influence quantities (temperature, pressure, polarity and recombination effects) have been applied. The position of the chamber effective point of measurement, and the numerical values of the scaling factor, fluence correction factor and $s_{w,air}$ used were the values recommended in the four protocols compared.

A comparison was made first of the $N_{D,air}$ factors of cylindrical and plane parallel chambers determined according to the electron beam method recommended in TRS-381 and the other three protocols. The comparison between TRS-381 and TRS-277 yielded differences smaller than 0.5%, which were basically caused by the difference between $p_{cel\text{-}glob}$ (TRS-277) and $p_{cel}k_{cel}$ (TRS-381). In the case of TG-39, in spite of the differences in various physical quantities and factors ($s_{graphite,air}$ for Co-60, W/e, β_{wall}, etc.) most discrepancies cancelled out and the factors for the plane parallel chambers were within 0.5% for the two protocols. The difference between TRS-381 and IPMEB was negligible in all cases.

The differences in the absorbed dose determined according to the three protocols were less than 1% for all the chambers when measurements were made in water. A large deviation (up to 2%) was found, however, between the absorbed dose values obtained using TRS-277, TRS-381 and TG-39 when the measurements were made in PMMA phantoms. This disagreement was mainly caused by the different scaling procedures plastic/water used in these protocols (C_{pl}), the fluence correction factor h_m, and the mean restricted mass stopping power ratio ($s_{w,air}$) versus the product of $s_{PMMA,air}$ by the ratio of the mean unrestricted mass collision stopping power of water to PMMA ($s_{w,PMMA}$) recommended in TG-39.

Ratios of the absorbed dose to water determined following TRS-277 and TG-39 to that obtained using TRS-381, for measurements carried out in PMMA with several ionization chambers are plotted in Figs 1 and 2. Note that these figures supersede the corresponding figures in Ref. [5], where results previous to 1998 were reported but a mistake related to the scaling of depths had been made.

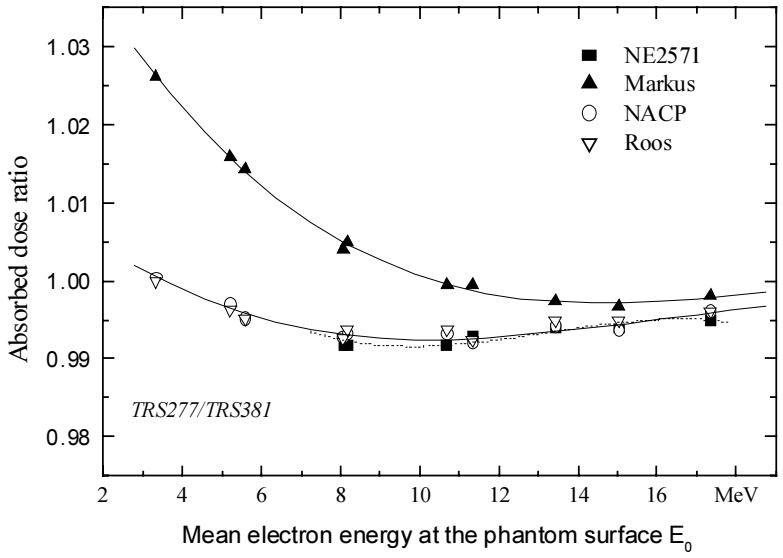

FIG. 1. Ratios of the absorbed dose to water determined according to TRS-277 and TRS-381 as a function of the mean energy at the phantom surface. Measurements performed in a PMMA phantom.

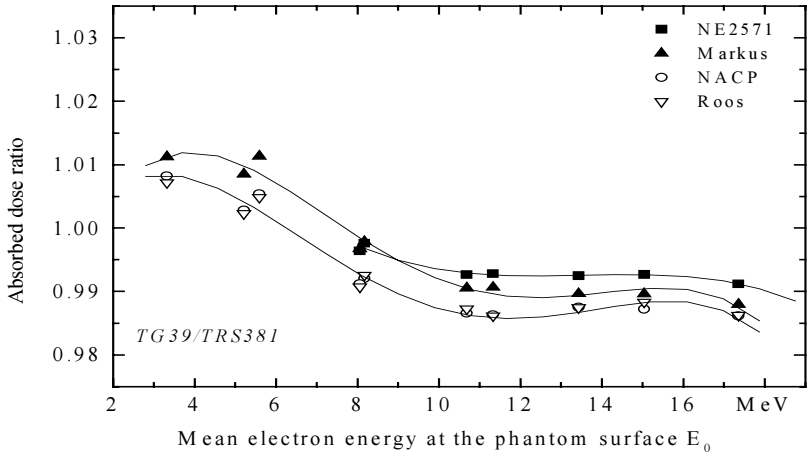

FIG. 2. Ratios of the absorbed dose to water determined according to TG-39 and TRS-381 as a function of the mean energy at the phantom surface. Measurements performed in a PMMA phantom.

7. Investigation on the scaling factor C_{pl}

The scaling factor C_{pl} is defined in TRS-381 as a material-dependent factor, that converts ranges and depths measured in plastic phantoms into the corresponding values in water. The recommended values are 1.123 for PMMA (for $\rho = 1.190$) and 0.967 for Solid Water WT1 (for $\rho = 1.020$).

To validate these values for the plastic phantoms used in our work, measurements of depth-ionization curves were performed in PMMA, Solid Water RMI-457 and water, using PTW Roos and NACP plane parallel ionization chambers, in electron beams of several energies (see Table IX).

The water phantom employed was an automated Radiation Field Analyser RFA 300 from Scanditronix. The solid water phantoms, PMMA and RMI-457, consisted of 30 × 30 cm^2 slabs with thickness varying from 2 mm to 10 mm and 2 mm to 50 mm, respectively.

TABLE IX. MEASUREMENT CONDITIONS OF DEPTH-IONIZATION DISTRIBUTIONS IN PLASTIC PHANTOMS

	PMMA	Solid Water RMI-457
Nominal energy (MeV)	6, 12, 20	6, 9, 12, 16, 20
Field size	25 × 25 cm^2	25 × 25 cm^2
Plane parallel chamber	PTW Roos	PTW Roos and NACP-02
Monitor chamber	NE-2571	NE-2571
$p_{P,T}$ correction	Yes	Yes
p_s, p_{pol} correction	No	No

All measurements were made at an SSD of 1 m in electron beams produced by a Clinac 2100 C linear accelerator, having nominal electron beam energies of 6, 9, 12, 16 and 20 MeV. A NE-2571 cylindrical ionization chamber was used as external monitor, placed in air at the lowest position of the treatment head, with its build-up cap. The tip of the monitor chamber was positioned just within the light field to ensure negligible perturbation in the measurements of the electron field. Readings obtained from the plane parallel ionization chambers were divided by the monitor chamber readings, thus eliminating the effects of drift in the output of the linear accelerator throughout the experiments.

Each solid phantom material had one slab with a cavity to accept an ionization chamber. The slabs were position to maintain a fixed SSD. In this procedure one or more slabs are moved from underneath the chamber to a position above the chamber or vice versa. Thus the total number of slabs in the solid phantom stack remained constant and the SSD also remained constant. The couch supporting the stack of slabs was not moved during these measurements. To provide adequate backscatter, at least 10 cm of the solid phantom material were placed under the point of measurement at all times.

Depth dose curves in plastic have been derived in an approximate manner from depth ionization curves in PMMA and Solid Water RMI-457 [8], correcting each data point by the factor $\frac{(S/\rho)_{plastic}}{(S/\rho)_{water}} s_{w,air}$ where the values of the (S/ρ)-ratio were taken from Ref. [9]. No significant differences were found between $R_{50,w}/R_{50,plastic}$ obtained from the ionization and from the dose curves (see Tables X and XI).

A scaling factor was determined from the ratio $R_{50,w}/R_{50,plastic}$ for all the depth-dose curves measured. Good agreement was found between the value calculated by us for PMMA (1.121) and the C_{pl} factor given in TRS-381 (1.123) for a density of 1.190 g cm^{-3} (see Fig. 3).

In the case of Solid Water RMI-457, although the density stated by the manufacturer (1.030 g cm^{-3}) was slightly different than the value quoted in TRS-381 for WT1 (1.020 g cm^{-3}), the C_{pl} given for this material in TRS-381 was used first without including the ratio ρ_{user}/ρ_{table} recommended in TRS-381. The discrepancy between C_{pl} and the ratio $R_{50,w}/R_{50,plastic}$ measured from our depth-dose curves was significant (see Fig. 4).

These results suggested that the Solid Water materials WT1 and RMI-457 were very different. Therefore, an estimation of the density of SW RMI-457 was made, obtaining ρ = 1.062 ± 0.4% g cm^{-3}, which is different from the values published by Tello et al. [10] (1.045 g cm^{-3}) and Nisbet and Thwaites [11] (1.04 g cm^{-3}) for the same material. In light of this, the

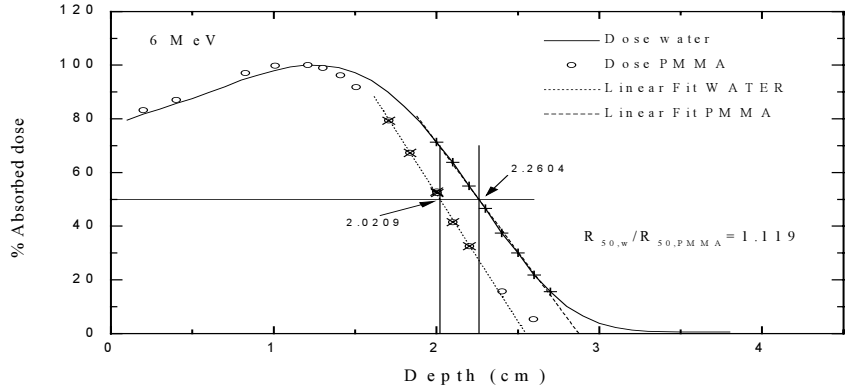

FIG. 3. Depth dose curves of a 6 MeV electron beam determined in water and PMMA with a Roos plane parallel chamber. The scaling factor has been determined as the ratio $R_{50,w}/R_{50,PMMA}$.

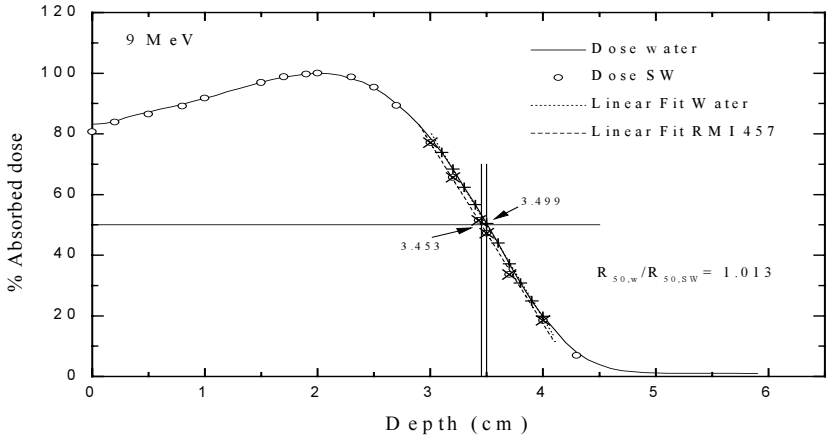

FIG. 4. Depth dose curves of a 9 MeV electron beam determined in water and SW RMI-457 with a Roos plane parallel chamber. The scaling factor has been determined as the ratio $R_{50,w}/R_{50,SW}$.

need for measuring the density of the material, and include the ratio ρ_{user}/ρ_{table} in the use of C_{pl}, as recommended by TRS-381 [1] becomes evident.

Using the ratio ρ_{user}/ρ_{table} together with the value of C_{pl} given in TRS-381, a value for this product equal to 1.007 was obtained for SW RMI-457, in excellent agreement with the ratios $R_{50,w}/R_{50,plastic}$ determined in this work (see Table X). This provides an experimental confirmation of the Monte Carlo calculated values given in TRS-381.

TABLE X. DETERMINATION OF THE SCALING FACTOR FOR A SOLID WATER RMI-457 PHANTOM WITH DENSITY 1.062 g cm^{-3} [a]

$\overline{E}_0$ (MeV)	5.51	8.16	11.32	15.15	19.28	Mean for all energies measured	SDOM [b]
$\frac{R^J_{50,W}}{R^J_{50,SW}}$	1.009	1.011	1.001	1.011	1.004	1.007	0.002
$\frac{R^D_{50,W}}{R^D_{50,SW}}$	1.010	1.013	1.002	1.011	0.997	1.007	0.003

[a] Note that this scaling factor should be compared with the product $C_{pl}\ \rho_{user}/\rho_{table}$ as recommended in TRS-381. In this case, ρ_{user}=1.062 g cm^{-3} and ρ_{table}= 1.020 g cm^{-3}; combined with C_{pl} = 0.967, the product yields 1.007.

[b] Standard deviation of the mean value.

TABLE XI. DETERMINATION OF THE SCALING FACTOR FOR A PMMA PHANTOM WITH DENSITY 1.190 g cm^{-3}

$\overline{E}_0\ (MeV)$	5.51	11.32	19.28	Mean for all energies measured	SDOM [a]
$\frac{R^J_{50,W}}{R^J_{50,PMMA}}$	1.120	1.119	1.123	1.121	0.001
$\frac{R^D_{50,W}}{R^D_{50,PMMA}}$	1.119	1.119	1.125	1.121	0.002

[a] Standard deviation of the mean value.

Figures 5 and 6 show depth-dose curves determined in water and plastic phantoms. The depths in plastic have been scaled according to the results obtained in this work, 1.121 for PMMA and 1.007 for Solid Water RMI-457. The difference between the two families of curves (water and plastic) is less than 0.5% for all measured depths.

8. Fluence correction factor

8.1. First determination of fluence correction factors (1998)

A first set of determinations of the h_m factor for PMMA was performed from the measurements carried out in water and in PMMA for absorbed dose determinations. The factor was obtained as

$$h_m = \frac{M_{water}(z_{ref,water})}{M_{PMMA}(z_{ref,PMMA})} \tag{3}$$

where $z_{ref,PMMA}$ is obtained from $z_{ref,water}$ using a scaling factor $C_{pl} = 1.123$ [1].

The measurements were performed in water and PMMA phantoms in the electron beams produced by a Clinac 18 and a Clinac 2100 C, covering a range of mean energies $\overline{E}_z$ from 1.8 to 12.5 MeV. The measurement conditions were SSD=100 cm, field size 10 × 10 cm^2, depth of maximum dose in water and scaled depths in PMMA. In all the measurements, corrections for p_{PT}, p_s and p_{pol} were applied to the chamber readings M. NACP and Roos plane parallel chambers were used with a NE-2590 Dose Master electrometer. The results are presented in Table XII.

The discrepancy between h_m in TRS-381 and that obtained from Eq. (3) was about 1% for the two chambers. Due to the difficulty of reproducing the measurement conditions for the two phantoms, this difference was included in the measurement uncertainty.

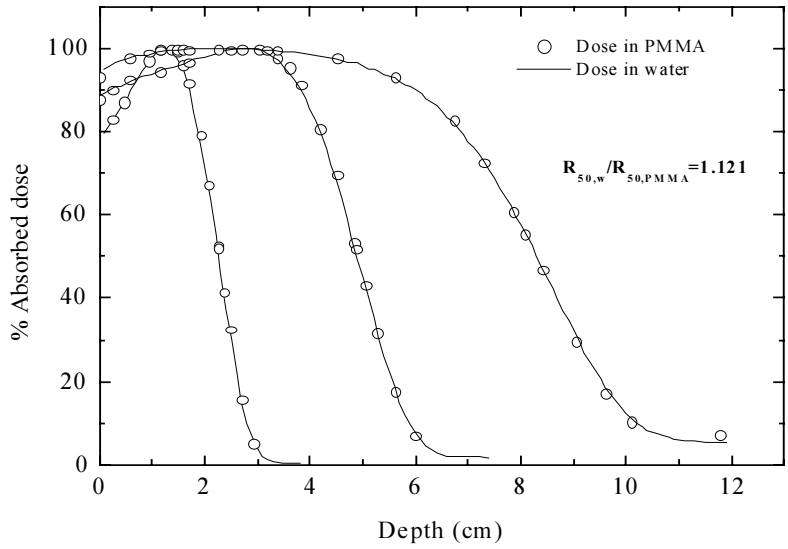

FIG. 5. Depth dose distributions of electron beams with nominal energies 6, 12 and 20 MeV, measured in water and PMMA. Depths in PMMA have been corrected by a scaling factor of 1.121, determined experimentally for PMMA with ρ = 1.190 g cm^{-3}.

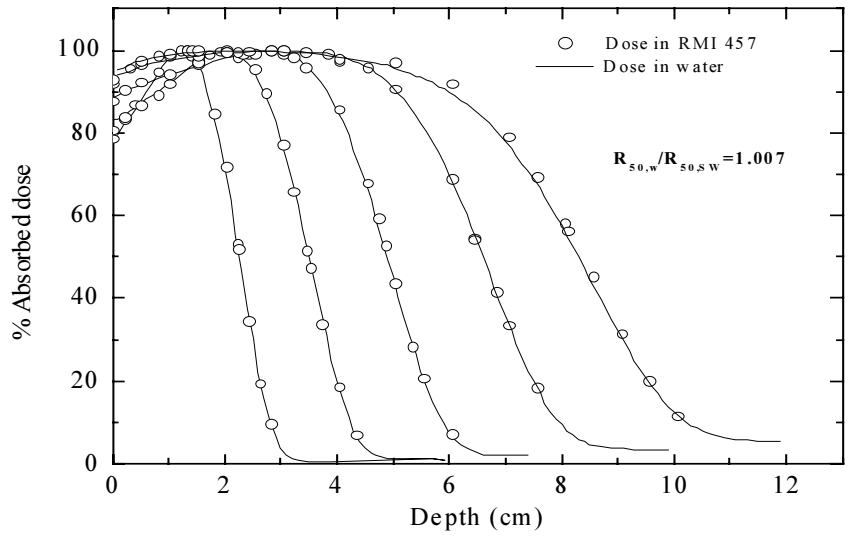

FIG. 6. Depth dose distributions of electron beams with nominal energies 6, 9, 12, 16 and 20 MeV, measured in water and Solid Water RMI-457. Depths in SW RMI-457 have been corrected by a scaling factor of 1.007, determined experimentally for SW RMI-457with ρ = 1.062 g cm^{-3}.

TABLE XII. COMPARISON BETWEEN THE FLUENCE CORRECTION FACTORS DETERMINED IN THIS WORK (1998) AND THE h_m VALUES GIVEN IN TRS-381

$\overline{E}_z\ (MeV)$	NACP-02	Roos (PTW)	h_m (TRS-381)	NACP-02 Difference %	Roos (PTW) Difference %
1.86	1.019	1.003	1.009	0.98	0.57
2.45	1.003	0.999	1.009	0.64	0.95
3.50	1.004	0.996	1.008	0.44	1.20
4.10	1.004	0.999	1.008	0.39	0.93
4.83	1.001	0.999	1.008	0.70	0.93
6.24	1.008	1.003	1.007	0.07	0.40
8.18	1.004	0.995	1.005	0.09	0.95
8.90	1.003	1002	1.005	0.17	0.29
12.53	0.997	0.995	1.003	0.63	0.84

8.2. Second determination of fluence correction factors (1999)

Common measurement conditions had been agreed by the participants of the project during a meeting in 1998 with the purpose of decreasing the uncertainty of the measurements. These conditions have been described above.

The fluence correction factor h_m may be obtained as the ratio of the detector readings at the depth of maximum ionization (on the central axis) in a water phantom and at the depth of maximum ionization in another phantom material.

$$h_m = \left(\frac{\phi_{water}}{\phi_{plastic}} \right)_{R_{100}} = \frac{\left(M_{water}(p_{P,T})_{water} \right)_{R_{100,water}}}{\left(M_{plastic}(p_{P,T})_{plastic} \right)_{R_{100,plastic}}} \tag{4}$$

Following the conditions agreed, the fluence correction factor h_m was determined for PMMA and Solid Water RMI-457 using a NE-2571 cylindrical ionization chamber and NACP, PTW Markus and PTW Roos plane parallel ionization chambers.

Measurements were performed in electron beams produced by three linear accelerators covering a range of nominal energies from 4 to 20 MeV. The field size was 15 × 15 cm^2 without electron cone, at SSD = 1 m (see Table XIII).

The in-water ionization measurements were made in a 30 × 30 × 30 cm^3 water phantom (produced by MED-TEC). In order to maintain the constancy of the nominal SSD and the chamber depth, the water level was closely monitored for water evaporation. It is emphasized that during all measurements the surface of the water and plastic phantoms were always maintained at the same level, thereby the couch was not moved in this experiment. Consequently, the uncertainty resulting from the experimental set-up was minimised.

For each energy, three sets of measurements were taken: plastic/water/plastic. The electron cone was not used in order to have enough space for exchanging the phantom without moving the gantry or the couch.

All electrometer readings were corrected for pressure and temperature. A cylindrical ionization chamber NE-2571 was used as external monitor, placed in air at the lowest position

TABLE XIII. MEASUREMENT CONDITIONS FOR THE NEW DETERMINATIONS OF h_m

	PMMA phantom	Solid water phantom
Radiation unit	Clinac 18 and Clinac 2100C #768	Clinac 2100C #1336
Nominal energy (MeV)	4 – 18	6 – 20
$\overline{E_0}\ (MeV)$	3.31 – 17.11	5.51 – 19.28
Measurement depth	Depth of maximum ionization	Depth of maximum ionization
$\overline{E_z}\ (MeV)$	1.89 – 12.52	2.63 – 12.73
Field size (No Cone)	15 × 15 cm^2	15 × 15 cm^2
Monitor chamber	NE – 2571	NE – 2571
$p_{P,T}$ correction	Yes	Yes
p_s, p_{pol} correction	No	No

of the treatment head, with its build-up cap. The fluctuations of the room temperature can result in corrections of the monitor chamber of the same order as the h_m values; therefore the room and phantom temperatures were measured frequently (every 10 seconds) throughout the measurements. Five readings were taken at each point, and the experiment was performed three times (on different days) in most cases.

The h_m values obtained are plotted as a function of the mean energy at depth $\overline{E}_z$ in Figs 7 and 8 for PMMA and RMI-457, respectively. These values are given in Tables XIV and XV including the standard deviation of the mean value of the determinations

The difference between the values of h_m obtained in a PMMA phantom with several chambers was lower than the standard deviation of the measurements; thus it can be concluded that there is no significant difference between the type of chambers used. The measured values are about 0.5% lower than those given in TRS-381 for the range of energies used.

In the case of h_m for Solid Water RMI-457, due to the large number of measurements the dispersion of the measurements was lower (1 SD < 0.5%) than for PMMA. However, a larger discrepancy was found between the measured values for this material and the values recommended in TRS-381 than for PMMA. This discrepancy decreases when the energy increases, probably due to a lower uncertainty in the positioning of the chamber at the depth of maximum absorbed dose.

The largest differences of the water/RMI-457 ratios between this work and TRS-381 correspond to measurements with the PTW Roos and NE-2571 chambers. These values are in agreement with the results published by Tello et al. [10] for cylindrical chambers. Figure 8 shows a dependence with the chamber type, in contrast with the results for PMMA.

In spite of being extremely careful with the performance of this experiment, we have not been able to decrease the standard deviation of the measurements to a level negligible in relation to the values of the parameters to be determined. The fluctuations in the room temperature lead to corrections of 0.5% or more in the readings of the chamber when placed in the plastic phantom or in air (monitor chamber), and it is not possible to assure that the temperature of the chamber cavity air is the same as that read on the thermometer. Therefore, an error could have been introduced instead of performing a correction for this effect.

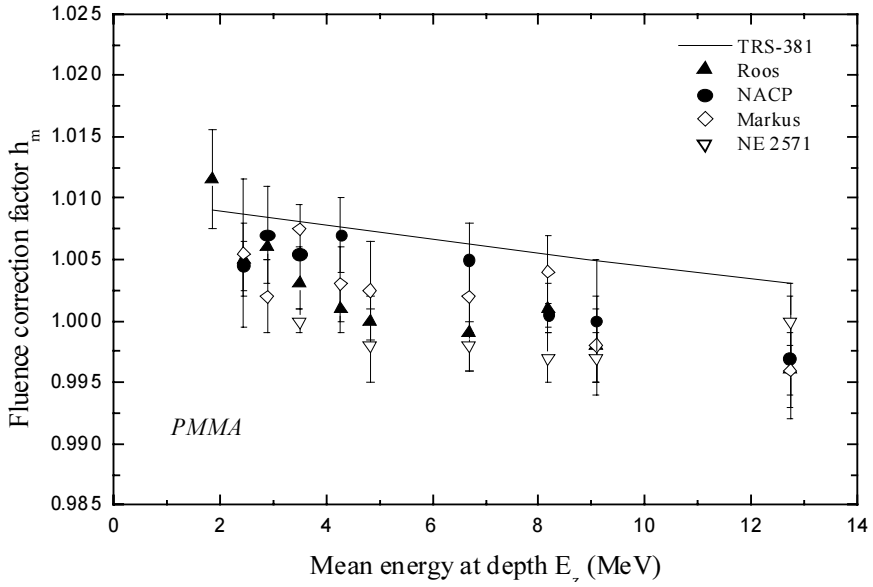

FIG. 7. Fluence ratios h_m for PMMA as a function of the mean energy at depth. Measurements performed with different ionization chambers. The uncertainty bars correspond to the standard deviation of the mean values shown.

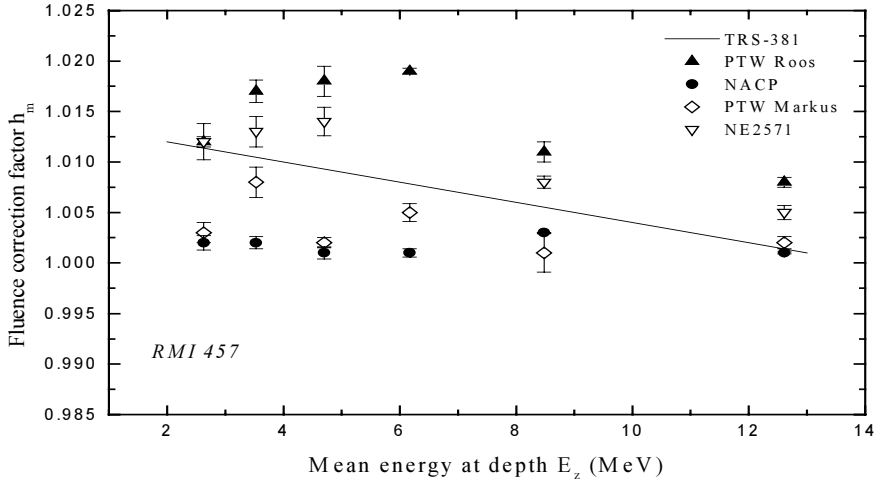

FIG. 8. Fluence ratios h_m for Solid Water RMI-457 as a function of the mean energy at depth. Measurements performed with different ionization chambers. The uncertainty bars correspond to the standard deviation of the mean values shown.

TABLE XIV. EXPERIMENTALLY DETERMINED FLUENCE CORRECTION FACTORS h_m FORSOLID WATER RMI-457

$\overline{E_z}$ (MeV)	PTW Roos	PTW Markus	NACP-02	NE 2571
2.63	1.012 ± 0.0006	1.003 ± 0.001	1.002±0.0.0006	1.012 ± 0.002
3.53	1.017 ± 0.001	1.008 ± 0.002	1.002 ± 0.0006	1.013 ± 0.001
4.70	1.018 ± 0.001	1.002 ± 0.0006	1.001 ± 0.006	1.014 ± 0.001
8.48	1.011 ± 0.001	1.001± 0.002	1.001 ± 0.004	1.008 ± 0.0007
12.6	1.008 ± 0.0004	1.002 ± 0.0004	1.001 ± 0.001	1.005 ± 0.0007

TABLE XV. EXPERIMENTALLY DETERMINED FLUENCE CORRECTION FACTORS h_m FOR PMMA

$\overline{E_z}$ (MeV)	PTW Roos	PTW Markus	NACP-02	NE 2571
1.86	1.012 ± 0.004	–	–	–
2.45	1.005 ± 0.003	1.006 ± 0.006	1.005 ± 0.002	–
2.89	1.006 ± 0.001	1.002 ± 0.003	1.007 ± 0.004	–
3.50	1.003 ± 0.002	1.008 ± 0.002	1.006 ± 0.0005	1.000 ± 0.001
4.28	1.001 ± 0.002	1.003 ± 0.003	1.007 ± 0.003	–
4.83	1.000 ± 0.002	1.003 ± 0.004	–	0.998 ± 0.003
6.69	0.999 ± 0.003	1.002 ± 0.004	1.005 ± 0.003	0.998 ± 0.002
8.18	1.001 ± 0.002	1.004 ± 0.003	1.001 ± 0.001	0.997 ± 0.002
9.08	0.998 ± 0.003	0.998 ± 0.004	1.000 ± 0.005	0.997 ± 0.002
12.73	0.996 ± 0.003	0.996 ± 0.001	0.997 ± 0.005	1.000 ± 0.003

REFERENCES

[1] INTERNATIONAL ATOMIC ENERGY AGENCY, The Use of Plane Parallel Ionization Chambers in High Energy Electron and Photon Beams — An International Code of Practice for Dosimetry, Technical Reports Series No 381, IAEA, Vienna (1997).

[2] AMERICAN ASSOCIATION OF PHYSICISTS IN MEDICINE, Task Group 39: The calibration and use of plane parallel ionization chambers for dosimetry of electron beams: An extension of 1983 protocol, Med. Phys. **21** (1994) 1251.

[3] INTERNATIONAL ATOMIC ENERGY AGENCY, Absorbed Dose Determination in Photon and Electron Beams — An International Code of Practice, Technical Reports Series No 277, IAEA, Vienna (1987).

[4] INSTITUTION OF PHYSICS AND ENGINEERING IN MEDICINE AND BIOLOGY, Working Party, The IPEMB code of practice for electron dosimetry for radiotherapy beams of initial energy from 2 to 50 MeV based on an air kerma calibration. Phys. Med. Biol. 41 (1996) 2557.

[5] INTERNATIONAL ATOMIC ENERGY AGENCY, Dose determination with plane parallel ionization chambers in therapeutic electron and photon beams. IAEA SSDL Newsletter. 40 (1999) 4–16.

[6] LIZUAIN, M.C., LINERO, D., PICON, C., ANDREO, P., Determination of absorbed dose to water in electron beams with plane parallel chambers. Comparison between IAEA TRS-381, TRS-277 and AAPM TG-39 recommendations. Medical & Biological Engineering & Computing **35**, sup. 2: 889 (1997).

[7] BOAG, J.W., CURRANT, J., Current collection and ionization recombination in small cylindrical ionization chambers exposed to pulsed radiation, Br. J. Radiol. **53** (1980) 471.

[8] ANDREO, P., personal communication (1999).

[9] INTERNATIONAL COMMISSION ON RADIATION UNITS AND MEASUREMENTS, Tissue Substitutes in Radiation Dosimetry and Measurement, ICRU Report 44, ICRU, Bethesda, MD (1989).

[10] TELLO, V.M., TAILOR, R.C., HANSON, W.F., How water equivalent is solid material for output calibration of photon and electron beams? Med. Phys. **22** (1995) 1177.

[11] NISBET, A., THWAITES, D., An evaluation of epoxy resin phantom materials for electron dosimetry. Phys. Med. Biol. **43** (1998) 1253.

EXPERIMENTAL DETERMINATION OF p_{cav} FACTORS FOR CYLINDRICAL IONISATION CHAMBERS IN ELECTRON BEAMS

Å. PALM, O. MATTSSON
Department of Radiation Physics,
Göteborg University,
Göteborg, Sweden

Abstract

The electron beam method recommended for calibrating plane parallel ionisation chambers involves cavity correction factors for cylindrical chambers. The cavity correction factors in the IAEA TRS-381 Code of Practice are based on measurements at R_{100} in a PMMA phantom using PMMA cylindrical chambers having different cavity radii. In the present work the recommended data were confirmed for electron beams delivered by modern medical accelerators by using the very same phantom and ionisation chambers that were used in the original work. From another series of measurements, using four specially designed wall-less chambers in a graphite phantom, the linear relation between p_{cav} and the chamber radius that is the basis for the experimental method, was verified. The method was also used to determine the cavity correction factors for a set of Farmer-like graphite chambers placed in water. Compared to the TRS-381 Code of Practice a smaller correction was found for the cavity perturbation for the graphite chambers used in water.

1. Introduction

When an air-filled cavity is inserted into a medium irradiated by electrons, the electron fluence will be perturbed, compared to the undisturbed medium irradiated under identical conditions. The perturbation at a certain depth depends on the shape and the size of the air cavity and on the radiation beam quality. In the TRS-381 Code of Practice [1] a correction factor denoted by p_{cav} is applied to account for the fluence perturbation. The effect is mainly of concern when using cylindrical ionisation chambers, while the effect is negligible for properly designed plane parallel chambers. However, cylindrical ionisation chambers are often used for the cross-calibration of plane parallel chambers, preferably in a high-energy electron beam [1, 2]. Consequently, the fluence perturbation correction factors for the cylindrical chambers are of importance also for plane parallel chamber dosimetry.

The fluence perturbation correction factors recommended by most dosimetry protocols are based on the experimental work of Johansson et al. [3]. These correction factors were determined using cylindrical PMMA chambers with different cavity radii, but with the same cavity length. The measurements were made in a PMMA phantom at the depths of maximum ionisation for the different chambers. Johansson et al. found a linear relation between the fluence perturbation correction factor and the cavity radius, in contradiction to the $\sqrt{r}$ – dependence predicted by Harder [4]. To our knowledge no other theoretical approach has been presented.[1] A few subsequent experimental studies on p_{cav} for cylindrical chambers have been published [5–9]. However, most of them depend on the original data. Wittkämper et al. [9] and Van der Plaetsen et al. [8] determined the cavity correction factors for a cylindrical NE2571 chamber by normalizing to the values of Johansson et al. for $\overline{E}_z$=14.2 MeV. Huq et al. [6], and Reft and Kuchnir [5] determined the cavity correction factors at depths beyond d_{max} for Farmer type cylindrical ionisation chambers by using p_{cav} values taken from Table VIII of the TG-21 protocol [10], which is based on the values of Johansson et al.

[1] Note from reviewers. An improved theoretical approach by Svensson and Brahme ("Recent advances in electron and photon dosimetry", in: *R*adiation Dosimetry, Physical and Biological Aspects (Orton, C.G., Ed.), Plenum Press, New York (1986) 87–170), taking into account the angular spread of the radiation, yields a linear dependence which is in agreement with the experimental results.

The aim of the present project was to experimentally determine a new set of p_{cav}-factors to be used for Farmer-like graphite chambers placed in water. Measurements were made at two depths; at the depth of maximum ionisation, and with the effective point of measurement of the chambers at the reference depth. In order to study any influence of the different spectral distribution of the electron beams delivered by modern medical accelerators compared to those used by Johansson et al., the original experiment was repeated using the very same ionisation chambers and PMMA phantom. Another series of measurements, using four specially designed wall-less chambers in a graphite phantom, was made in order to verify the linear relation between p_{cav} and chamber radius that is the basis for the experimental method.

2. Material and methods

Measurements were made with a set of cylindrical ionisation chambers, which were identical except for the cavity radius. Based on the equality of absorbed dose to water determined with different ionisation chambers irradiated under identical conditions and using the formalism given in the TRS-381 Code of Practice, the following relation is obtained

$$M^{\mathrm{cyl}} N_{\mathrm{D,air}}^{\mathrm{cyl}} s_{\mathrm{w,air}} p_{\mathrm{wall}}^{\mathrm{cyl}} p_{\mathrm{cel}}^{\mathrm{cyl}} p_{\mathrm{cav}}^{\mathrm{cyl}} = M^{\mathrm{ref}} N_{\mathrm{D,air}}^{\mathrm{ref}} s_{\mathrm{w,air}} p_{\mathrm{wall}}^{\mathrm{ref}} p_{\mathrm{cel}}^{\mathrm{ref}} p_{\mathrm{cav}}^{\mathrm{ref}} . \quad (1)$$

Here, *ref* denotes the chamber chosen as the reference chamber used for normalisation, and *cyl* denotes any other chamber. For the cylindrical chambers used in this work, the perturbation correction factors p_{wall} and p_{cel} cancel out in equation (1). In photon beams the cavity correction factors, p_{cav}, can be considered unity [1] and equation (1) is reduced to

$$M_{\mathrm{X\text{-}ray}}^{\mathrm{cyl}} N_{\mathrm{D,air}}^{\mathrm{cyl}} = M_{\mathrm{X\text{-}ray}}^{\mathrm{ref}} N_{\mathrm{D,air}}^{\mathrm{ref}} . \quad (2)$$

Thus by irradiating the chambers to the same absorbed dose in photon beams the ratio of the absorbed dose to air chamber factors of the chambers can be determined. This ratio is assumed to be independent of beam quality for high-energy photon beams.

In electron beams p_{cav} must be included resulting in the following equation

$$M_{\mathrm{e}}^{\mathrm{cyl}} N_{\mathrm{D,air}}^{\mathrm{cyl}} p_{\mathrm{cav,e}}^{\mathrm{cyl}} = M_{\mathrm{e}}^{\mathrm{ref}} N_{\mathrm{D,air}}^{\mathrm{ref}} p_{\mathrm{cav,e}}^{\mathrm{ref}} . \quad (3)$$

By combining equation (2) and (3) the ratio of the cavity correction factors for the chambers in electron beams is obtained as

$$\frac{p_{\mathrm{cav,e}}^{\mathrm{cyl}}}{p_{\mathrm{cav,e}}^{\mathrm{ref}}} = \frac{M_{\mathrm{X-ray}}^{\mathrm{cyl}}}{M_{\mathrm{X-ray}}^{\mathrm{ref}}} \Big/ \frac{M_{\mathrm{e}}^{\mathrm{cyl}}}{M_{\mathrm{e}}^{\mathrm{ref}}} . \quad (4)$$

Johansson et al. [3] found a linear relation between the ratio of the cavity correction factors in equation (4) and the cavity radius for each electron beam energy. By extrapolation to zero cavity radius, for which p_{cav} is unity, and re-normalisation, the absolute value of the cavity correction factor can be determined.

When a plane parallel chamber, for which the cavity correction factor is unity, is used as the reference chamber and the other chambers are identical cylindrical chambers having graphite or plastic central electrodes (i.e. p_{cel} is unity) the following equation, corresponding to equation (4), is obtained

$$p_{\mathrm{cav,e}}^{\mathrm{cyl}} = \frac{M_{\mathrm{X-ray}}^{\mathrm{cyl}}}{M_{\mathrm{X-ray}}^{\mathrm{pp}}} \frac{p_{\mathrm{wall,X-ray}}^{\mathrm{cyl}}}{p_{\mathrm{wall,X-ray}}^{\mathrm{pp}}} \Bigg/ \frac{M_{\mathrm{e}}^{\mathrm{cyl}}}{M_{\mathrm{e}}^{\mathrm{pp}}} . \tag{5}$$

As all the cylindrical chambers have the same p_{wall} in photon beams, here denoted $p_{\mathrm{wall,X-ray}}^{\mathrm{CYL}}$, equation (5) can be rewritten

$$p_{\mathrm{cav,e}}^{\mathrm{cyl}} \cdot k = \frac{M_{\mathrm{X-ray}}^{\mathrm{cyl}}}{M_{\mathrm{X-ray}}^{\mathrm{pp}}} \Bigg/ \frac{M_{\mathrm{e}}^{\mathrm{cyl}}}{M_{\mathrm{e}}^{\mathrm{pp}}} , \tag{6}$$

where k is a constant

$$k = \frac{p_{\mathrm{wall,X-ray}}^{\mathrm{pp}}}{p_{\mathrm{wall,X-ray}}^{\mathrm{CYL}}} . \tag{7}$$

The ratio in Equation (6) plotted as a function of cavity radius results in a linear relation for each electron beam energy. By linear extrapolation to zero radius k can be determined and p_{cav} derived[1].

Three investigations were performed. (I) The measurements by Johansson et al. [3] were repeated using the very same ionisation chambers and PMMA phantom. (II) Four cylindrical graphite-walled Farmer-like ionisation chambers with different cavity radius were built and used for the measurements in a water phantom together with a PTW Roos plane parallel chamber. (III) Another set of four cylindrical graphite chambers with different cavity radius were built and used for measurements in a graphite phantom together with an NACP plane parallel chamber.

The characteristics of the cylindrical chambers and the experimental details are given in Table I. Also given in the table are the depth of measurement in the electron beams, the phantom material, its size, and the plane parallel chamber type used. Water protective sleeves made of PMMA with a wall thickness of 0.9 mm were used for the in-water measurements. All measurements were performed using a Varian Clinac 2300CD linear accelerator.

The photon beam measurements were made in beams of 6 MV and 15 MV nominal energy, TPR_{10}^{20} = 0.68 and 0.76, respectively. The effective point of measurement, using a shift of 0.6r from the centre of the chamber for the cylindrical chambers and the front surface of the air cavity for the plane parallel chamber, was positioned at 5 g/cm^2 depth. A source to surface distance of 100 cm and a field size of 10×10 cm were used (15×15 cm for investigation (II)). When one of the cylindrical chambers was used as the reference chamber the mean value of $M_{\mathrm{X-ray}}^{\mathrm{cyl}} / M_{\mathrm{X-ray}}^{\mathrm{ref}}$ determined in the two photon beams was used.

[1] When the Farmer-like chambers were used in water together with a *R*oos chamber, this provided an estimate of $p_{\mathrm{wall,X-ray}}^{\mathrm{Roos}}$; $p_{\mathrm{wall}}^{\mathrm{Roos}}$ (TPR_{10}^{20}=0.68)=1.012±0.2%, and $p_{\mathrm{wall}}^{\mathrm{Roos}}$ (TPR_{10}^{20}=0.76)=1.009±0.2%. Here, only the experimentally determined standard uncertainty of k was considered. $p_{\mathrm{wall,X-ray}}^{\mathrm{CYL}}$ was taken from the TRS 277 Code of Practice [11].

TABLE I. CHARACTERISTICS OF THE SPECIALLY DESIGNED CHAMBERS USED IN INVESTIGATIONS (I) TO (III)

Cylindrical chamber [b]	Internal length (mm)	Internal radius (mm)	Wall material	Wall thickness (mm)	Electrode material	Electrode diameter (mm)
(I) R_{100}. PMMA phantom, 20 × 20 × 20 cm. NACP02 chamber						
JMLS3	15	1.5	Mixture [a]	0.5	Mixture [a]	1.0
JMLS5	”	2.5	”	”	”	”
JMLS7	”	3.5	”	”	”	”
(II) z_{ref} and R_{100}. Water phantom, 30 × 30 × 30 cm. PTW Roos chamber						
RK2	20	1.0	Graphite	0.5	Graphite	1.0
RK4	”	2.0	”	”	”	”
RK7	”	3.5	”	”	”	”
RK8	”	4.0	”	”	”	0.9
(III) R_{100}. Graphite phantom (bulk density 1.78 g/cm^3), 20 × 20 × 20 cm. NACP01 chamber						
OM4	16	2.0	Wall-less		Graphite	0.9
OM5	”	2.5	”		”	”
			”			
			”			
OM6	”	3.0			”	”
OM8	”	4.0			”	”

[a] Graphite and epoxy resin.

[b] JMLS3-7 refer to the chambers used by Johansson et al. [3], RK2-8 to the cylindrical graphite-walled Farmer-like chambers, and OM4-8 to the second set of graphite chambers.

Measurements were made in electron beams of 6, 8, 10, 12, 15 and 20 MeV nominal energy. The chambers were positioned at the peak of the depth ionisation curve or at the reference depths recommended in TRS-381. In the first case the depth of R_{100} was experimentally determined for each chamber and electron beam energy. In the latter case a shift of the effective point of measurement from the centre of the cylindrical chamber of 0.5r was used. A source to surface distance of 100 cm and a field size of 15 × 15 cm were used (13 × 13 cm for investigation (III)).

The measured charge was corrected for temperature, pressure, recombination, leakage and polarity. The corrections for ion recombination were determined using the two-voltage method ($V_1/V_2 = 3$). The polarity effects were derived from the measurements with positive and negative polarity, and were in most cases found negligible (<0.1%). The accelerator output during each series of measurements proved to be very stable (one of the chambers was used for repeated measurements during the measurement series and the quotient of the reading of two subsequent measurements was typically ≤0.2%) and therefore generally no external monitor chamber was used. Repeated measurements were made in order to estimate the reproducibility of the experimental procedure.

3. Results and discussion

From investigation (I), the linear relation between p_{cav} and the cavity radius, as previously reported by Johansson et al. [3], was confirmed. As described in Section 2, the cavity correction factors can be derived by using either one of the cylindrical chambers or a plane parallel chamber as reference. In Fig. 1, the good agreement between the p_{cav} factors determined using the smallest cylindrical PMMA chamber as a reference chamber and the factors determined using the plane parallel NACP chamber as reference can be seen. The maximum deviation (0.8%) was found for the lowest energy, for which it was impossible to position the larger cylindrical chambers at R_{100}.

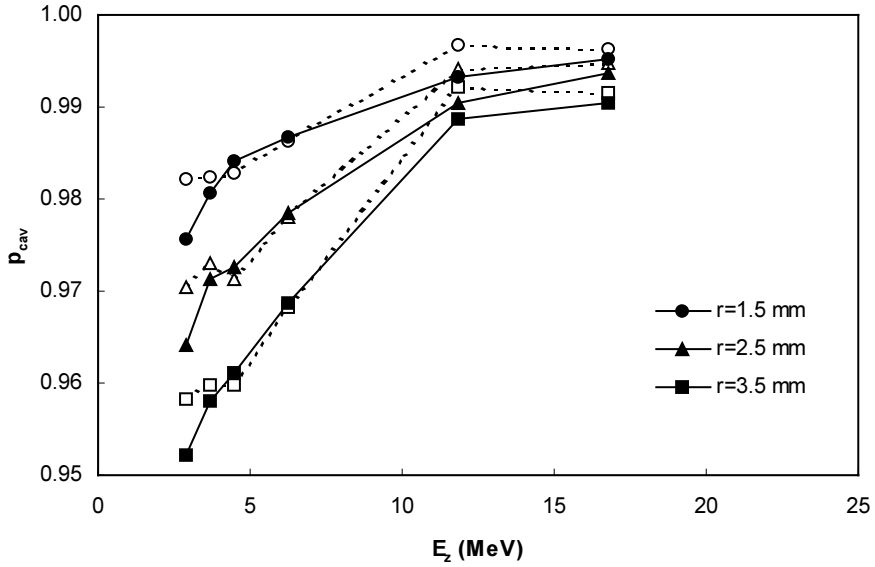

FIG. 1. p_{cav} *as a function of mean energy at depth z for cylindrical PMMA chambers placed at the depths of maximum ionisation in a PMMA phantom. Data from the present work using the same equipment as Johansson* et al. *[3]. Full lines and filled symbols: evaluated relative to the NACP-chamber; dotted lines and open symbols: evaluated relative to the smallest cylindrical chamber.*

In Fig. 2 mean values of the data obtained relative to the cylindrical and the NACP chamber are shown together with the data recommended in the TRS-381 Code of Practice [1]. p_{cav} is given as a function of the mean energy at depth z, $\overline{E}_z$, determined according to the recommendations in TRS-381. The agreement between the cavity correction factors determined in the present work and those recommended by the protocol is good. The two sets of data were determined using the very same instrumentation, but using different electron beams. Thus, any differences between the correction factors determined in this work and those given in TRS-381 should not be due to the characteristics of the electron beams used in this work.

In investigation (II), the measurements were first made with the effective point of measurement at the reference depth in water. A linear relation between p_{cav} and the cavity radius was obtained for the higher energies, but not for the lower energies. This makes it non-feasible to use the extrapolation method described above to derive the correction factors. A possible explanation can be the narrow depth dose profile in relation to the dimension of the chambers and the steep dose gradient around z_{ref} for the low-energy electron beams. The measurements were therefore repeated placing the chambers at R_{100} instead. This improved the situation, and an approximate linear relation was obtained. The resulting cavity correction

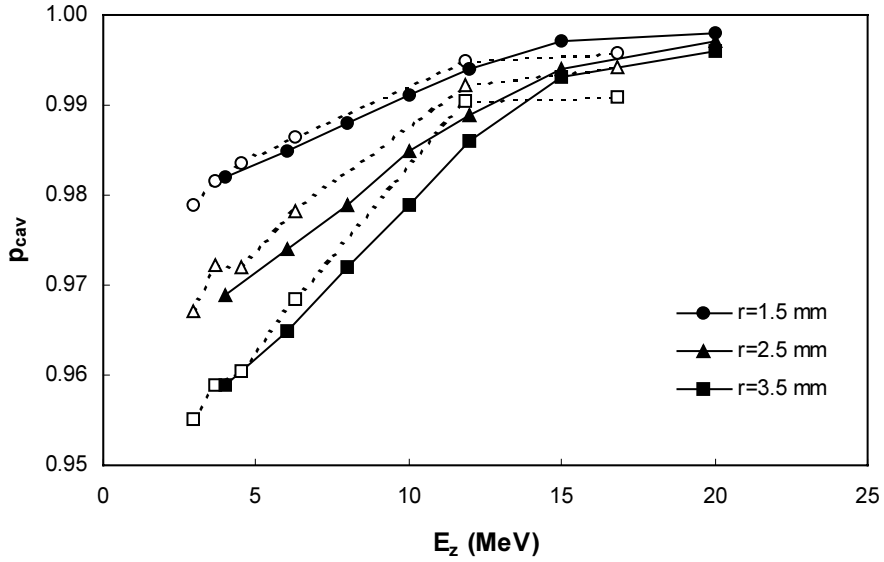

FIG. 2. p_{cav} *as a function of mean energy at depth z for cylindrical PMMA chambers placed at the depths of maximum ionisation in a PMMA phantom. Full lines and filled symbols: data from the TRS-381 Code of Practice [1]; dotted lines and open symbols: data from the present work (average of cylindrical and NACP chambers), using the same equipment as Johansson* et al. *[3].*

factors are presented in Table II. Again the agreement between the p_{cav} factors derived relative to the smallest cylindrical chamber and those determined relative to a plane parallel Roos chamber is good. Mean values of the two data series are given in Table II. The p_{cav} factors for the tabulated $\overline{E}_z$ values were obtained by linear interpolation. In Fig. 3 the data from Table II are compared with the data from the TRS-381 Code of Practice. A smaller correction was found compared to the protocol for the chambers used at R_{100} in water. For a 7-mm diameter chamber, which is similar to a Farmer chamber, the difference was larger than 1% for some

TABLE II. CAVITY CORRECTION FACTORS FOR FARMER-TYPE CHAMBERS OF DIFFERENT CAVITY RADIUS, r, USED IN WATER, EXTRAPOLATED FROM MEASUREMENTS AT THE DEPTHS OF MAXIMUM IONISATION

$\overline{E}_z$ [a]	p_{cav} [b]			
	3.15			
(MeV)	r = 1 mm	r = 2 mm	r = 3.5 mm	r = 4 mm
4	0.992	0.978	0.970	0.962
6	0.994	0.983	0.977	0.968
8	0.995	0.988	0.983	0.975
10	0.996	0.992	0.988	0.981
12	0.997	0.996	0.993	0.988
16	0.998	0.998	0.996	0.994

[a] The mean energy at depth was calculated according to the TRS-381 Code of Practice [1].

[b] The combined experimental standard uncertainty of the p_{cav} factors is estimated to be 0.4%.

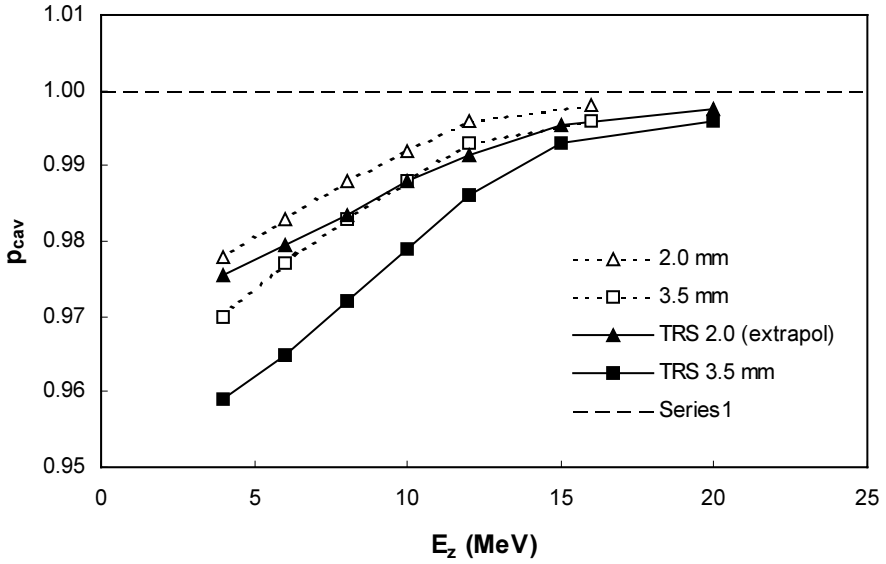

FIG. 3. p_{cav} *factors for graphite-walled Farmer-like chambers of cavity radius 2.0 and 3.5 mm at the depths of maximum ionisation in water, compared with data from the TRS-381 Code of Practice [1].*

energies. In-water calibration of the plane parallel chambers in electron beams with $\overline{E}_z$<15 MeV using the p_{cav}-values recommended in TRS-381 will thus underestimate the $N_{D,air}$ factor, and therefore any subsequent absolute dose determination.

In TRS-381 the input parameter for the selection of p_{cav} is the mean energy at the reference depth but the tabulated data is based on measurements at the depth of maximum ionisation. To study if the depth of measurement for the same value of $\overline{E}_z$ has any influence on the cavity correction factor, actual measurements at z_{ref} were compared with the corresponding factor obtained from Table II for the same $\overline{E}_z$. It was found that p_{cav} for a certain mean energy at depth was closer to unity when the chamber was placed at z_{ref} than at R_{100}. The deviation was of approximately the same magnitude as the estimated combined standard uncertainty of p_{cav} (see below), and was therefore not statistically verified.

The complex experimental set-up in water can cause a slightly weaker correlation in the linearity of p_{cav} versus chamber radius for the in-water measurements. Transition effects between water, PMMA and graphite and the unavoidable air volumes between the chambers and the water protective sleeves could cause unpredictable perturbations in electron beams. Investigation (III) was made in order to study the variation of p_{cav} with cavity radius in a wall-less situation where all other perturbation effects are minimised. The results are given in Fig. 4 and the linear relation between p_{cav} and the chamber radius is evident. It can be concluded that the measurement uncertainty during the electron beam measurements in water can be relatively large due to unpredictable perturbation effects.

The experimental standard uncertainty of the determined p_{cav} values was calculated by combining the uncertainty components of Eq. (5). From repeated measurements in photon and electron beams the experimental uncertainties of the M^{cyl}/M^{pp} quotients were estimated. A value of 0.2% was assigned for both photons and electrons. The uncertainty of the recombination correction was estimated to be 0.1%. The contribution due to the polarity effect

was estimated to be 0.1% in electron beams. In photon beams this component was assumed to be negligible. For the PMMA and Farmer-like chambers the value of the constant, k was given as the mean value of the determinations in five different electron beams (E_{nom}=6 MeV was excluded for reasons explained above). The standard uncertainty of the mean was 0.2%. For the graphite measurements this contribution was 0.5%. The uncertainty of the temperature and pressure correction was assumed to cancel out in the ratio. The uncertainty of the leakage corrections was assumed to be negligible. When the chambers are placed at the depth of maximum ionisation, the effective point of measurement of the chambers is positioned at somewhat different depths. We are aware that the equality in Eq. (1) is then strictly not valid and that $\overline{E}_z$ is not exactly the same at different depths. The mean energy at the depth of the plane parallel chamber was used throughout. The corresponding uncertainty was assumed to be included in the uncertainty of the constant, k. The combined experimental standard uncertainty of the p_{cav} values determined according to Eq. (5) was 0.4% for the PMMA and Farmer-like chambers, and 0.6% for the wall-less graphite chambers. The same uncertainties were assumed for the p_{cav} values determined according to Eq. (4).

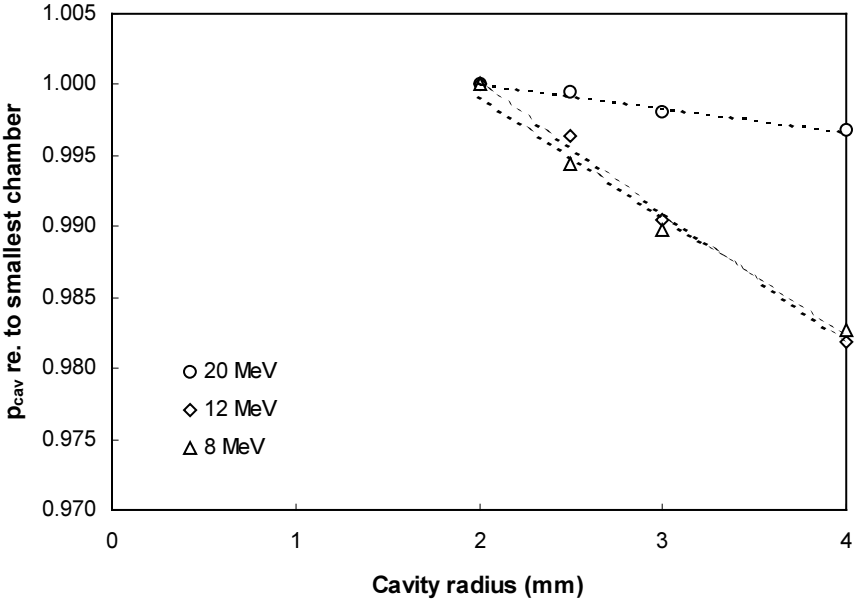

FIG. 4. The relative values of p_{cav} *as a function of cavity radius for a number of nominal electron energies, measured using wall-less chambers placed at the depths of maximum ionisation in a graphite phantom.*

4. Conclusions

The measurements using the three sets of cylindrical ionisation chambers placed at R_{100} in graphite, PMMA and water have confirmed the linear relation between p_{cav} and cavity radius found by Johansson et al. [3]. Repeating their measurements in PMMA gives approximately the same p_{cav} factors in the electron beams used in this work. We conclude that the characteristics of the electron beams is not of major importance. Compared to the TRS-381 Code of Practice [1], a smaller correction was found for the cavity perturbation for Farmer-like chambers when used in water. The difference is small for $\overline{E}_z \geq 15$ MeV. However, for plane parallel chambers calibrated at $\overline{E}_z < 15$ MeV in water the use of p_{cav}-values from TRS-381 will underestimate the $N_{D,air}$ factor, and consequently any subsequent absolute dose determination. Cavity correction factors to be used for measurements in water are given in

Table II. It can be concluded that the measurement uncertainty during electron beam measurements in water can be relatively large due to unpredictable perturbation effects. The present work indicates that the experimental method for the determination of the cavity correction factors is mainly limited to the measurements at depths corresponding to the maximum ionisation. Monte Carlo simulations would be very useful to determine cavity correction factors under other conditions.

ACKNOWLEDGEMENTS

The authors wish to thank Mr. R. Karlsson and Mr. A. Kristensson for making the ionisation chambers.

REFERENCES

[1] INTERNATIONAL ATOMIC ENERGY AGENCY, The Use of Plane Parallel Ionization Chambers in High Energy Electron and Photon Beams — An International Code of Practice for Dosimetry, Technical Reports Series No 381, IAEA, Vienna (1997).

[2] AMERICAN ASSOCIATION OF PHYSICISTS IN MEDICINE, The calibration and use of plane parallel ionization chambers for dosimetry of electron beams: An extension of the 1983 AAPM protocol report of AAPM Radiation Committee Task Group No. 39, Med. Phys. **21** (1994) 1251–1260.

[3] JOHANSSON, K.A., MATTSSON, L.O., LINDBORG, L., SVENSSON, H., Absorbed-dose determination with ionization chambers in electron and photon beams having energies between 1 and 50 MeV, Proc. Symp. National and International Standardization of Radiation Dosimetry, IAEA, Vienna (1978) 243–70.

[4] HARDER, D., Einfluss der Vielfachstreuung von Elektronen auf die Ionisation in gasgefüllten Hohlräumen, Biophysik **5** (1968) 157–168.

[5] REFT C., KUCHNIR, F.T., Measured overall perturbation factors at depths greater than d_{max} for ionization chambers in electron beams, Med. Phys. **26** (1999) 208–213.

[6] HUQ, M.S., YUE, N., SUNTHARALINGAM, N., Experimental determination of fluence correction factors at depths beyond d_{max} for a Farmer type cylindrical ionization chamber in clinical electron beams, Med. Phys. **24** (1997) 1609–1613.

[7] KUBO, H., Determination of replacement correction factors for “homogeneous” cylindrical chambers, Med. Phys. **22** (1995) 479–480.

[8] VAN DER PLAETSEN, A., SEUNTJENS, J., THIERENS, H., VYNCKIER, S., Verification of absorbed doses determined with thimble and parallel-plate ionization chambers in clinical electron beams using ferrous sulphate dosimetry, Med. Phys. **21** (1994) 37–44.

[9] WITTKÄMPER, F.W., THIERENS, H., VAN DER PLAETSEN, A., DE WAGTER, C., MIJNHEER, B.J., Perturbation correction factors for some ionization chambers commonly applied in electron beams, Phys. Med. Biol. **36** (1991) 1639–1652.

[10] AMERICAN ASSOCIATION OF PHYSICISTS IN MEDICINE, A protocol for the determination of absorbed dose from high-energy photon and electron beams. Task Group No. 21, Med. Phys. **10** (1983) 741.

[11] INTERNATIONAL ATOMIC ENERGY AGENCY, Absorbed Dose Determination in Photon and Electron Beams — An International Code of Practice, Technical Reports Series No 277, IAEA, Vienna (1987).

CALIBRATION OF PLANE PARALLEL CHAMBERS AND DETERMINATION OF p_{WALL} FOR THE NACP AND ROOS CHAMBERS FOR ^{60}Co γ-RAY BEAMS

Å. PALM, O. MATTSSON
Department of Radiation Physics,
Göteborg University,
Göteborg, Sweden

P. ANDREO
Dosimetry and Medical Radiation Physics Section,
Division of Human Health,
International Atomic Energy Agency,
Vienna

Abstract

Plane parallel ionization chambers of the type PTW-34001 Roos and Scanditronix NACP02 have been calibrated using the two N_K-based in-phantom procedures recommended in TRS-381 using a high-energy electron beam and a ^{60}Co γ-ray beam. For the NACP chamber the difference between the two $N_{D,air}$ chamber factors is of the same order as the experimental uncertainty. For the PTW Roos chamber, however, systematic disagreement has been obtained. The value determined in ^{60}Co is questioned; the reason for the discrepancy is thought to be the perturbation correction factor for the wall effect, p_{wall}. Values of p_{wall} have been measured comparing D_w determinations based on air-kerma and absorbed dose to water calibration procedures. A new p_{wall} factor for the Roos chamber in ^{60}Co γ-ray beams in water (1.009 ± 0.6%) is derived, which is not significantly higher than the p_{wall} given in TRS-381 (1.003 ± 1.5%), although it has a lower uncertainty. The chamber to chamber variation for six commercial PTW Roos chambers and a Roos prototype was found to be very small.

1. Introduction

The TRS-381 Code of Practice [1] recommends different methods for the calibration of plane parallel chambers. Discrepancies larger than 1.5% in $N_{D,air}$ chamber factors determined in electron and ^{60}Co γ-ray beams have been reported for the PTW-34001 Roos chamber, whereas good agreement has been found for the Scanditronix NACP02 chamber [2]. It has been suggested that the difference could be caused by the TRS-381 recommended value of the correction factor for the chamber wall perturbation, p_{wall}, for the Roos chamber in ^{60}Co γ-ray beams in water.

The aim of the present work is to provide additional data on the comparison of $N_{D,air}$ chamber factors determined in electron and ^{60}Co γ-ray beams. Preliminary results were presented at the 5th Biennial ESTRO Meeting on Physics for Clinical Radiotherapy [3][1]. For the PTW Roos chamber the results confirm the discrepancy in $N_{D,air}$ values observed by other participants of this project [2], when the data recommended in TRS-381 are used. Assuming that p_{wall} for the PTW Roos chamber is the reason for the discrepancy, new values of p_{wall} are experimentally determined by comparing absorbed dose measurements based on air-kerma, N_K, and absorbed dose to water, $N_{D,w}$, calibration procedures. The investigation also includes the analysis of the chamber to chamber variation of the PTW Roos type chamber. The implications of using the new p_{cav} factors suggested in Ref. [5] are discussed.

[1] The present contribution is a summary of a full paper published elsewhere [4].

2. Methods

2.1. Comparison of $N_{D,air}$ for plane parallel ionization chambers determined using two N_K-based calibration procedures

Plane parallel ionisation chambers of the type PTW-34001 Roos and Scanditronix NACP02 were calibrated using two N_K-based procedures where either an electron beam or a ^{60}Co γ-ray beam was used. The calibrations were performed according to the recommendations given in TRS-381 [1]. The $N_{D,air}^{pp}$ chamber factor was obtained by experimental cross-calibration against a reference Farmer chamber of type NE-2571, for which $N_{D,air}^{ref}$ was known.

The $N_{D,air}^{ref}$ factor for the reference chamber was determined from

$$N_{D,air}^{ref} = N_K^{ref}(1-g)\left[k_{att}k_m\right]^{ref}k_{cel}^{ref}, \tag{1}$$

where the air-kerma calibration factor, N_K^{ref}, was traceable to the BIPM through the Swedish Standard Dosimetry Laboratory. The $[k_{att}k_m]^{ref}$ and k_{cel}^{ref} factors were taken from TRS-381 [1].

The $N_{D,air}^{pp}$ chamber factor for a plane parallel chamber was obtained from

$$N_{D,air}^{pp} = N_{D,air}^{ref}\left[\frac{M^{ref}}{M^{pp}}\frac{p_{wall}^{ref}}{p_{wall}^{pp}}\frac{p_{cav}^{ref}}{p_{cav}^{pp}}p_{cel}^{ref}\right], \tag{2}$$

where M^{ref} and M^{pp} are, respectively, the average readings of the reference and the plane parallel chambers in a high-energy electron beam ('the electron beam method') or in a ^{60}Co γ-ray beam. The mean energy at depth for the electron beam method was 13.1 MeV. The perturbation correction factors were taken from TRS-381 [1].

2.2. Determination of p_{wall} for ^{60}Co γ-ray beams for the NACP and Roos type chambers

Assuming the $N_{D,air}^{pp}$ factor derived from the electron beam method to be equal to the $N_{D,air}^{pp}$ resulting from the ^{60}Co γ-ray beam, p_{wall} factors for the plane parallel chambers in ^{60}Co γ-ray beams in water were obtained from

$$p_{wall}^{pp} = \left[\frac{M^{ref}}{M^{pp}}\right]_{Co}\left[\frac{M^{pp}}{M^{ref}}\right]_{e}\frac{\left(p_{wall}^{ref}\cdot p_{cel}^{ref}\right)_{Co}}{\left(p_{cav}^{ref}\cdot p_{cel}^{ref}\right)_{e}} \tag{3}$$

The p_{wall} factors were also derived from a comparison of the absorbed dose to water determined using $N_{D,w}$ and $N_{D,air}$ factors [6],

$$p_{wall}^{pp} = \frac{N_{D,w}^{pp}}{N_{D,air}^{pp}s_{w,air}}. \tag{4}$$

The latter procedure depends on the calibration factors supplied by a standards laboratory through the ratio $N_{D,w}/N_K$. In the present work N_K was traceable to the BIPM, and $N_{D,w}$ was traceable to the BIPM and/or PTB. The $N_{D,air}^{pp}$ chamber factor was determined from the electron beam method.

3. Results and discussion

Table I gives the results for the $N_{D,air}$ chamber factors of the Scanditronix NACP02 and the PTW Roos chambers. The experimental standard uncertainty of the $N_{D,air}$ factors was estimated to be 0.3%. The PTW Roos chamber factors resulting from calibrations in the ^{60}Co γ-ray beam are about 1% higher than the $N_{D,air}$ factors determined in the electron beam, whereas the two methods agree within the uncertainty of the measurements for the Scanditronix NACP02 chamber.

For the Scanditronix NACP02 chamber we conclude that the experimentally determined correction factor for the wall perturbation in ^{60}Co γ-ray beams agrees well with the value recommended in TRS-381 within the uncertainty of our experimental procedure (see Table II). However, the mean value of the p_{wall} factor for the PTW Roos chambers derived from the two N_K-based calibrations is 1.014, in comparison with 1.003 as recommended in TRS-381. The chamber to chamber variation for six commercial PTW Roos chambers and a Roos prototype chamber has been found to be very small.

Using the $N_{D,w}/N_{D,air}$ procedure, different values of the p_{wall} factor were obtained depending on whether the $N_{D,w}$ calibration was traceable to BIPM or PTB (see Table III). When the calibration was traceable to PTB the agreement with the value given in TRS-381, taken from Medin et al. [6], was excellent. In order to remove the influence of the two primary standards, the p_{wall} factors were corrected using the ratio of the mean value of all absorbed-dose-to-water and air-kerma primary standards. The values of p_{wall}^{corr}(PTB) and p_{wall}^{corr}(BIPM) were then consistent, yielding a mean value of 1.009 for the PTW Roos chamber.

The difference of about 0.5% between the p_{wall} factor obtained using the N_K-based methods and the $N_{D,w}/N_{D,air}$ procedure can only be explained in terms of a systematic experimental uncertainty or uncertainties associated with the different perturbation factors in the electron and ^{60}Co γ-ray beams used in the determination. A new value for the p_{wall} factor for the PTW Roos chamber in water in ^{60}Co γ-ray beams is therefore proposed (1.009) derived as the weighted average of the different determinations.

The results of the present work depend on the value of p_{cav} for the NE-2571 chamber in electron beams in water. Using the new p_{cav} values suggested in Ref. [5] would eliminate the discrepancy in $N_{D,air}$ found for the PTW Roos chamber using the two N_K-based calibration procedures. The p_{wall} factors for the PTW Roos chamber would be reduced by about 1%, but the difference between the p_{wall} factor obtained from the two methods would remain. The agreement with the p_{wall} factor given in TRS-381 would be excellent, but would result from the cancellation of the impact of the new p_{cav} combination. For the Scanditronix NACP02 chamber, the use of the new p_{cav} values would introduce a reduction of about 1% in $N_{D,air}^{pp}$ factors determined in electron and ^{60}Co γ-ray beams.

TABLE I. EXPERIMENTALLY DERIVED $N_{D,air}$ CHAMBER FACTORS (mGy/nC) FOR A SCANDITRONIX NACP02, A PROTOTYPE ROOS, AND SIX COMMERCIAL PTW-34001 ROOS PLANE PARALLEL IONIZATION CHAMBERS

The $N_{D,air}$ factors were determined by cross calibration against a reference NE-2571 cylindrical chamber in a 20 MeV (nominal energy) electron beam and a ^{60}Co γ-ray beam in water. The standard deviation of the mean value of at least four calibrations was 0.1% or less. The experimental standard uncertainty of the $N_{D,air}$ factors was estimated to be 0.3%. The last column gives the quotient of the $N_{D,air}$ chamber factors determined using the two methods.

Chamber type - serial no.	$N_{D,air}$ (mGy/nC)		Ratio ^{60}Co/electrons
	20 MeV e^- beam	^{60}Co γ-ray beam	
NACP02 - 2003	164.5	163.8	0.996 ± 0.4%
Roos FK6 - 05 (prototype)	70.64	71.58	1.013 ± 0.4%
PTW Roos - 0057	77.32	78.10	1.010 ± 0.4%
PTW Roos - 0080	72.34	73.23	1.012 ± 0.4%
PTW Roos - 0083	71.95	72.72	1.011 ± 0.4%
PTW Roos - 0084	71.74	72.52	1.011 ± 0.4%
PTW Roos - 0085	72.26	73.04	1.011 ± 0.4%
PTW Roos - 0086	72.14	72.94	1.011 ± 0.4%

TABLE II. EXPERIMENTALLY DERIVED CORRECTION FACTORS FOR THE PERTURBATION DUE TO THE CHAMBER WALL, p_{wall}, IN ^{60}Co γ-RAY BEAMS IN WATER FOR A SCANDITRONIX NACP02, A PROTOTYPE ROOS, AND SIX COMMERCIAL PTW-34001 ROOS PLANE PARALLEL IONIZATION CHAMBERS

The perturbation factors were determined by assuming that the $N^{pp}_{D,air}$ chamber factors derived by cross-calibration against a reference cylindrical NE-2571 chamber in an electron beam and in a ^{60}Co γ-ray beam were identical, see Eq. (3). The experimental standard uncertainty was 0.4%; the values of p_{wall} for the two types of plane parallel chambers given in TRS-381 [1] are included for comparison.

Chamber type – serial no.	p_{wall} in a ^{60}Co γ-ray beam in water	
	Eq. (3)	TRS-381
NACP02 - 2003	1.020	1.024
Roos FK6 - 05 (prototype)	1.016	1.003
PTW Roos - 0057	1.013	
PTW Roos - 0080	1.015	
PTW Roos - 0083	1.014	
PTW Roos - 0084	1.014	
PTW Roos - 0085	1.014	
PTW Roos - 0086	1.014	

TABLE III. EXPERIMENTALLY DERIVED CORRECTION FACTORS FOR THE PERTURBATION DUE TO THE CHAMBER WALL, p_{wall}, IN ^{60}Co γ-RAY BEAMS IN WATER FOR A PROTOTYPE ROOS, AND SIX COMMERCIAL PTW-34001 ROOS PLANE PARALLEL IONIZATION CHAMBERS

The perturbation factors were determined by assuming that the absorbed dose to water in a ^{60}Co γ-ray beam determined with a plane parallel chamber having $N_{D,w}^{pp}$ (calibrated in a ^{60}Co γ-ray beam) and $N_{D,air}^{pp}$ (calibrated in an electron beam) factors were identical, see Eq. (4). Columns 2 and 3 give values of the p_{wall} factors determined using $N_{D,w}^{pp}$ calibrations traceable to the BIPM and to PTB respectively. $N_{D,air}^{pp}$ was in the two columns traceable to the BIPM through the N_K calibration of the reference cylindrical chamber. Columns 4 and 5 give the corresponding values, p_{wall}^{corr}, corrected to take into account the differences in primary standards at different standards laboratories. The experimental standard uncertainty was 0.3%.

Chamber type – serial no.	p_{wall} in a ^{60}Co γ-ray beam in water			
	p_{wall}^{uncorr} (BIPM)	p_{wall}^{uncorr} (PTB)	p_{wall}^{corr} (BIPM)	p_{wall}^{corr} (PTB)
Roos FK6 - 05 (prototype)	1.011	1.006	1.008	1.010
PTW Roos - 0057	1.014	1.003	1.011	1.007
PTW Roos - 0080	1.015	1.004	1.012	1.008
PTW Roos - 0083	1.011		1.008	
PTW Roos - 0084	1.009		1.006	
PTW Roos - 0085	1.012		1.009	
PTW Roos - 0086	1.010		1.007	

REFERENCES

[1] INTERNATIONAL ATOMIC ENERGY AGENCY, The Use of Plane Parallel Ionization Chambers in High Energy Electron and Photon Beams — An International Code of Practice for Dosimetry, Technical Reports Series No 381, IAEA, Vienna (1997).

[2] INTERNATIONAL ATOMIC ENERGY AGENCY, Dose determination with plane parallel ionization chambers in therapeutic electron and photon beams, IAEA SSDL Newsletter 40 (1999) 4–16.

[3] PALM, Å., MATTSSON, O., ANDREO, P., Wall correction factors for plane parallel ionization chambers, Radiother. Oncol. 51 Suppl. **1** (1999) 50 (Abstract).

[4] PALM, Å., MATTSSON, O., ANDREO, P., Calibration of plane parallel chambers and determination of p_{wall} for the NACP and Roos chambers for ^{60}Co γ-ray beams, Phys. Med. Biol. **45** (2000) 971–981.

[5] PALM, Å., MATTSSON, O., Experimental determination of p_{cav} factors for cylindrical ionisation chambers in electron beams (this volume).

[6] MEDIN, J., ANDREO, P., GRUSELL, E., MATTSSON, O., MONTELIUS, A., ROOS, M., Ionization chamber dosimetry of proton beams using cylindrical and plane parallel chambers. N_w versus N_K ion chamber calibrations, Phys. Med. Biol. **40** (1995) 1161–1176.

TESTING OF THE CODE OF PRACTICE AT DIFFERENT ELECTRON ENERGIES AND PHANTOM MATERIALS

A. BJÖRELAND, H. SVENSSON
Department of Radiation Physics,
Umeå University,
Umeå, Sweden

Abstract

The aim of this investigation is to compare results of absorbed dose determinations in electron beams using methods based on measurements with plane parallel ionization chambers (TRS-381) and on the Fricke dosimetry. In order to exclude uncertainties in the air-kerma calibration of the reference cylindrical ionization chamber and in the εG-value of the Fricke dosimeter, dosimetry comparisons were made also using these two dosimetry systems in a ^{60}Co beam. Assuming that the air–kerma calibration was correct and applying the interaction coefficients from TRS-381 would have given an εG of 352.4 $\times 10^{-6} m^2 kg^{-1} Gy^{-1}$ which is in excellent agreement with published values. This indicates that the measurement procedure is reliable. Comparing dose determinations using the so called "electron method" from TRS-381 measuring with a NACP-02 chamber and using the Fricke method gave a ratio $D_{w,NACP}/ D_{w,Fricke} = 0.998 \pm 0.003$ (1SD) in the electron energy range, E_Z from 3 to 36 MeV, thus showing that the procedures used from the TRS-381 agree closely with more direct methods (i.e. Fricke). It was shown that the uncertainty would increase if ionization chamber measurements were made in plastics.

1. Introduction

The IAEA code of practice, TRS-381 [1], recommends water as the reference medium for absorbed dose measurements both for photon and electron beams. However, at low electron beam energies (below 10 MeV) solid phantoms in slab form may sometimes be used for practical reasons. Also in this case the absorbed dose determination must refer to water. As the IAEA code of practice uses the same expression when measurements are made in plastic as when measurements are made in water this requires converting of the meter reading and reference depth to equivalent quantities in water.

The task of this work was to test the methods to determine the absorbed dose to water through measurements in water and plastic according to the methods recommended in the TRS-381 and to compare the results to the protocol AAPM TG-39 [2] and measurements made using ferrous sulfate dosimetry, Fricke.

2. Electron fluence correction factor, h_m

When measurements have been carried out in plastic an equivalent depth in water must be determined. The requirement for equivalent depth is that the mean energy is the same in the two materials. The magnitude of the electron fluence in plastic might differ from that at equivalent depth in water due to differences in the scattering properties of the two materials. To correct for this, a factor h_m is employed by the TRS-381 and an approximate relation can be written

$$\phi_w\left(z_{ref,water}\right) \approx \phi_{plastic}\left(z_{ref,plastic}\right) h_m$$

where ϕ is the electron fluence. At the equivalent depths, ϕ_w and $\phi_{plastic}$ can be assumed to be proportional to the meter reading (M) in water and plastic respectively. The reason is that M is proportional to the absorbed dose to air in the air cavity which in turn is proportional to the product of the electron fluence and collision stopping power of air. The collision stopping powers are the same in the two materials and therefore cancels in the equation.

$$M_{Q,w}\left(z_{ref,w}\right) = M_{Q,plastic}\left(z_{ref,plastic}\right) h_m$$

The h_m factor can therefore directly be measured as the ratio of the temperature and pressure corrected chamber readings at the reference points in water and plastic. This method requires the use of depth scaling to find the equivalent depth in plastic which introduces further uncertainties in the measurements. The measurements, in the two materials have been performed at the ionization maximum. The results would be closely the same if instead the ionization maximum in plastic had been the reference depth and the equivalent depth in water had been determined using the scaling procedure, as commented in TRS-381 [1]. This is so as the depth ionization curves have fairly broad maxima, see Fig. 1.

2.1. Measurement of the h_m factor

The measurements of the h_m factor for PMMA were made at the energies at depth corresponding to E_z 2.9, 5.4 and 13.0 MeV from a Varian Clinac 2300 C/D using two different types of plane parallel ion chambers, NACP-02 and PTW 34001 (Roos). The measurements were made at the ionization maximum in both PMMA and water using a constant source to chamber distance of 105 cm, i.e. the effective point of measurement was placed 5 cm below the isocenter point. To correct for possible variations in the output from the accelerator an external monitor chamber was used. The only correction applied to the measurements was for the difference in temperature between water and PMMA since the pressure was found to be constant, during the measurements at each energy.

2.2. Results of the h_m factor measurement

The depth of ionization maximum was determined for each individual measurement at each energy, using the two types of detectors, by varying the amount of material above the detector, see Fig. 1. Both detectors gave the same depth of ionization maximum except for the measurement at 20 MeV in water. The difference between the depth of ionization maximum at 20 MeV in water measured using the NACP-02 and the PTW Roos chamber was approximately 2 mm. This difference is most probably due to the flat depth dose distribution at high energies and therefore large uncertainty in finding the maximum.

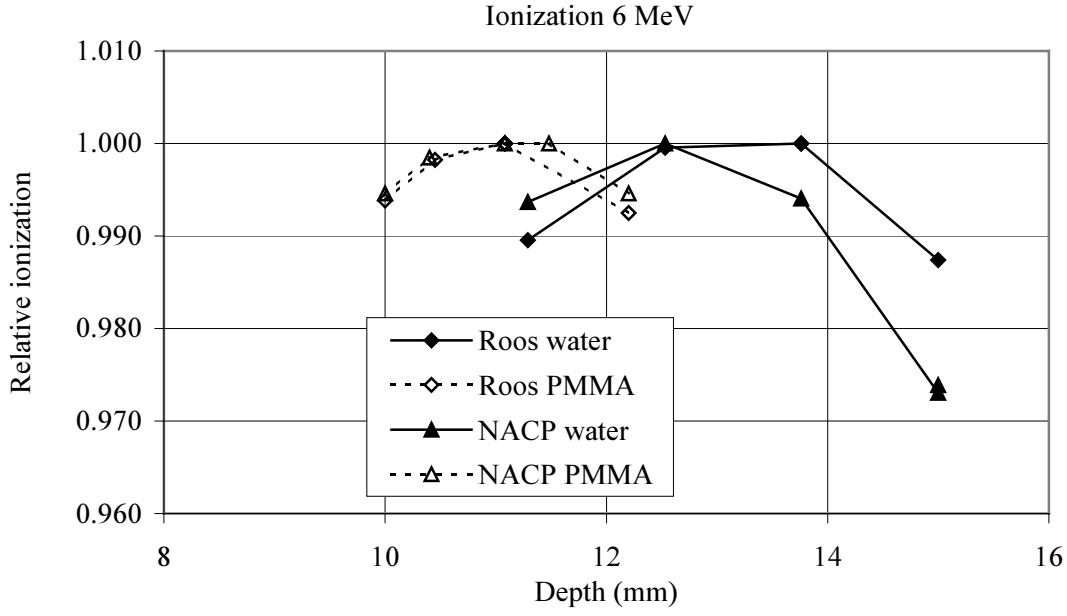

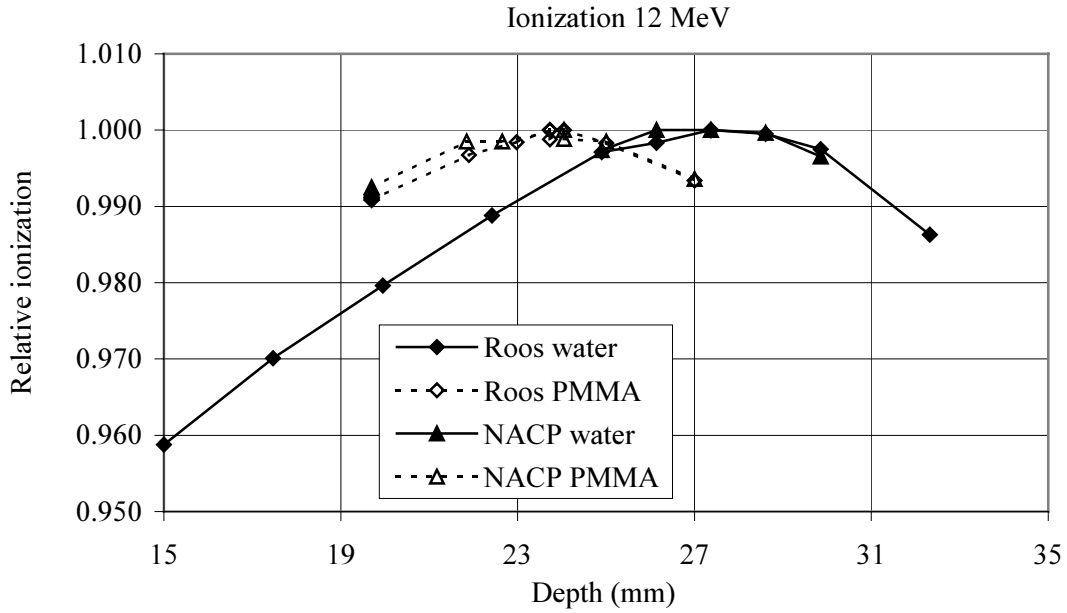

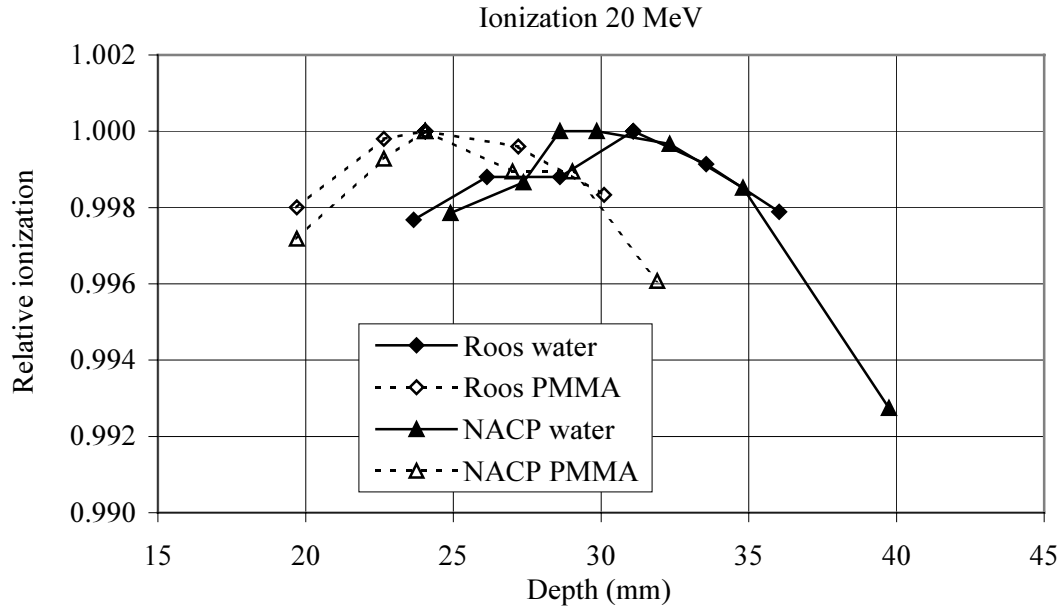

Figure 1 (a–c). Measurements of depth of ionization maximum in water and PMMA at a constant source to chamber distance of 105 cm using the plane parallel ionization chambers PTW Roos *and NACP-02. The nominal electron energies 6 (a), 12 (b) and 20 (c) MeV corresponds to energies at surface* E_0 *of 5.7, 11.7 and 19.7 MeV.*

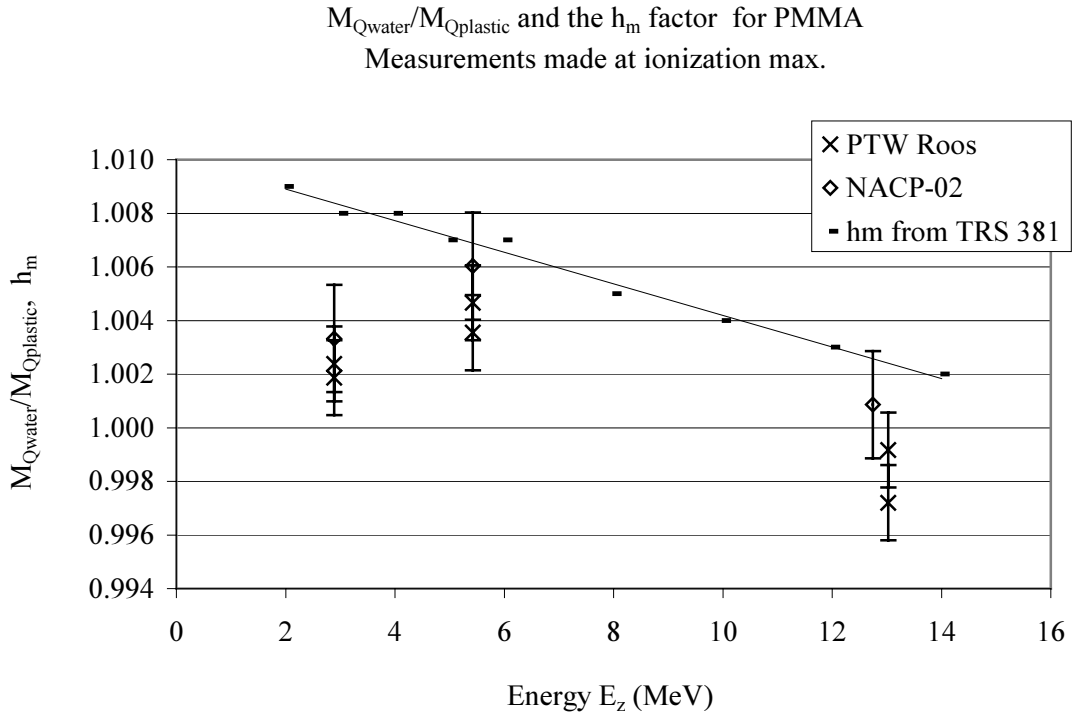

Figure 2. Comparison of measurements, using plane parallel ionization chambers (NACP-02 and PTW R*oos), of the ratio MQwater/MQplastic at ionization maximum in water and PMMA and tabulated values of the h_m factor for PMMA. The two points, at each energy, using the PTW* R*oos chamber are from two different measuring occasions. Energies at depth in water (Ez) from table XII TRS-381.The error bars represents the statistical uncertainty of the measurements of the ratio MQwater/MQplastic.*

The measured ratio $M_{Qwater}/M_{Qplastic}$ for PMMA is slightly lower than the tabulated h_m values in TRS-381. The maximum deviation, ca 0.5% at the lowest energy E_z 2.9 MeV, between measured and tabulated values might be due to the sharp peak in the depth dose distribution at this low energy and therefor the difficulty in finding the exact ionization maximum in both media. Considering the fact that the measurements were made at ionization maximum instead of at the dose maximum, the statistical uncertainty in the measurement of $M_{Qwater}/M_{Qplastic}$ (approximately 0.2% 1 SD) and that the sharp peak in the depth ionization curve at 6 MeV can cause an error of up to 1% for a mispositioning of the detector of only ±1 mm, the TRS-381 [1] values are just inside the experimental values.

3. Comparison with the Fricke dosimeter

To investigate the absorbed dose to water determinations based on the methods and data in the two protocols IAEA TRS-381 [1] and AAPM TG-39 [2] measurements were performed in water using a NACP-02 ion chamber and the Fricke dosimeter. The determinations of the energies at surface, $E_{0,}$ and at measuring depth (reference depth) E_z, were made according to the procedures in the IAEA code of practice using central axis depth dose data measured with a diode detector.

The Fricke dosimeter was calibrated in water against a cylindrical reference ion chamber using ^{60}Co radiation. This procedure was used to insure that the Fricke dosimetry system did not introduce a systematical error. The reference chamber was the same chamber as that used as the cylindrical reference chamber for the inter-calibration of the plane parallel chamber in the electron beam. The calibration gave a $\varepsilon_m G$ value of $352.4 \times 10^{-6} \pm 0.13\%$ (1SD) $m^2\ kg^{-1}\ Gy^{-1}$ which is in good agreement with published data [3], [4]. The long term stability, over

one year, of the Fricke dosimetry system was within 0.4% (1SD), based on 14 measurements in a fixed geometry using a ^{60}Co source. The readout system was a Varian Cary 219 spectrophotometer.

3.1. Results of the Fricke measurements

TABLE 1. RATIO OF THE ABSORBED DOSE TO WATER ACCORDING TO THE DOSIMETRY PROTOCOLS IAEA TRS-381 OR AAPM TG-39, USING PLANE PARALLEL IONIZATION CHAMBER NACP-02, AND ABSORBED DOSE TO WATER DETERMINED USING FRICKE DOSIMETRY. THE MEASUREMENTS AT EACH ENERGY ARE MADE AT DIFFERENT MEASURING OCCASIONS. THE 1 SD FRICKE IS ONE STANDARD DEVIATION OF THE DOSE OBTAINED FROM THE 2 TO 4 FRICKE CAPSULES IRRADIATED AT EACH MEASURING SESSION AND ENERGY

Energy E_0 MeV	$D_{w,IAEA}$/ $D_{w,Fricke}$	$D_{w,AAPM}$/ $D_{w,Fricke}$	$D_{w,AAPM}$/ $D_{w,IAEA}$	1SD Fricke
5.7	1.001	0.995	0.995	0.10%
	0.997	0.992	0.995	0.03%
8.6	0.995	0.990	0.995	0.43%
	0.996	0.992	0.995	0.26%
11.7	0.995	0.987	0.992	0.28%
	0.997	0.990	0.992	0.14%
	0.996	0.988	0.992	0.23%
15.4	1.002	0.996	0.993	0.54%
	0.999	0.992	0.993	0.09%
19.7	0.996	0.988	0.992	0.19%
	1.001	0.993	0.992	0.26%
9.92*	1.003	0.997	0.994	0.13%
29.1*	0.993	0.985	0.992	0.04%
45.1*	0.999	0.991	0.993	0.07%

*Energies from a Scanditronix MM50 accelerator with scanned electron beam.

The difference between the two protocols, for the ionization chambers in use (NACP-02 and the cylindrical reference chamber described below), is mainly due to the difference in the tabulated stopping power ratios at the measuring depth. The calibration factor for the plane parallel chamber ($N^{pp}_{D,air}$ in TRS-381 and N^{pp}_{gas} in TG-39) is dependent on the absorbed dose to air calibration factor for the cylindrical reference chamber. In TG-39 the calculation of the reference chamber absorbed dose to air factor (N_{gas}) is carried out according to AAPM TG-21 [5]. In TG-21 there is an inconsistency in the calculation procedure of the N_{gas} factor regarding the air humidity and the wall correction factor [6], [7], [8]. The suggested correction of 1.003 in Ref. [8] of N_{gas} has been employed in the calculation of the values in table 1 for the AAPM protocol. The dose values using TG-39 is consistently lower than the dose based on TRS-381. Disregarding the correction would increase the differences by 0.3%.

The difference in the plane parallel chamber calibration factors ($N^{pp}_{D,air}$ and N^{pp}_{gas}) calculated using the protocols depend also on the choice of cylindrical reference chamber as the correction factors depend on chamber wall and build-up cap material and their dimensions. The cylindrical reference chamber in this comparison had a graphite wall and

build-up cap with a total thickness of 0.51 g/cm^2 and a graphite central electrode, the cavity inner dimensions were 5.6 mm in diameter and a length of 21.3 mm. This chamber was calibrated at the Swedish standard laboratory in 1995 and the air kerma calibration factor was checked against a reference chamber calibrated in 1999 prior to the measurements. Three separate calibrations of the NACP-02 chamber were performed at the highest available energy from the Varian Clinac 2300 C/D (E_0 19,7 MeV) and the standard deviation of the calibration factor for the plane parallel chamber was 0.2%.

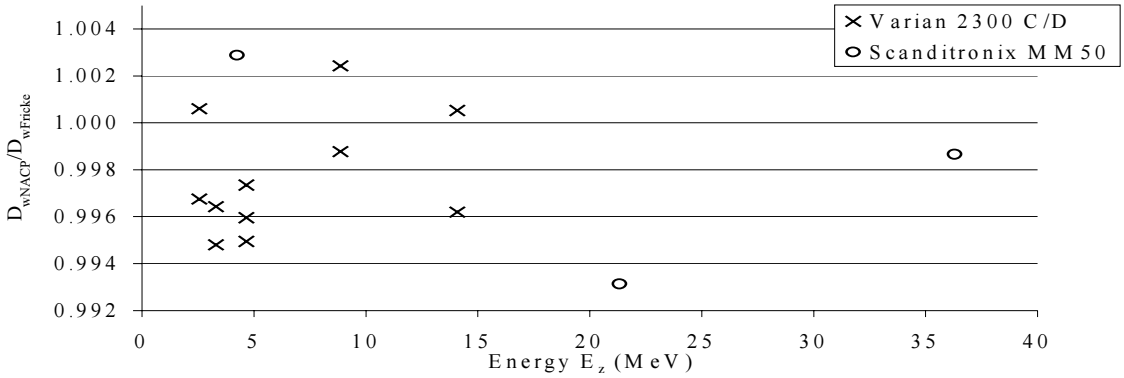

Figure 3. Ratio of dose to water determined using ionization chamber (NACP-02) and chemical dosimeter (Fricke) as a function of energy at measuring depth (E_z).

The two voltage method of TRS-381 gave a recombination in the pulsed scanned beam of 1.014 for the (E_0) 9,9 MeV beam, 1.010 for (E_0) 29.1 MeV and 1.015 for (E_0) 45.1 MeV at a chamber potential of 400V. The same relative difference in recombination, between the three energies, was observed using three other plane parallel ionization chambers operated at different polarizing voltages. The recombination in pulsed beam at a chamber potential of 400V was 1.003±0.001 at all energies. The relatively large difference in recombination in pulsed scanned beams is due to different lateral dose distribution, at depth of the elementary beam, at different energies and to the different scanning patterns, at different energies, designed to obtain a homogeneous fields.

The total statistical uncertainty (1SD) for a single measurement, using the Fricke dosimeter is between 0.4 and 0.7% including long term stability of the Fricke system, standard deviation of the result from different capsules at the same energy and statistical uncertainty at the check of the $\varepsilon_m G$ value. The standard deviation of the mean value at measurement of each energy is of course much smaller. The overall uncertainty of the ionization chamber measurement stated in TRS-381 is 2,9% for the inter-calibration method.

4. Conclusions

- The measured values of the h_m factor, using the described method and considering the statistical and positioning uncertainty, does not contradict the tabulated values in TRS-381.

- The ratio of dose to water measured using the NACP-02 chamber and the chemical dosimeter ($D_{wNACP}/D_{wFricke}$) is close to unity, the mean value is 0.998 ± 0.003 (1 SD).

- There seems to be no change in the ratio ($D_{wNACP}/D_{wFricke}$) as a function of energy in the interval 2–35 MeV. This is a strong indication that both the procedures and the data in the TRS-381 protocol as well as that the assumption of an overall perturbation factor of unity, for the NACP-02 chamber down to electron energies of 2 MeV, is correct.

REFERENCES

[1] INTERNATIONAL ATOMIC ENERGY AGENCY, The Use of Plane Parallel Ionization Chambers in High Energy Electron and Photon Beams — An International Code of Practice for Dosimetry, Technical Reports Series No 381, IAEA, Vienna (1997).

[2] AMERICAN ASSOCIATION OF PHYSICISTS IN MEDICINE TG-39, The calibration and use of plane parallel ionization chambers for dosimetry of electron beams: An extension of the 1983 AAPM protocol report of AAPM Radiation Therapy Committee Task Group No. 39, Med. Phys. **21** (8) (1994) 1251–1260.

[3] SVENSSON, H., BRAHME, A., Ferrous sulphate dosimetry for electrons. A re-evaluation, Acta Radiologica Oncology **18** (1979).

[4] KLASSEN, N.V., SHORTT, K.R., SEUNTJENS, J., ROSS, K.C., Fricke dosimetry: the difference between $G(Fe^{3+})$ for ^{60}Co γ-rays and high energy x-rays. Phys. Med. Biol. **44** (1999) 1609–1624.

[5] AMERICAN ASSOCIATION OF PHYSICISTS IN MEDICINE TG-21, A protocol for the determination of absorbed dose from high-energy photon and electron beams, Med. Phys. **10** (6) (1983) 741–771.

[6] SCHULZ, R.J., ALMOND, P.R., KUTCHER, G., LOEVINGER, R., NATH, R., ROGERS, D.W.O., SUNTHARALINGAM, N., WRIGHT, K.A., Clarification of the AAPM Task Group 21 protocol, Med. Phys. **13** (5) (1986) 755–759.

[7] ROGERS, D.W.O., ROSS, C.K., The role of humidity and other correction factors in the AAPM TG-21 dosimetry protocol, Med. Phys. **15** (1) (1988) 40–48.

[8] ATTIX, F.H., Equations for N_{gas} and N_{air} in terms of N_X and N_K, Med. Phys. **16** (5) (1989) 803–806.

Appendix
PUBLICATIONS ISSUED WITHIN THE FRAMEWORK OF THIS PROJECT

LIZUAIN, M.C., LINERO, D., PICÓN, C., ANDREO, P., Determination of Absorbed Dose to Water in Electron Beams with Plane Parallel Chambers. Comparison between IAEA TRS-381, TRS 277 and AAPM TG-39 Recommendations. Medical and Biological Engineering and Computing **35** Suppl. Part 2 (1997) 889 (Abstracts of the World Congress on Medical Physics and Biomedical Engineering, Nice, France, 1997).

VÉLEZ, G.R., BRUNETTO, M., GERMANIER, A., A Comparison of Methods for Calibrating a Plane Parallel Ionization Chamber in the User's Beam. Medical and Biological Engineering and Computing **35** Suppl. Part 2 (1997) 891 (Abstracts of the World Congress on Medical Physics and Biomedical Engineering, Nice, France, 1997).

ROOS, M., Design and Performance of Electron Chambers. Radiotherapy & Oncology **51** Suppl. 1 (1999), p. S10 (Abstracts of the 5th Biennial ESTRO Meeting on Physics for Clinical Radiotherapy, Göttingen, Germany, 1999).

ROOS, M., DERIKUM, K., KRAUSS, A., On the Effective Point of Measurement of Plane Parallel Chambers in Electron Beams. Radiotherapy & Oncology **51** Suppl. 1 (1999), p. S11 (Abstracts of the 5th Biennial ESTRO Meeting on Physics for Clinical Radiotherapy, Göttingen, Germany, 1999).

VAN DER PLAETSEN, A., PALMANS, H., THIERENS, H., Verification of the IAEA Code of Practice TRS-381 in Therapeutic Electron Beams using Ferrous Sulfate Dosimetry. Radiotherapy & Oncology **51** Suppl. 1 (1999), p. S20 (Abstracts of the 5th Biennial ESTRO Meeting on Physics for Clinical Radiotherapy, Göttingen, Germany, 1999).

PALM, Å., MATTSSON, O., p_{cav} for Cylindrical Ionization Chambers in Electron Beams. Radiotherapy & Oncology **51** Suppl. 1 (1999), p. S20 (Abstracts of the 5th Biennial ESTRO Meeting on Physics for Clinical Radiotherapy, Göttingen, Germany, 1999).

ROOS, M., CHRIST, G., On the Selection of Stopping Power Ratios Water/Air in Electron Beams. Radiotherapy & Oncology **51** Suppl. 1 (1999), p. S38 (Abstracts of the 5th Biennial ESTRO Meeting on Physics for Clinical Radiotherapy, Göttingen, Germany, 1999).

PALM, Å., MATTSSON, O., ANDREO, P., Wall Correction Factors for Plane Parallel Ionization Chambers. Radiotherapy & Oncology **51** Suppl. 1 (1999), p. S50 (Abstracts of the 5th Biennial ESTRO Meeting on Physics for Clinical Radiotherapy, Göttingen, Germany, 1999).

LIZUAIN, M.C., PICÓN, C., LINERO, D., ANDREO, P., Fluence Correction Factor in PMMA for Electron Beam Dosimetry. Comparison with the h_m Values Recommended in the IAEA TRS-381 and IPEMB Protocols. Radiotherapy & Oncology **51** Suppl. 1 (1999), p. S54 (Abstracts of the 5th Biennial ESTRO Meeting on Physics for Clinical Radiotherapy, Göttingen, Germany, 1999).

LIZUAIN, M.C., LINERO, D., PICÓN, C., ANDREO, P., Absorbed Dose Determination in Electron Beams with Plane Parallel Ionization Chambers: A Comparison of Different Codes of Practice (IAEA TRS-381, AAPM TG-39 and IPEMB). Radiotherapy & Oncology **51** Suppl. 1 (1999), p. 56 (Abstracts of the 5th Biennial ESTRO Meeting on Physics for Clinical Radiotherapy, Göttingen, Germany, 1999).

PALM, Å., MATTSSON, O., ANDREO, P., Calibration of plane parallel chambers and determination of p_{wall} for the NACP and Roos chambers for ^{60}Co γ-ray beams, Phys. Med. Biol. **45** (2000) 971–981.

PARTICIPANTS IN THE CO-ORDINATED RESEARCH PROJECT

Andreo, P.	Dosimetry and Medical Radiation Physics Section, Division of Human Health, International Atomic Energy Agency, P.O. Box 100, A-1400 Vienna, Austria
Björeland, A.	Department of Radiation Physics, University Hospital, S-901 85 Umeå, Sweden
Brunetto, M.	Grupo de Espectroscopía, Facultad de Matemática, Astro y Física (FaMAF), Universidad Nacional de Córdoba (UNC), Ciudad Universitaria, 5000 Córdoba, Argentina
Bustos, S.	CEPROCOR – CONICOR, Alvarez de Arenales 230, 5000 Córdoba, Argentina
Christ, G.	Radiologische Universitätsklinik, Abteilung Med. Physik, Universität Tübingen, Tübingen, Germany
Derikum, K.	Physikalisch-Technische Bundesanstalt (PTB), Gruppe für Photonen- und Elektronendosimetrie, Laboratorium 6.43, Bundesallee 100, Pf 33 45, D-38023 Braunschweig, Germany
DuSautoy, A.	National Physical Laboratory (NPL), Centre for Ionising Radiation Metrology, Queen's Road, Teddington, Middlesex TW11 0LW, United Kingdom
Germanier, A.	CEPROCOR, Alvarez de Arenales 230, 5000 Córdoba, Argentina
Krauss, A.	Physikalisch-Technische Bundesanstalt (PTB), Gruppe für Photonen- und Elektronendosimetrie, Laboratorium 6.43, Bundesallee 100, Pf 33 45, D-38023 Braunschweig, Germany
Linero, D.	Servicio de Física y Protección Radiológica, Institut Català d'Oncologia, Av. Gran Vía s/n, km 2,7, E-08907 L'Hospitalet, Barcelona, Spain
Lizuain, M.C.	Servicio de Física y Protección Radiológica, Institut Català d'Oncologia, Av. Gran Vía s/n, km 2,7, E-08907 L'Hospitalet, Barcelona, Spain

Mattsson, O.	Department of Radiation Physics, Göteborg University, S-413 45 Göteborg, Sweden
Palm, Å.	Department of Radiation Physics, Göteborg University, S-413 45 Göteborg, Sweden
Palmans, H.	Standard Dosimetry Laboratory, University of Ghent, Proeftuinstraat 86, B-9000 Ghent, Belgium
Picón, C.	Servicio de Física y Protección Radiológica, Institut Català d'Oncologia, Av. Gran Vía s/n, km 2,7, E-08907 L'Hospitalet, Barcelona, Spain
Roos, M.	Physikalisch-Technische Bundesanstalt (PTB), Gruppe für Photonen- und Elektronendosimetrie, Laboratorium 6.43, Bundesallee 100, Pf 33 45, D-38023 Braunschweig, Germany
Saldaña, O.	Instituto Oncológico Nacional, Panama City, Panama
Svensson, H.	Radiation Physics Department, Norlands Universitetssjukhus (NUS), University of Umeå, S-901 85 Umeå, Sweden
Thierens, H.	Standard Dosimetry Laboratory, University of Ghent, Proeftuinstraat 86, B-9000 Ghent, Belgium
Van der Plaetsen, A.	Radiotherapie-Oncologie, A.Z. St. Lucas, Groene Briel 1, B-9000 Ghent, Belgium
Vélez, G.	Facultad de Matemática, Astro y Física (FaMAF), Universidad Nacional de Córdoba (UNC), Hospital San Roque, Córdoba, Argentina

Research Co-ordination Meetings
Vienna, Austria: 2–5 December 1996
Barcelona, Spain: 30 March–3 April 1998

Consultants Meeting
Vienna, Austria: 29 November–3 December 1999

RECENT IAEA PUBLICATIONS ON DOSIMETRY AND MEDICAL PHYSICS

1999 Calibration of Brachytherapy Sources: Guidelines on Standardized Procedures for the Calibration of Brachytherapy Sources at Secondary Standard Dosimetry Laboratories (SSDLs) and Hospitals (IAEA-TECDOC-1079)

1999 Techniques for High Dose Dosimetry in Industry, Agriculture and Medicine, Proceedings of an International Symposium, Vienna, 2–5 November 1998 (IAEA-TECDOC-1070)

1999 SSDL Network Charter: IAEA/WHO Network of Secondary Standard Dosimetry Laboratories (IAEA/WHO/SSDL/99)

1998 Design and Implementation of a Radiotherapy Programme: Clinical, Medical Physics, Radiation Protection and Safety Aspects (IAEA-TECDOC-1040)

1998 Determinación de la Dosis Absorbida en Haces de Fotones y Electrones, Código de Práctica Internacional (OIEA Colección de Informes Tecnicos No. 277, Segunda Edición). This supersedes the first Spanish edition of 1990

1998 Accidental Overexposure of Radiotherapy Patients in San José, Costa Rica. Special Publication Series (STI/PUB/1027)

1997 Quality Assurance in Radiotherapy, Proceedings of a Joint IAEA–ISRO Working Meeting on National Programmes, 1995 (IAEA-TECDOC-989)

1997 The Use of Plane Parallel Ionization Chambers in High Energy Electron and Photon Beams: An International Code of Practice for Dosimetry (Technical Reports Series No. 381)

1997 Absorbed Dose Determination in Photon and Electron Beams: An International Code of Practice (Technical Reports Series No. 277, Second Edition). This supersedes the first edition of 1987

1996 Review of Data and Methods Recommended in the International Code of Practice IAEA Technical Reports Series No. 277, Absorbed Dose Determination in Photon and Electron Beams (IAEA-TECDOC-897)

1996 Radiation Dose in Radiotherapy from Prescription to Delivery, Proceedings of an IAEA Seminar in Rio de Janeiro, 1994 (IAEA-TECDOC-896)

1995 Atomic and Molecular Data for Radiotherapy and Radiation Research, Final Report of a Co-ordinated Research Programme (IAEA-TECDOC-799)

1994 Calibration of Dosimeters used in Radiotherapy: A Manual sponsored by the IAEA and WHO (Technical Reports Series No. 374). This supersedes IAEA Technical Reports Series No. 185

1994 Radiation Dose in Radiotherapy from Prescription to Delivery, Proceedings of an IAEA Seminar in Leuven, 1991 (IAEA-TECDOC-734)

1994 Measurement Assurance in Dosimetry, Proceedings of a Symposium, Vienna, 24–27 May 1993 (STI/PUB/930)